AN ACOUSTIC IMPEDANCE METER AND ITS VALUE AS A DIAGNOSTIC TOOL

By

PAUL WAYNE WHALEY

Bachelor of Science
Oklahoma State University
Stillwater, Oklahoma
1971

Master of Science
Oklahoma State University
Stillwater, Oklahoma
1973

Submitted to the Faculty of the
Graduate College of the
Oklahoma State University
in partial fulfillment of
the requirements for
the Degree of
DOCTOR OF PHILOSOPHY
December, 1975

AN ACOUSTIC IMPEDANCE METER

AND ITS VALUE AS A

DIAGNOSTIC TOOL

Thesis Approved:

Larry D. Tuttle
Thesis Adviser

David Jennings

R. F. Lowery

J. E. Bose

N. N. Durham
Dean of the Graduate College

PREFACE

An important field of application for an acoustic impedance meter is audiology. Although static acoustic impedance has been used before as a diagnostic tool, there are drawbacks to the acoustic impedance bridge used in those studies. It was felt that if an acoustic impedance meter could be designed which reduced or eliminated those drawbacks, then there might be additional valuable diagnostic information in static acoustic impedance profiles. The purpose of this study is to design a suitable acoustic impedance meter and then test its application as a diagnostic tool.

My special thanks go to my thesis adviser, Dr. Larry Zirkle, who provided many helpful suggestions and comments. Appreciation is also expressed to the other committee members, Dr. Richard Lowery, Dr. David Jennings, and Dr. James Bose, for their helpful comments during the course of this study.

Thanks go to Mr. Gary Beeby, Staff Audiologist at Oklahoma State University's Speech and Hearing Clinic, for his suggestions and his assistance in obtaining normal hearing subjects for the clinical study included in this dissertation. Particular thanks also go to Dr. Thomas Stokinger, Chief of the Audiology and Speech Pathology Service of

Veterans Administration Hospital, Oklahoma City, Oklahoma, for his help in furnishing the subjects with known middle ear malfunctions, and to the Ear, Nose and Throat section, Surgical Service, for providing the diagnoses.

Personal gratitude is extended to my wife, Karen, for her understanding and sacrifice during this research and for her help in typing draft copies of this manuscript. The author also wishes to acknowledge the assistance of Mr. Eldon Hardy in drawing the figures in this dissertation. Finally, a note of thanks is given to Mrs. Lynn Danvers for her comments on the manuscript and for her help in preparing the final copy.

This work was supported in part by a Biomedical Support Grant from the U. S. Public Health Service (NIH) to Oklahoma State University and by the OSU Center for the Systems Sciences. Also, the School of Mechanical and Aerospace Engineering provided support for which the author is grateful.

TABLE OF CONTENTS

LIST OF TABLES

LIST OF FIGURES

NOMENCLATURE

Z_o = input acoustical impedance to the ear canal

Z_e = input acoustical impedance at the eardrum

ρ_a = density of air

C_a = speed of sound in air

S = cross-sectional area of ear canal model

x = length of ear canal model

C = wave propagation velocity of eardrum model

σ = mass per unit area in eardrum model

E = modulus of elasticity of eardrum model

t = plate thickness of eardrum model

ν = Poisson's ratio for eardrum model

P = pressure forcing function amplitude

y = transverse displacement of eardrum model

ω = frequency, in radians per second

K_a = ω/C_a wave number for air

K^2 = ω/C wave number for eardrum model, squared

Z_m = input mechanical impedance of ossicular chain

K_{me} = spring effect of middle ear volume

b = outer radius of annular plate

d = inner radius of annular plate

V_{me} = volume of middle ear cavities

Q = shear per unit length for eardrum model

K_d = effective spring constant of outer segment of eardrum

M_m = mass of malleus

ℓ_m = length of malleus

M_I = mass of incus

ℓ_I = length of incus

R_c = mechanical input resistance to the cochlea

k_S = spring constant of stapedius muscle

k_t = spring constant of tensor tympani muscle

P_t = pressure measured in known calibration impedance

P_m = pressure measured next to the diaphram in the probe microphone

P_s = source pressure in microphone calibration

P_c = reference pressure in independent calibration of probe microphone

P_K = pressure measured in unknown test impedance

P_{OC} = open circuit pressure response

P_r = reference pressure

G_T = complex ratio of output pressure measured next to the probe microphone diaphram to the reference pressure for the calibration test

G_m = transfer function for probe microphone calibration

G_K = complex ratio of output pressure measured next to the probe microphone diaphram to the reference pressure for the unknown test impedance

G_{OC} = complex ratio of output pressure measured next to the probe microphone diaphram to the reference pressure for the open circuit response

G_{OS} = transfer function for erroneous open circuit response

U_t = volume velocity flowing through the known acoustical test impedance

U_b = volume velocity flowing through the source impedance

U_m = volume velocity flowing through probe microphone impedance

U_c = volume velocity flowing through the load for microphone calibration

Z_b = internal source impedance of acoustic impedance meter

Z_M = impedance of probe microphone

Z_c = value of acoustic impedance of the B&K coupler supplied for probe tube calibration

Z_s = internal source impedance of piezoelectric transducer

Z_K = unknown test impedance

U_K = volume velocity flowing through unknown test impedance

C_m = value of acoustical capacitance for probe microphone

R_m = value of acoustical resistance for probe microphone

L_m = value of acoustical inertance for probe microphone

CHAPTER I

INTRODUCTION

Preliminary Considerations

Instruments used in conventional impedance audiometry measure only one of the three components of acoustic impedance. This dissertation concerns the design of a device capable of measuring all three impedance components. In addition, a clinical investigation is conducted to determine the value of such a device in obtaining additional diagnostic information.

In order to discuss the concept of acoustical impedance and an acoustic impedance meter, it is appropriate to describe the analogy method commonly used in analysis of acoustical systems. Mathematically, acoustical behavior is governed by the wave equation, the same equation for vibration of continuous bodies (strings, bars, membranes, plates), with pressure and volume velocity the independent variables. While the concept of pressure is straightforward, the concept of volume velocity is elusive in that the "volume" is unspecified. Thus, it is common practice to define acoustical systems analogously in terms of electrical circuits which are easier to understand. Pressure is analogous to voltage, and volume velocity is analogous to current. Acoustical

circuits defined in this manner may be analyzed using linear, lumped parameter methods provided that the physical dimensions of the acoustical system are small compared to a wavelength of those sound waves present. Lumped acoustical elements are defined as resistors (porous material or capillary tube), capacitors (enclosed volume with rigid walls), and inertances (a hole or a short tube). Thus, the electrical analogy is appropriate as the acoustical circuit is identical to the electrical circuit when linear, lumped parameter techniques apply.

When applied properly, the analogy method is an acceptable engineering approach. However, particular consideration should be given to three aspects: (1) The wavelength criterion should be carefully examined to identify applicability of linear, lumped parameter techniques. When that wavelength criterion is not met, other analytical techniques should be used. (2) Acoustical elements are not as pure and linear as electrical elements, and use of the analogy method sometimes obscures that fact. (3) The analogy method has sometimes been applied to mechanical systems. Since volume velocity of a vibrating mechanical element is well defined, the analogy method is not necessary and should not be used.

The analogy method is not used in the design of this acoustic impedance meter. Analysis and design are carried out in terms of acoustical circuits, with pressure and volume velocity the independent variables. Thus, the reader is reminded that acoustical elements are not as pure as

electrical elements; and a more accurate validation and evaluation of the acoustic impedance meter is possible.

The definition of the acoustical impedance concept is comparable to other physical systems: mechanical impedance is defined as force divided by velocity; electrical impedance is defined as voltage divided by current; and acoustical impedance is defined as pressure divided by volume velocity. There are three main parts of acoustical impedance: resistance, compliance, and inertance. Mathematically, acoustical impedance is a simple concept, but physically there is a major obstacle. It is not possible with conventional technology to measure volume velocity. A method of avoiding that technical difficulty is formulated in Chapter II in the development of the acoustic impedance meter.

Various ways to measure acoustic impedance have been described by Beranek (1). To avoid measuring volume velocity, some researchers have used constant volume velocity sources (2) (3). There are two problems with this: (1) This technique introduces an error in the phase (3); and (2) The assumption of constant volume velocity depends on a large internal source impedance. The value of the internal source impedance of acoustical devices is difficult to check so the accuracy of that assumption may be overlookd.

Another method of measuring acoustical impedance is an acoustical bridge circuit (4). The acoustical bridge circuit is similar to an electrical half bridge, containing a variable known impedance on one leg and an unknown impedance on

the other. The known impedance is adjusted until a null is reached and the bridge is balanced. This technique has had wide use in audiology, but there has been some question concerning the accuracy of resistance (5). Bridge circuits for use in audiology have two weaknesses: (1) They are limited to compliance measurements because there is no inertance leg. (2) They are inherently limited in upper frequency range, and their accuracy depends on the accuracy of acoustical reference resistors (5). Most acoustical resistors possess some inertance and have nonlinear characteristics (2).

Conventional impedance tests in audiology fall into two categories: static impedance and dynamic impedance or tympanometry. Static impedance is the passive impedance of the ear measured in absence of middle ear muscle activity and with atmospheric pressure in the ear canal. Dynamic impedance or tympanometry is the change in ear impedance which results from middle ear muscle reflex activity or varying pressure in the ear canal (6). While static impedance is frequently denoted as absolute impedance, dynamic impedance is sometimes called relative impedance because change of impedance is the quantity of interest. Dynamic impedance is measured at 220 hz and 660 hz. A tympanogram is a plot of impedance change versus ear canal pressure. Dynamic acoustic impedance has had more widespread clinical application than static acoustic impedance because of the difficulty involved in accurately measuring static impedance.

Static Impedance Profiles

Static acoustic impedance is the quantity to be measured in this dissertation. Studies concerning static impedance and its use in audiology have yielded limited clinical results. For a more complete discussion of this see Lilly (6).

Metz (7) discovered that the static acoustical input impedance of the human ear bears a relationship to the pathological conditions of the middle ear. Since that time various researchers (Zwislocki (4), Feldman (8) (9) (10), Jerger (11)) have published studies of static impedance and its relationship to middle ear pathology. The overall conclusion of these studies is that otitis media and otosclerosis exhibit high levels of resistance and reactance. However, this is not precise, as some normal levels are indistinguishable from otosclerosis because of their wide confidence bands (12).

There are two weaknesses of previous static impedance studies in audiology. First, the acoustic impedance bridge used in these studies has two weaknesses which have already been mentioned: (1) The bridge had no provision for measuring inertance; and (2) Acoustical reference resistances are very difficult to design with purity and linearity. Inertance and resistance may play a significant part of ear impedance in the case of ear pathology. Second, in previous studies of static acoustic impedance the effect of the ear

canal was assumed to be shunt compliance. The volume of the ear canal was measured, and that volume was used to calculate acoustical compliance. Whether or not the ear canal behaves only as a shunt compliance is not known. There may also be resistance and inertance effects. The effect of the ear canal on impedance profiles was experimentally determined for this dissertation. By measuring impedance at the two extremes of eartip insertion into the ear canal and noting the effect on static impedance, one can account for the ear canal's effect without making assumptions as to its dynamic behavior.

A valuable engineering tool in the analysis and design of dynamic systems is the frequency response or Bode plot. Using this test one can estimate the parameter values of a system when its general properties are known. In a similar manner, if the system's static input acoustical impedance is measured at several frequencies, the resulting plot is called an impedance profile. It is possible that such an impedance profile contains additional information about the pathological condition of the middle ear. Although previous studies have shown gross changes of impedance with different pathological conditions, there is no relationship between detailed structural information of the middle ear and impedance profiles (6). This problem in audiology is a potential field of application for the acoustic impedance meter described in this dissertation. In order to systematically investigate the possibility of such diagnostic information present in

static impedance profiles, an improved method of measuring acoustic impedance is necessary. Such an improved method is the acoustic impedance meter of this dissertation.

The objective of this dissertation is two-fold. First, an acoustic impedance meter which is capable of measuring all three components of acoustic impedance is designed and evaluated. Second, since this acoustic impedance meter's primary field of application is audiology, a study of impedance profiles as a diagnostic criterion is also undertaken. A preliminary test of the concept of impedance profiles as a diagnostic criterion is desirable to provide support for further investigation and to indicate whether the acoustic impedance meter is capable of measuring changes of the magnitude expected with pathological conditions. A mathematical model which shows impedance profile shape differences with model parameter variations would be valuable in providing preliminary support of that concept.

Mathematical modeling of the auditory system is not a new concept. Auditory models have been used to aid in understanding the ear's function, to study the effect of the middle ear's pathological conditions, and to study the effects of noise exposure (13) (14) (15). These auditory models range from a very complicated mechanical model (14) to a simple electrical analog model (14) (15). There are no mathematical models which are capable of reflecting changes in impedance profile due to a specific malfunctioning middle ear mechanism. Zwislocki (13) showed changes in impedance of

a mathematical model due to simulated gross effects, but a description of a specific mechanism and of its effect on impedance profiles is lacking. Onchi attempted a model which included much of the middle ear's detail (14). The problem with that mathematical model, however, is that some of the validation depended on psychological testing. A more recent model is similar to that of Onchi but takes advantage of additional information and follows a more sound validation procedure (16). This model is still inappropriate, however, as it does not include damping. Details of the mathematical model simulations of pathology developed for this research are described in Chapter III.

Procedure

This dissertation concerns the design and testing of an acoustic impedance meter for use in audiology. Design criteria and procedures are described in Chapter II. Since no attempt has been made in the past to relate specific pathological conditions of the middle ear to static impedance profile shape, a preliminary study is done using an improved mathematical model of the human ear. The purpose of this study is to investigate those changes in static impedance profile shape which may be expected with specific pathological conditions of the middle ear. This study is described in Chapter III.

In Chapter IV three questions are answered to show improvements of this static impedance test over previous

methods. First, a test was completed to tell whether the depth of the eartip's insertion into the ear canal affects the impedance profile's shape. Second, consideration is given to the effect of auditory nonlinearity on impedance profile shape. If the ear is even slightly nonlinear, then the intensity level of testing may also be important. Third, data repeatibility is checked. If a particular person has a distinct impedance profile shape on any given day, then for this test to be valid that shape must be the same on any other given day.

A study is conducted to test the clinical applicability of static impedance profiles and their sensitivity to middle ear conditions. Subjects with previously identified normal hearing and subjects with previously diagnosed cases of middle ear pathologies were tested. Impedance profiles are plotted which correspond to specific pathological conditions, and results are noted.

Finally, Chapter V is a listing of this research's conclusions and recommendations for future study.

CHAPTER II

ACOUSTIC IMPEDANCE METER

Introduction

The design, evaluation, and general requirements of the acoustic impedance meter are described here. In order to accurately determine changes of impedance profile shape, a better method of measuring resistance and a method for measuring inertance are required. This acoustic impedance meter must be capable of measuring resistance and total reactance (both capacitance and inertance) in those ranges of magnitude and frequency which are important in the detection of middle ear pathology.

Some preliminary discussion of linear, lumped parameter techniques and their application to acoustical systems is necessary to establish those aspects which are important. Lumped models of acoustical elements have traditionally depended on the assumption that physical dimensions are small compared to a wavelength (1). There are three lumped acoustical elements: an acoustical compliance is a simple enclosed volume with stiff walls; an acoustical inertance is a short tube; and an acoustical resistance is some porous material which absorbs sound waves. Preliminary to these definitions is the basic assumption that the acoustical

system's physical dimensions are small compared to the sound's wavelength.

When the length of a small tube is longer than a wavelength, lumped parameter modeling may not be used. Such a tube may be approximated by a network similar to the transmission line models used in electrical and fluid power lines. This network is only an approximation, however, because distributed parameter systems are different from lumped parameter systems. Therefore, for any given acoustical system at low frequencies lumped parameter modeling results might be acceptable; while as frequency increases, the results may deteriorate because this wavelength criterion begins to fail. This consideration plays an important part in the acoustic impedance meter's evaluation.

The most difficult acoustical element to design is the resistor. Almost all acoustical resistors possess some inertance and have nonlinear characteristics (2). Since resistance is inherently a direct current concept depending only on steady flow conditions, a pure resistor doesn't depend on frequency. Therefore, little is known about the frequency properties of impure acoustical resistors. The measured direct current characteristics of some acoustical resistors are shown in Figure 1. All of these are nonlinear. The sintered disks are supposedly the best commercially available acoustical resistors. The ceramic rods shown are fluidic resistors and so were not expected to be very good acoustical

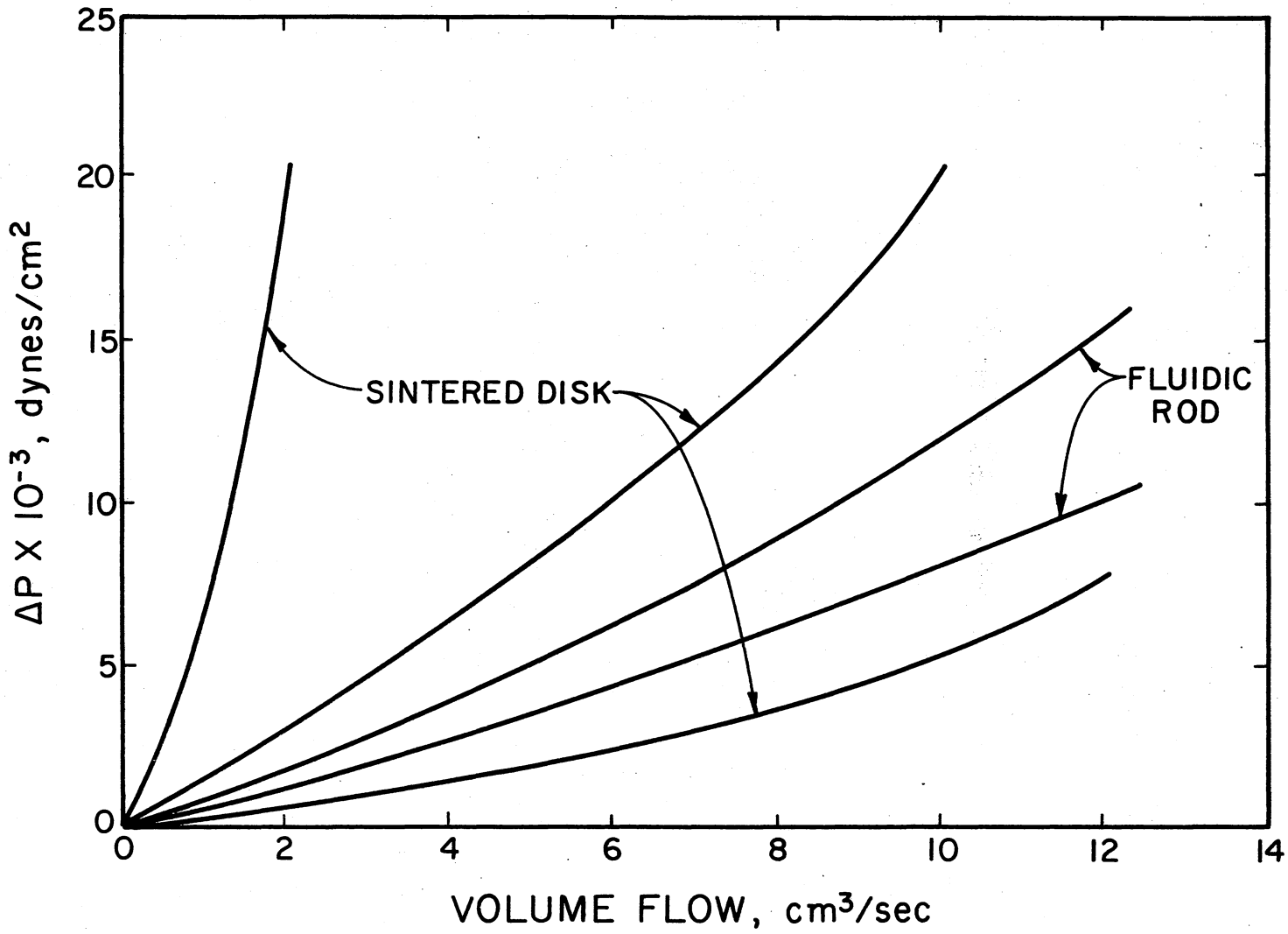

Figure 1. Direct Current Characteristics of Some Acoustical Resistors

resistors. Surprisingly their linearity appears to be as good if not better than that of the sintered disks.

A different acoustical resistor was used for this study. For a long tube the input impedance is real and constant with frequency, as can be shown by the following equation.

$$Z_i = \frac{\rho_0 C}{S} \cdot \frac{A+B}{A-B}$$

where A = complex amplitude of incident sound wave;

B = complex amplitude of reflected sound wave.

If the tube is infinite, then B = 0, and $Z_i = \rho_0 C/S$, which is real. Therefore, the input impedance of such tubes is a pure resistance. This differs from traditional resistors in that it represents a complex network's input impedance and not the direct current pressure flow characteristic. It is likely that the measured direct current pressure-flow characteristic may be different from the input impedance to the infinite tube. There is a large source of error since this resistance is inversely proportional to the square of the tube's diameter; therefore, small errors in measuring the tube's diameter can have a large effect.

Enclosed cavity acoustical compliances are contaminated by flexible cavity walls and by leaks. Flexible walls can add stiffness effects, and leaks can add inertance and resistance effects. When acoustical compliances are constructed to avoid these two possibilities, their purity is very good. Therefore, because of their purity infinite tube resistance and enclosed

cavity compliance were used in the calibration and evaluation of the acoustic impedance meter.

Description

A schematic of the acoustic impedance meter is shown in Figure 2. A horn driver is connected to a four millimeter diameter probe tube from a Bruel and Kjaer (B&K) probe tube kit through a coupler shaped inside like a reversed exponential horn for impedance matching purposes. Steel wool is inserted into the probe tube to reduce resonance effects. There is a hole machined in the side of the coupler to allow the insertion of a Bruel and Kjaer quarter-inch reference condenser microphone at the inlet to the source probe tube. A microphone probe tube is fixed into the earpiece inside the source probe tube and is connected to a Bruel and Kjaer half-inch condenser microphone.

The acoustic impedance meter may be represented by the acoustical circuit shown in Figure 3. In order to determine a relationship between P_t, P_r, and Z_t, U_t must be determined, and that is not possible directly. It is assumed that the circuit of Figure 3 may be represented by Thevenin's equivalent circuit theorem. Thevenin's equivalent circuit theorem states that for linear, lumped parameter system elements a pressure source driving an impedance may be replaced with a pressure source of value equal the open circuit pressure with all sources equal to zero in series with the back

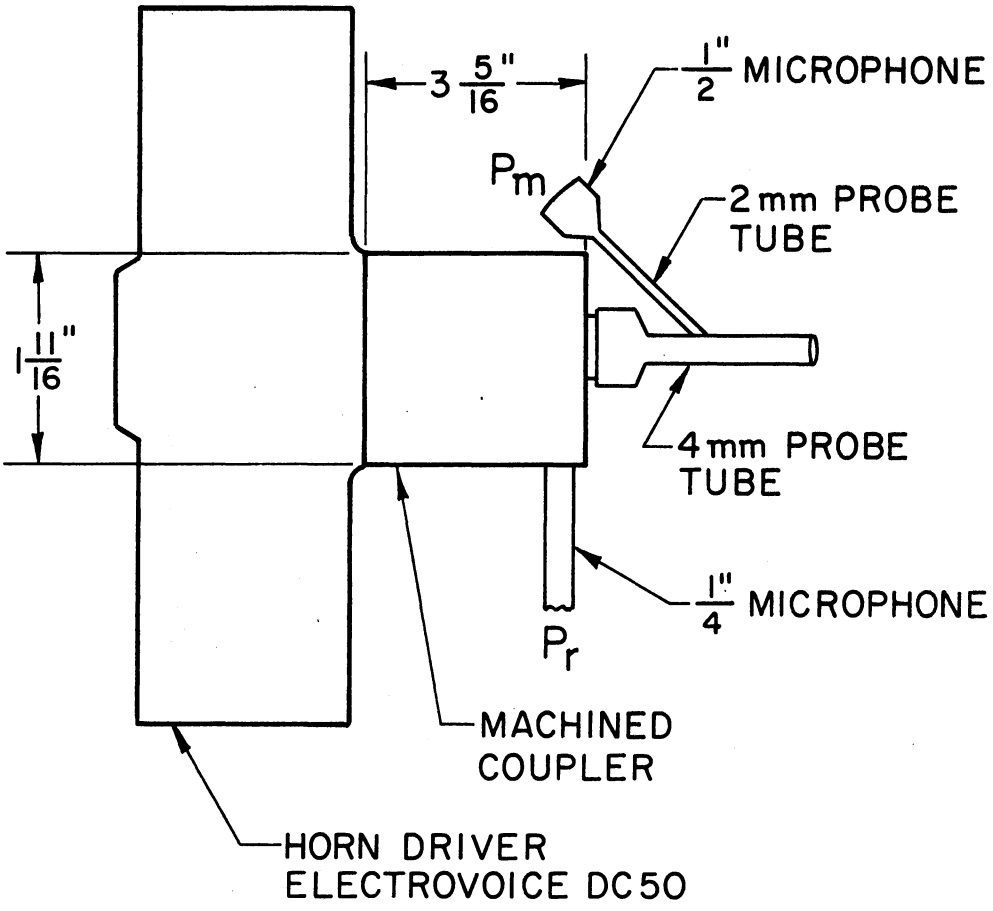

Figure 2. Schematic of the Acoustic Impedance Meter

impedance of the source as seen from the load (17). The physical dimensions of the device of Figure 2 are small compared to the wavelength of sounds below about 1400 hz; therefore, for such frequencies Thevenin's equivalent circuit theorem applies. This equivalent circuit is shown in Figure 4. The impedance Z_b is the measured back impedance of the source, while Z_M is shown as a series impedance because of the physical configuration of the probe microphone.

In order to measure some unknown impedance inserted in the place of Z_t in Figure 4, it is necessary to calculate U_t. If P_{OC}, Z_b, and Z_M are known, it is possible to calculate U_t. In order to measure P_{OC} it is necessary to block all volume velocity flow from the output of the probe tubes. Since the probe microphone is used to measure P_{OC}, there will be some drain of volume velocity and so some error in P_{OC}. Therefore, an estimate of Z_M is necessary in order to calculate P_{OC}. A measurement of Z_b is possible if Z_t of Figure 4 is known, since volume velocity drain through these two elements must be calculated. An estimate of Z_M is thus also necessary for the calculation of Z_b. The determination of Z_M is described next.

Figure 5 is the acoustical circuit of the probe tube calibration set-up provided by B&K along with the acoustical circuit for the probe tube. The source is a piezoelectric transducer, and Z_c is a coupler cavity. The elements shown for the microphone probe tube impedance are to be obtained from a parameter fit to frequency response data. The

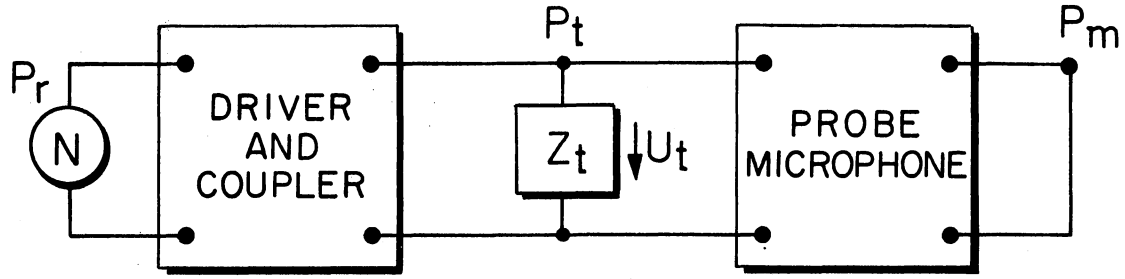

Figure 3. Acoustical Circuit of the Acoustic Impedance Meter

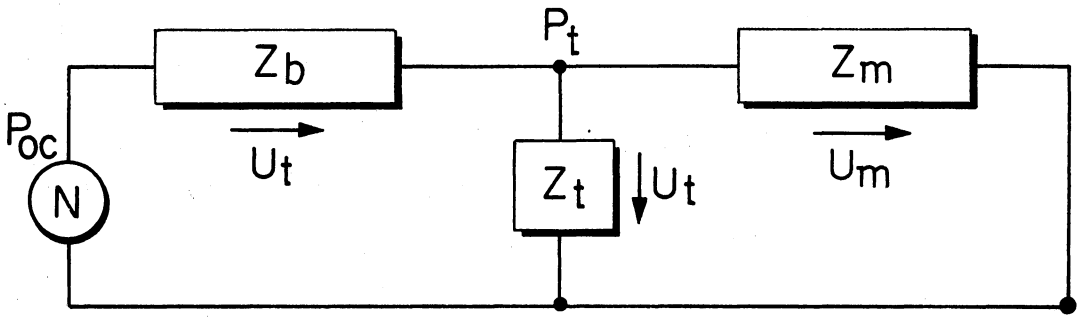

Figure 4. Thevenin's Equivalent Circuit for the Acoustic Impedance Meter

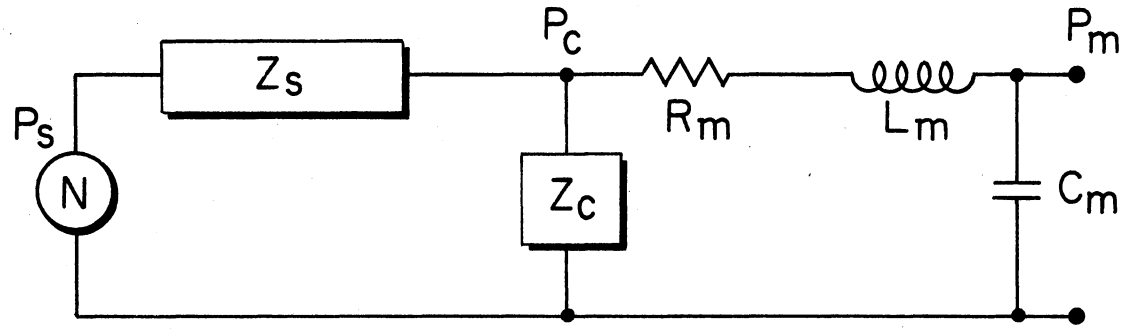

Figure 5. Acoustical Circuit of the Probe Tube Calibration

measured transfer function P_m/P_c is shown plotted in Figure 6 along with the second-order system equation. The general second-order system equation fits that data quite well. At the peak amplitude the phase shift is -90°. The data begins to deviate significantly from theory at higher frequencies, but that is because of a quarter wavelength resonance at about 2450 hz. Recall the discussions at the introduction to this chapter which noted that results using lumped parameter models can be expected to deteriorate at higher frequencies. In spite of this, low frequency data is a good validation for this type of model for the probe microphone.

From the data of Figure 6 an estimate may be made of the two parameters which describe any second-order system: damping ratio and natural frequency. Using charts on the response characteristics of second-order systems, the following parameters are estimated (17).

damping ratio = .35

natural frequency = 720 hz

Making the following definition,

$$\frac{P_m}{P_c} = \frac{1}{\frac{S^2}{\omega_c^2} + \frac{2\xi S}{\omega_c} + 1}$$

where

ω_c = natural frequency;

ξ = damping ratio,

this transfer function may be equated to that obtained from Figure 5.

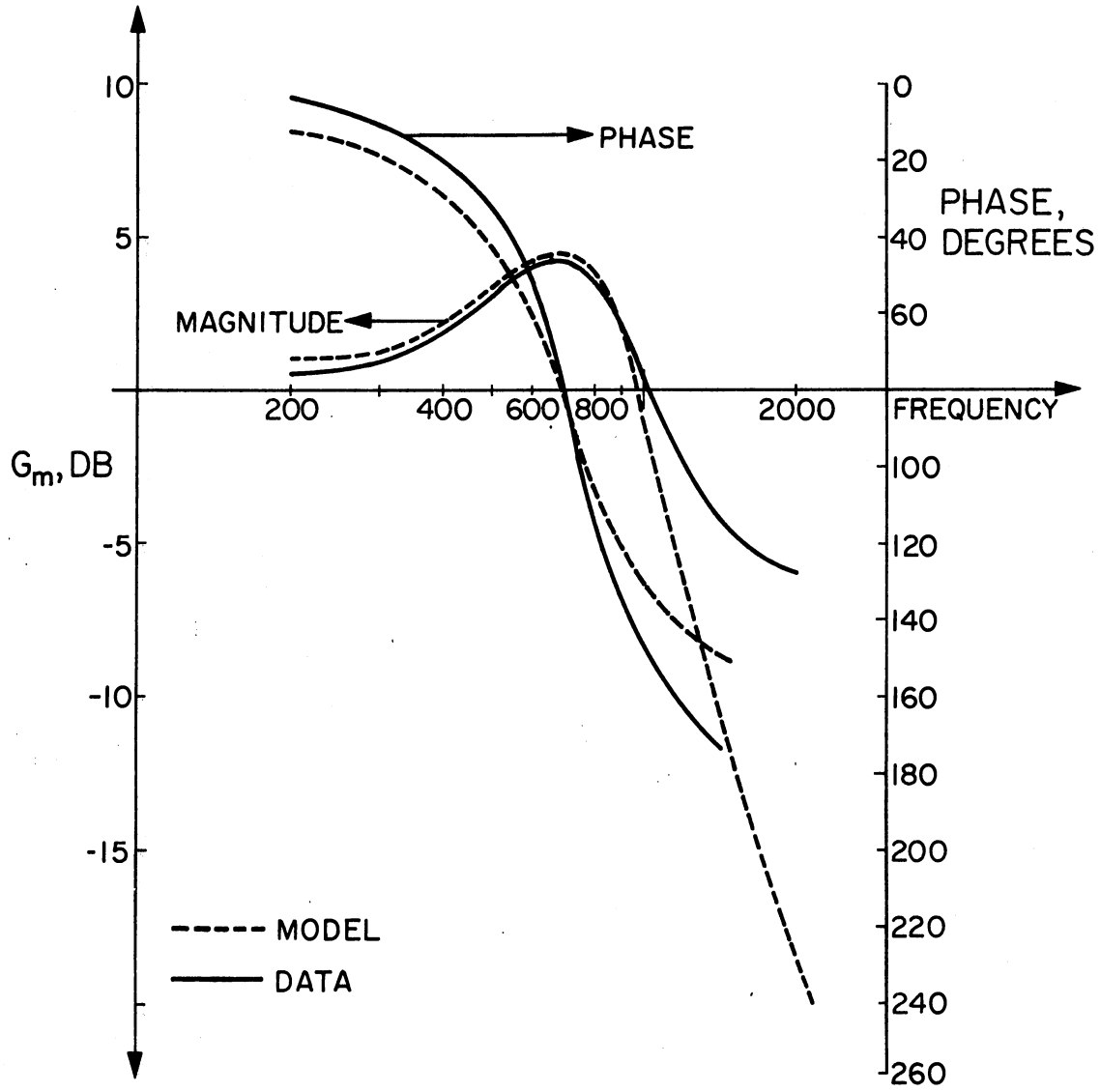

Figure 6. Measured Transfer Function of Probe Microphone Compared With Theory

$$\frac{1}{\frac{S^2}{\omega_c^2} + \frac{2\xi S}{\omega_c} + 1} = \frac{1}{1 - \omega^2 L_m C_m + j\omega R_m C_m} \quad .$$

For this to be true the following must be true:

$$L_m C_m = 1/\omega_c^2$$

$$R_m C_m = 2\xi/\omega_c \quad ,$$

giving two equations and three unknowns. However, B&K gives an estimate of the equivalent volume of their probe tube coupled with the one-half inch condenser microphone (18). Using that value of $V_m = .02 cm^3$, the following estimate is made.

$$C_m = \frac{V_m}{\rho_A C_A^2} = 13.84 \times 10^{-9} \quad ,$$

where V_m = equivalent volume of the one-half inch microphone cartridge coupled with the probe tube. Using this value for C_m, the other two microphone impedance elements may be calculated.

$$L_m = .354$$

$$R_m = 11200$$

As a check, L_m may be calculated independent of the above on the basis of acoustical inertance of a tube. Using that approach the following quantity results.

$$L_m' = .212$$

The two inertances do not agree probably because the bend in the microphone probe tube affects the inertance calculated by the second method. On this basis it is likely

that the original estimate of C_m is better. That estimate of Z_M is given below.

$$Z_M = 11200. + j(.354\omega - \frac{1}{13.84 \times 10^{-9}\omega})$$

Referring to Figure 4, if Z_t is replaced by a plug which blocks the probe tube, then the resultant pressure P_{OC}' at that point may be measured and the following definition made.

$$\frac{P_{OC}'}{P_r} = \frac{G_{OS}}{G_m}$$

where G_{OS} = measured open circuit transfer function

G_m = measured microphone transfer function.

P_{OC}' is not the open circuit pressure but may be used to calculate the open circuit pressure.

$$P_{OC} - P_{OC}' = U_m Z_b$$

Referring again to Figure 4, a node equation yields the following:

$$\frac{P_{OC} - P_t}{Z_b} = \frac{P_t}{Z_t} + \frac{P_t}{Z_M} \quad .$$

Substituting for P_{OC}, the result is

$$\frac{P_{OC}' + U_m' Z_b - P_t}{Z_b} = \frac{P_t}{Z_t} + \frac{P_t}{Z_M} \quad .$$

Collecting terms and solving for Z_b, the result is

$$Z_b = \frac{P_{OC}' - P_t}{\frac{P_t}{Z_t} + \frac{(P_t - P_{OC}')}{Z_M}} \quad .$$

Now making the following definition,

$$\frac{P_t}{P_r} = \frac{G_T}{G_m} \quad ,$$

where G_T = measured known impedance transfer function, Z_b becomes

$$Z_b = \frac{(G_{OS}/G_T - 1)Z_T}{1 + (1 - G_{OS}/G_T)\ Z_T/Z_M} \quad .$$

Now the properties of Thevenin's equivalent circuit of Figure 4 are known, and if Z_T is replaced by some unknown impedance Z_K, a node equation yields the following:

$$\frac{P_{OC} - P_K}{Z_b} = \frac{P_K}{Z_K} + \frac{P_K}{Z_M} \quad .$$

Making the following definitions,

$$\frac{P_K}{P_r} = \frac{G_K}{G_m}$$

$$\frac{P_{OC}}{P_r} = \frac{G_{OC}}{G_m} \quad ,$$

and substituting, solving for Z_K the result is

$$Z_K = \frac{G_K}{(G_{OC} - G_K)/Z_b - G_K/G_m} \quad .$$

These equations and the associated data are included in a computer program given in Appendix B, along with instrumentation details. That program includes a calcomp plotting routine for ease in providing the resultant plots of acoustic impedance versus frequency.

In summary, first an approximation to the form of the microphone probe tube impedance is assumed. Transfer function data is measured on the microphone probe tube, and the

elements of the assumed form of the microphone probe tube impedance are determined through a curve fit to this data. Next, using the microphone impedance and loading the impedance meter with a known compliance, the value of the back impedance of the source is measured. If both these are known, then volume velocity flowing through the unknown impedance to be measured may be calculated; and since pressure is measured with the probe microphone, unknown impedance may be calculated.

Validation and Evaluation

As was noted at the first of the introduction to this chapter, the requirement of this acoustic impedance meter is that it accurately measure resistance and reactance over those magnitudes and frequencies which are important in the detection of middle ear pathology. It is the purpose of this section to determine whether that criterion is met. To do that six acoustical elements are used to test the acoustic impedance meter: three different compliances, two different long-tube resistors, and one capillary tube fluidic resistor. Those acoustical elements were chosen on the basis of the expected impedance levels which are important in middle ear pathology detection as reported by previous researchers.

At this point a few comments concerning the length of the long-tube resistors are needed. Theoretically an infinite tube is required, but reality demands some

realizable compromise. It was determined by testing several different lengths that tubes of twice the longest wavelength are of sufficient length to prevent quarter wavelength resonances over this frequency range. Traditionally, infinite tubes may be simulated by appropriate damping material at the end to absorb sound waves that would otherwise be reflected back to the source. However because of the small diameter of those tubes, such damping material was unnecessary.

Figure 7 shows the test results for the two long tubes and the fluidic resistor. Theoretical levels are dashed lines. The two long-tube resistors look quite good as far as predicted level and constancy with frequency. Their associated reactance levels are reasonable because of the unavoidable reactance of coupling between the long tube and the probe tubes of the acoustic impedance meter. Recall that in the introduction to this chapter it was anticipated there might be an error between the theory and the practice, as the theory depends on the inverse of the square of tube diameter. The difference between the theory and measurement in Figure 7 is consistent with this error.

The results of the fluidic resistor in Figure 7 are not as good as those of the long-tube resistor. The fact that the level depends on frequency is not surprising since the capillary tube fluidic resistor has some inertance and the characteristic is nonlinear. Two things about the fluidic resistor should be mentioned. First, this fluidic resistor

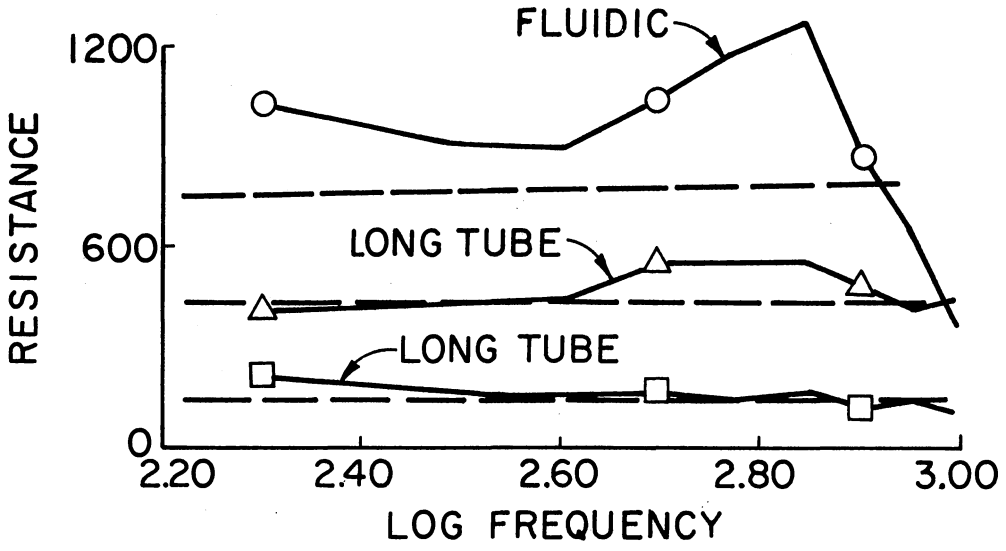

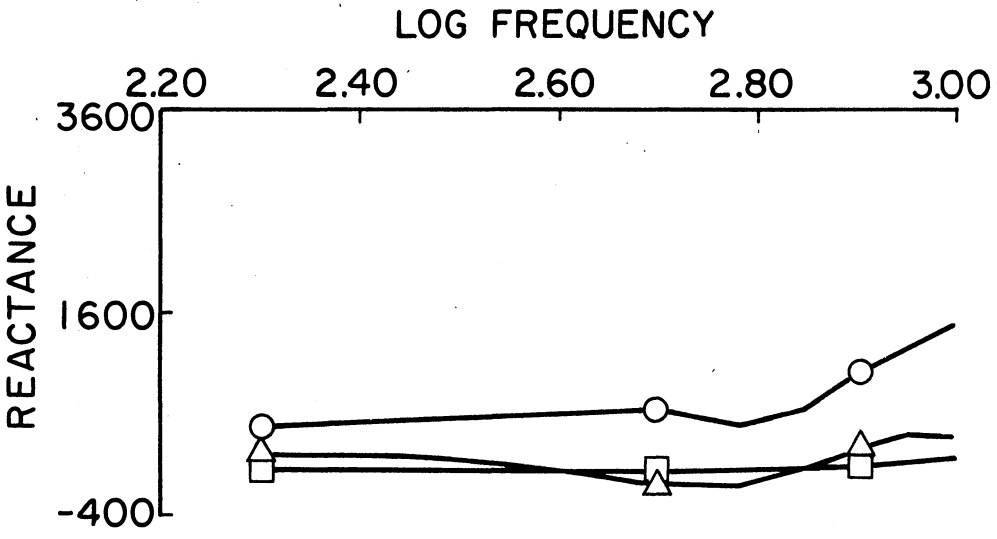

Figure 7. Test Results for Acoustical Resistors

is similar to the capillary tube resistor which has been used in previous bridge circuits. Figure 7 shows the accuracy of such an element in an alternating current condition. Second, notice the fairly high mass reactance associated with the fluidic resistor.

The discrepancy between data and theory of the fluidic resistor in Figure 7 at high frequency is probably because of discrepancy in the microphone calibration model and non-linear effects. First, the assumed microphone model effectively attenuates the data of the transfer function at high frequency. This attenuation has the effect of reducing resistance. Second, the source probe tube contains considerable resistance. Since acoustical resistors are typically nonlinear, the acoustic impedance meter itself is probably nonlinear. The increased fluidic resistance causes an increased sound pressure, encouraging nonlinear effects.

The levels of acoustical resistance which may be anticipated with pathological conditions of the middle ear may be determined from existing literature. The value for normal ear resistance ranges from about 300 to 500 cgs units (9). Resistance increases to about 800 or 1000 with otosclerosis and serous otitis media, but the increased level depends on degree of otosclerosis or otitis media (4). The resistance levels shown in Figure 7 cover this range quite well. The data above was taken with bridges which are for impedance at the eardrum, while this study is for impedance at the entrance to the ear canal. More comparable data was reported

in an older study which reports a normal resistance level at the entrance to the ear canal of around 200 cgs units (19). The overall conclusion is that the acoustic impedance meter is capable of measuring resistance in the magnitude range of interest in predicting pathology.

Figure 8 shows the compliance test results. Theoretical predictions are solid circles. A syringe was used to vary the test volume. The small resistance level is because of a small amount of damping material included with the test impedance. This small resistance is necessary because the acoustic impedance meter has large errors present when the load is not damped, as demonstrated in Figure 9. When the resistance is low and the reactance is high, errors in phase angle can have a significant effect. This normally occurs at low frequencies. For the impedance Z_1 of Figure 9, a small error in phase may cause a significant error in resistance because rotation of the impedance vector about the origin amounts to a large change in resistance without a significant change in reactance. For the impedance Z_2 of Figure 9, small variations in phase will not have a significant effect on the overall accuracy of impedance.

The acoustic impedance meter is sensitive to changes of compliance, and these levels are consistent with levels expected in the human ear. The earlier study for impedance in the ear canal gives normal reactance levels starting at -600 cgs units at 200 hz and sloping upward with frequency (19). With ossicular discontinuity this level decreases to

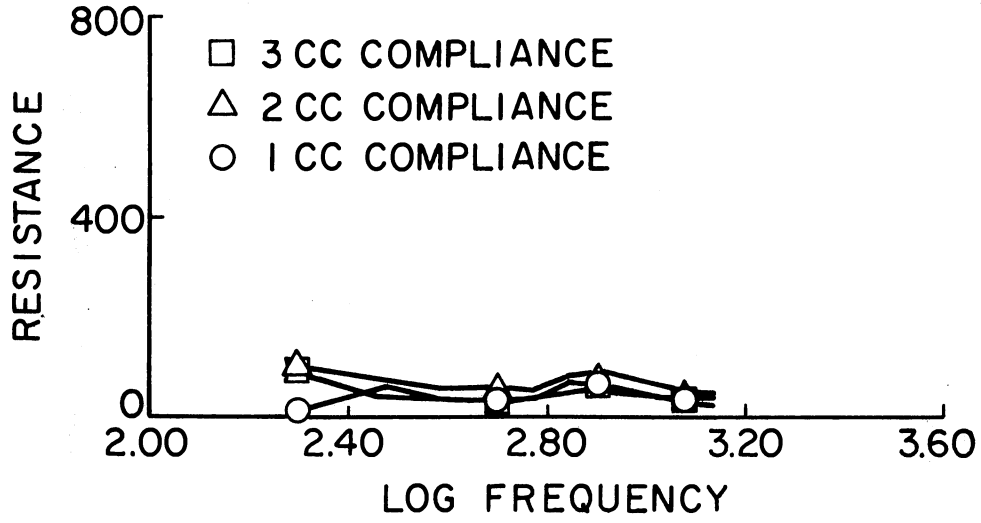

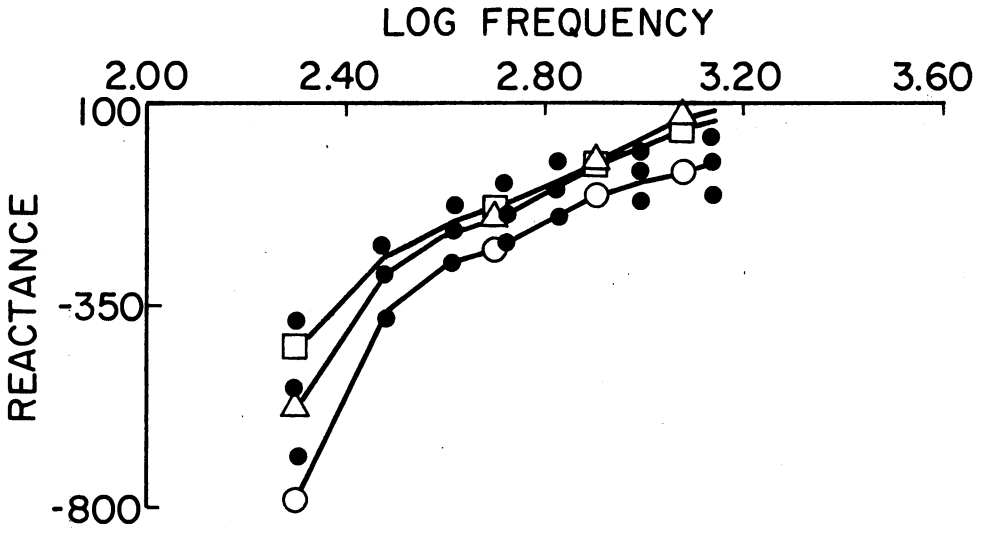

Figure 8. Test Results for Acoustical Compliance

about -1000 at 200 hz. The compliance sensitivity covers the expected ranges of impedance well.

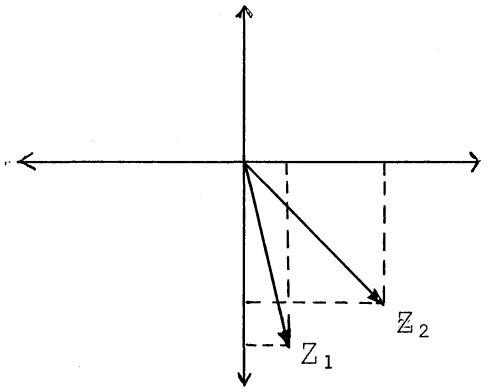

Figure 9. Demonstration of Phase Errors

Discussion

This acoustic impedance meter has two limitations. First, the upper frequency limit is about 1000 hz, relatively low for auditory application. This is because the assumed model for the microphone probe tube deviated significantly from data at frequencies higher than 1000 hz, as shown in Figure 6. This deviation might be reduced by improving the microphone probe tube model, or by shortening the probe tube to increase the frequency where resonance first occurs. The use of probe tubes is necessary because of size limitations in the ear, but if a microphone were available which was

small enough to fit into the ear canal beside a source without need for a probe tube, then this problem could be eliminated. Second, the phase angle voltmeter used in this study is accurate to within two degrees. This is adequate in measuring acoustic impedance at most frequencies, but when reactance is much higher than resistance these errors can have a large effect. These frequency dependent errors are demonstrated in Figure 9. The frequency range of reliable operation of this acoustic impedance meter is 200 hz - 1000 hz.

This frequency range is smaller than the 125 hz - 1500 hz frequency range of the Zwislocki bridge, although the frequency range of the Zwislocki bridge is sometimes reduced by its inability to measure inertance (4). While the frequency limitations of the Zwislocki bridge are inherent, the frequency limitations of this acoustic impedance meter are subject to design criteria, as the theory of operation does not depend on frequency. The frequency range of the acoustic impedance meter may be improved by miniaturization and by shortening or eliminating the probe tubes. This will increase the lowest frequency where resonance effects first occurs, thus allowing a higher frequency range.

Although the frequency range is relatively narrow, considerable detail is included by measuring impedance at several frequencies. Impedance profiles should offer improvements over static impedance measured at a single frequency because of the additional detail.

In summary, the theory of operation of the acoustic impedance meter is described. Sensitivity to changes of impedance are tested in the laboratory using the two acoustical elements which appear to be the most accurate; that is, acoustical compliance and infinite tube acoustical resistors. Results show that the acoustical impedance meter is sensitive to impedances which are expected in human ears. Further testing of the acoustic impedance meter in a clinical environment is necessary to establish whether audiology application is appropriate. In addition, consideration of impedance profiles as a diagnostic procedure is part of that clinical testing. Using a mathematical model, a preliminary investigation of impedance profiles in diagnosis is given in Chapter III.

CHAPTER III

MATHEMATICAL MODEL

Introduction

Consideration has not been given in the literature to the shape of impedance profiles and their relationship to the middle ear's physical properties (6). As a preliminary investigation of that concept this chapter describes simulations of middle ear pathology using a mathematical model. The mathematical model is designed to reproduce input acoustical impedance to the human ear with particular emphasis on the mechanical behavior of the eardrum and on the function of the middle ear muscles. The eardrum has been modeled with linear, lumped parameter elements in the past, but in light of mode shapes published by Bekesy (20) a distributed parameter system is more appropriate. The middle ear has been shown to possess high intensity nonlinear effects, but little is known about these effects (21). Even though a strong case can be established for the low-level linearity of the ear, hearing occurs over wide ranges of intensity, so nonlinearity is considered in the model (22).

Description of Model Parameters

Figure 10 shows the mathematical model along with the schematic drawing of the human ear. The ear canal probably has some damping and curvature associated with it, and the flexibility of the walls and presence of serumen might provide compliance and resistance. Since the precise nature of this effect is not known, the ear canal is modeled as a straight rigid tube with no damping.

The eardrum is very complex. According to Bekesy (20), it behaves mechanically like both a flat plate and a membrane. Toward the center near the region of connection to the malleus, the eardrum behaves like a rigid disk with no flexure. The malleus is connected to the eardrum all along the malleus length and rotates about a point near the ear canal above. This makes the eardrum vibrate asymmetrically. Moving toward the outer edge, the mass density and thickness decrease and flat plate flexural stiffness begins to have an effect, until at the point of attachment to the ear canal the eardrum behaves like a membrane (20).

To accurately model the eardrum, significant effects must be included. The asymmetry is probably not a significant effect since the input acoustical impedance depends on the average impedance. The varying eardrum properties may be a significant effect, but an accurate analysis of that case would be very difficult. As a compromise, the eardrum is modeled as follows. A rigid disk is connected to the malleus. Eardrum displacements are small, so malleus

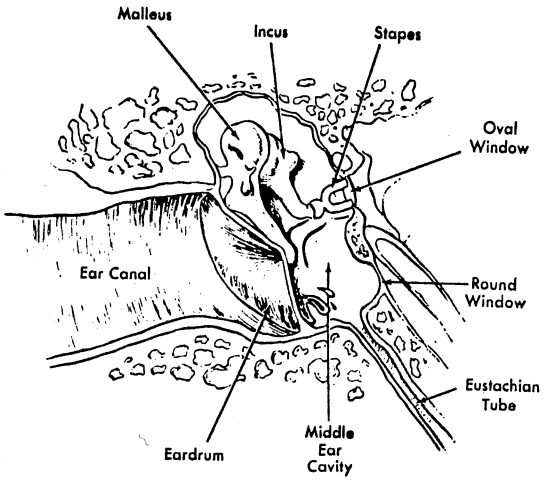

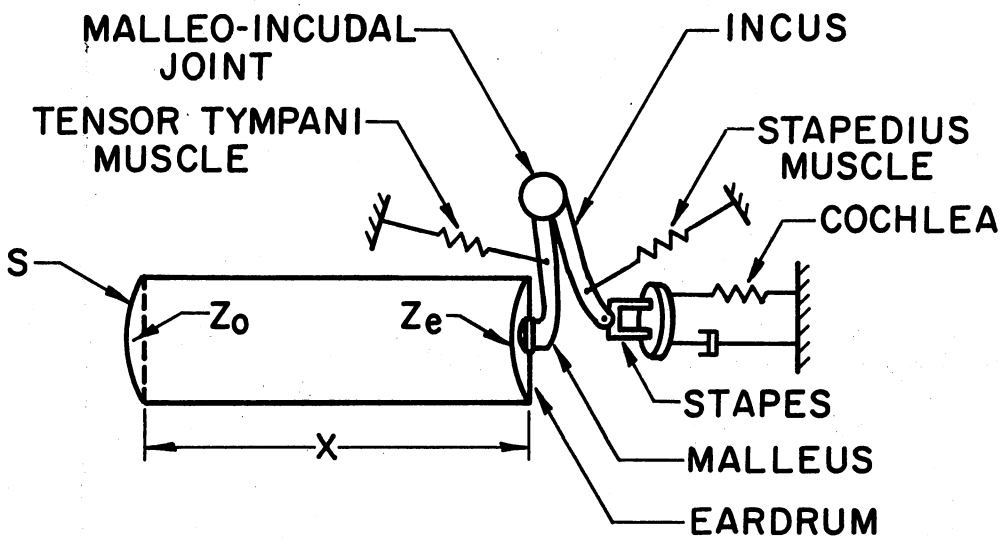

Figure 10. Schematic of the Ear (23) and Mathematical Model Configuration

rotation effects on the eardrum are neglected. An annular flat plate comprises the outer portion of the eardrum. Although the eardrum is conically shaped, it is felt that this is not a significant effect. At the outer edge of the eardrum, the membrane effect was modeled as a linear spring.

The effect of the middle ear cavity is assumed to be an acoustical capacitance. This is not shown directly on Figure 10 but is lumped with the stiffness effect of the ossicles. The ossicles are known to vibrate in at least three distinct stable modes, and their vibration is three-dimensional (20). For purposes of modeling the auditory system in terms of static acoustic impedance profiles, a two-dimensional model is assumed. The middle ear muscles are primarily a stiffness at intensities low enough to exclude the acoustic reflex (24). Therefore, the muscles are modeled as springs. Their static characteristics have not been measured for the human auditory muscles, but frog skeletal muscle data do exist (21) (22). It is assumed that these data are similar to those for a human. Two muscle spring models are formulated: (1) A linear model is included for debugging computer runs and also to investigate the validity of linear modeling; and (2) A nonlinear model is inlcuded because the above frog data is nonlinear (24).

The cochlea behaves primarily as a resistance (22). However, to provide simulation of otosclerosis a cochlear stiffness is also included. This stiffness effect is usually much smaller than the resistance, but pathological conditions

of the middle ear might cause it to become significant. This model of the auditory system should include sufficient detail for simulation of middle ear pathology. For details concerning eardrum boundary conditions, derivation of equation, and parameter selection, the reader is encouraged to consult Appendix A. Those details are beyond the scope of this discussion so are not given here.

The mathematical model described above was used to study possible nonlinear effects and to simulate middle ear pathological conditions as a preliminary consideration of impedance profiles in audiology.

Results and Discussion

Figure 11 compares typical impedance data collected on normal human ears with the impedance profile plots calculated for the linear and nonlinear mathematical models. There is a hump in the resistance curve at about 200 hz which has not been observed in data collected on human ears. Notice that the nonlinear ossicle model tends to reduce the height of that hump, indicating that the nonlinear ossicle model is closer to actual ear behavior than is the linear model. The mathematical model does not reproduce actual data as well as it was hoped; however, the object of this study is impedance profile changes associated with pathology.

The two attempted middle ear pathology simulations which were chosen on the basis of those pathologies anticipated in Chapter IV's clinical study are eardrum perforations and

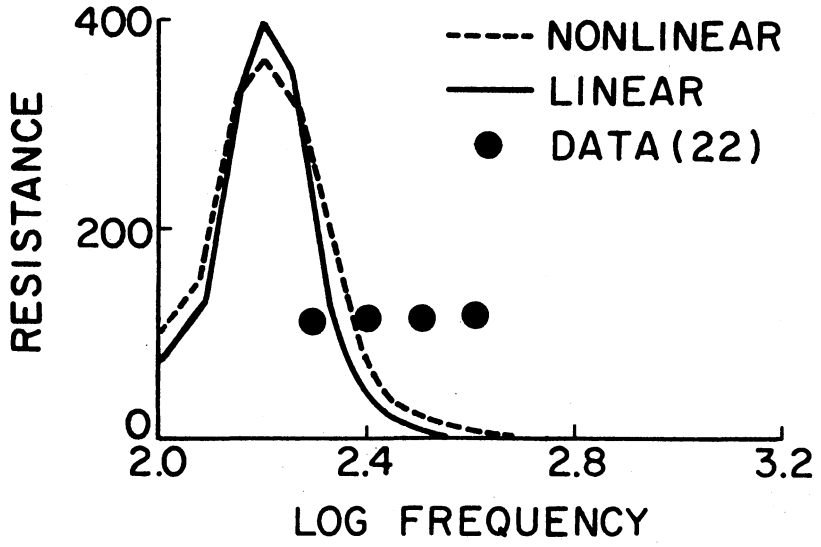

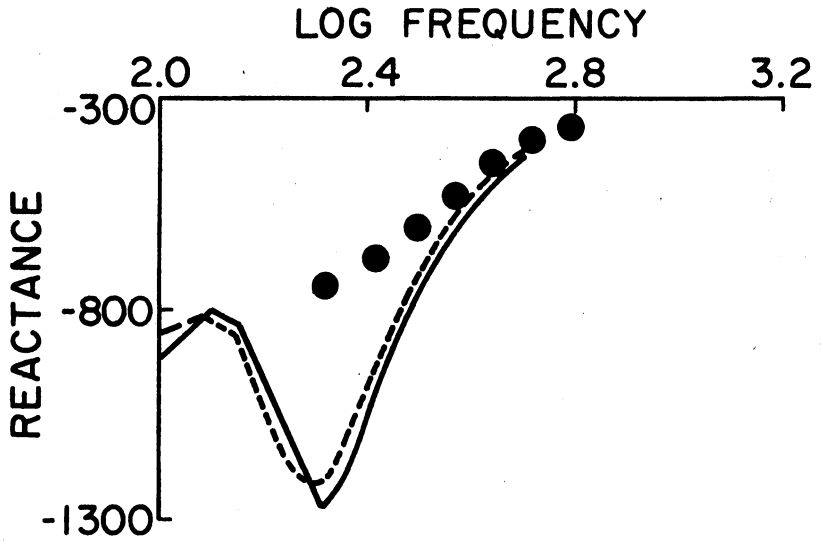

Figure 11. Linear and Nonlinear Models Compared With Data

serous otitis media. These two simulations are given in Figures 12 and 13, and for them the linear mathematical model was used. For perforations in the eardrum it is assumed that the primary dynamic effect is a reduced eardrum stiffness. By reducing the eardrum stiffness parameter a hole in the eardrum is simulated as shown in Figure 12. The resistance peaks sharply at low frequencies, but there is little effect on reactance. For serous otitis media it is assumed that the primary dynamic effect is an increased stiffness because of reduced middle ear cavity volume. By reducing the middle ear cavity volume serous otitis media is simulated. The change of impedance profile for this simulation is slight, as shown in Figure 13.

The purpose of this mathematical model is to support the concept of impedance profile shape as a diagnostic criterion. That purpose has been partially satisfied, as Figure 12 shows a difference in impedance profile shape with simulation of eardrum perforation. There is a large peak in resistance at low frequency without appreciable effect on reactance. For simulation of serous otitis media shown in Figure 13, however, there is little change in impedance profile. This may be because it was assumed that the dynamic effect of serous otitis media is only reduced middle ear cavity volume, but there may also be an addition of resistance. The mathematical model has no provision for middle ear resistance and does not accurately reproduce normal ear

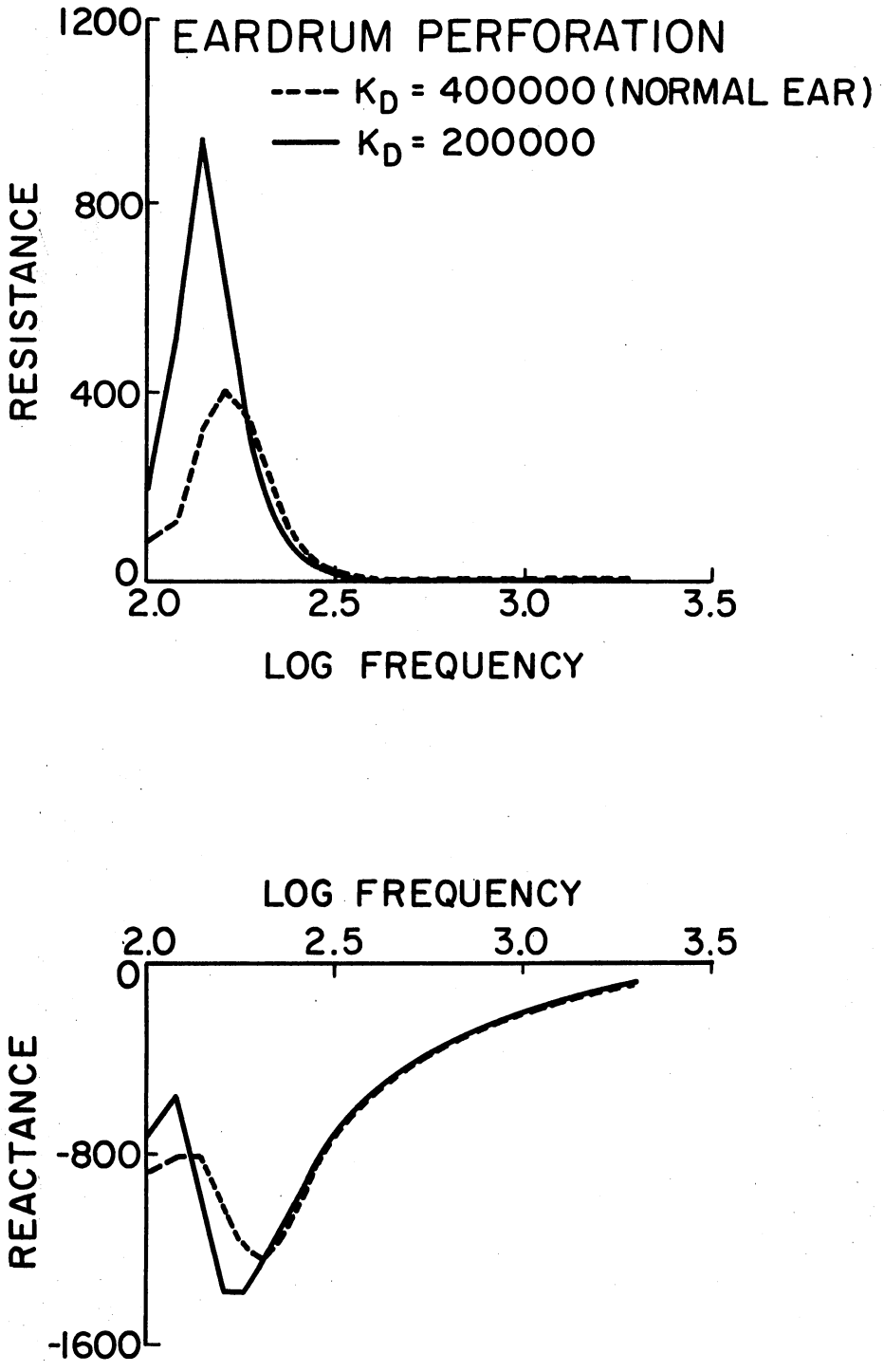

Figure 12. Eardrum Perforation Simulation

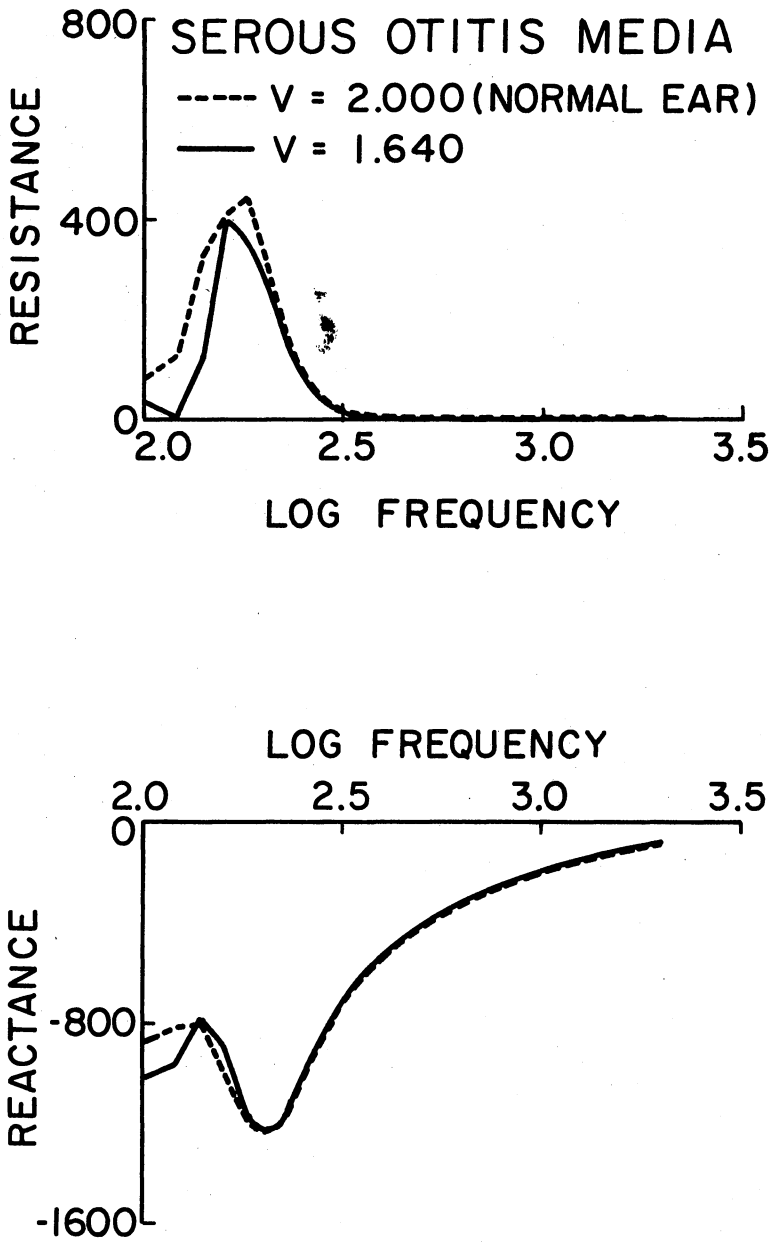

Figure 13. Serous Otitis Media Simulation

impedance. In addition, ability to simulate other middle ear pathologies has not been demonstrated.

In summary, there are two results of this preliminary study. First, the model exhibits differences between impedance profile shape of linear and nonlinear ossicular muscle models, suggesting that nonlinear behavior of these muscles may be important in hearing. Second, although the model did not accurately predict normal impedance profiles, differences in impedance profile shape related to the assumed dynamic effects of middle ear pathology were identified. These two results are preliminary support for impedance profile shape as a diagnostic tool. Experimental investigation of that concept is given in Chapter IV.

CHAPTER IV

CLINICAL STUDY

Introduction

As previously stated in Chapter I, the purpose of this dissertation has two parts: (1) to design and build an acoustic impedance meter capable of measuring impedance profiles; and (2) to investigate impedance profile shape and attempt to determine its diagnostic significance. The first part of that purpose was completed in the design and evaluation of the acoustic impedance meter described in Chapter II. Impedance profile shape as a potential diagnostic tool was partially investigated in Chapter III using a mathematical model of the ear, but impedance profiles should be experimentally evaluated. That experimental evaluation of impedance profiles is described in this chapter.

Two other aspects not previously considered are reported in this chapter: (1) The effect of distance from the impedance meter eartip to the eardrum is very important because shape differences due to the ear canal must be identified for impedance profiles to provide valuable information. (2) The effect of intensity variations below the acoustic reflex threshold should be considered as the nonlinear mathematical mathematical model used in this dissertation showed

variations in impedance profile with different intensity levels. Auditory nonlinearity is known to exist and is examined (21).

Procedure

The experimental evaluation was conducted by measuring impedance profiles on normal ears and on pathological ears and by comparing the profile shapes between the two groups. Ten subjects who had air and bone conduction pure-tone thresholds within normal limits comprised the normal hearing population. No subjects in the normal group had pure-tone air conduction thresholds greater than 10 DB bilaterally throughout the frequency range (250-8000 hz). The audiometer was calibrated to 1969 ANSI standards. The following subjects made up the pathological group: six cases of sensory neural hearing loss, four cases of otosclerosis, two cases of serous otitis media, two cases of radical mastoidectomy, and three cases of chronic otitis media with perforation. Audiograms and case history information were taken on the sensory neural population and on the subjects with middle ear pathology. This information may be found in Appendix C.

In testing each subject, the acoustic impedance meter was attached to the ear as demonstrated in Figure 15. The half-inch condenser microphone and probe tube, when unattached from the horn driver and reference microphone, may be easily fitted to an eartip. The eartips used were those already commercially available for use in tympanometry.

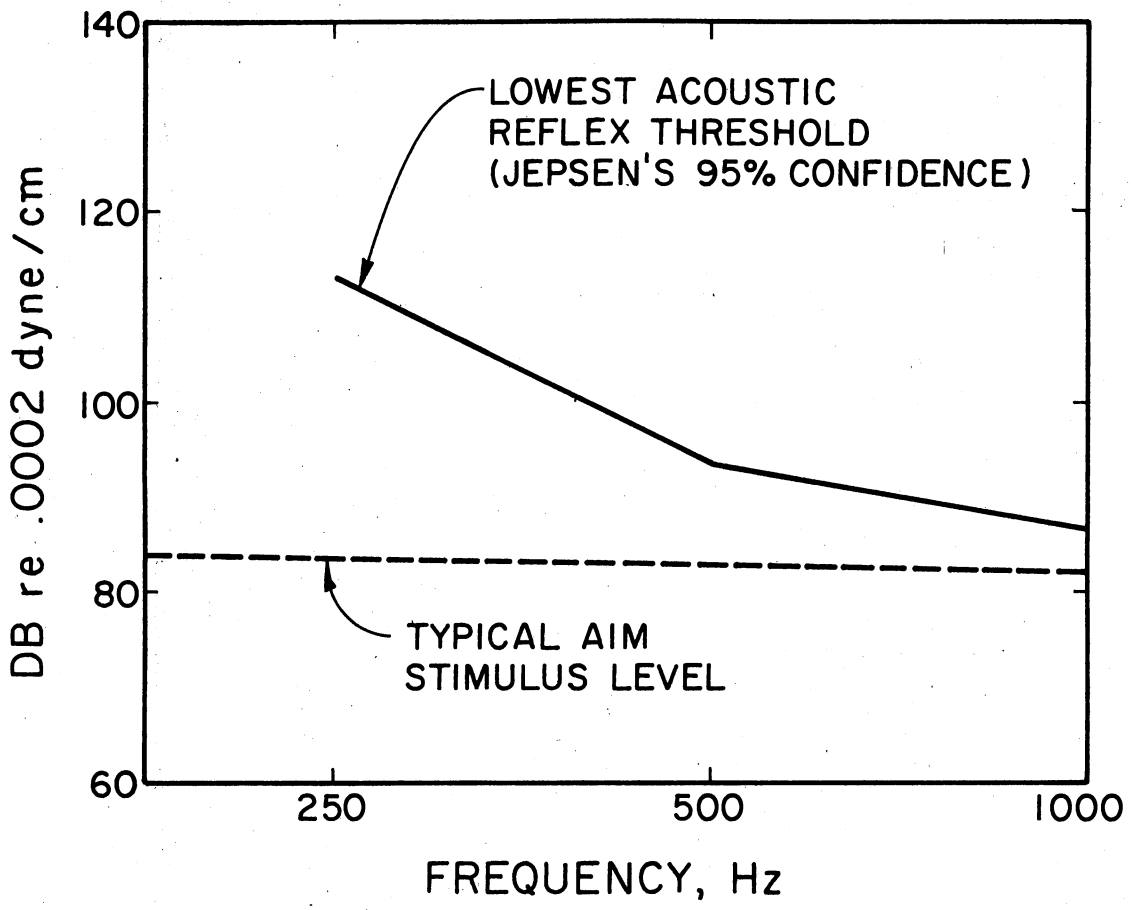

Figure 14. Minimum Acoustic Reflex Threshold

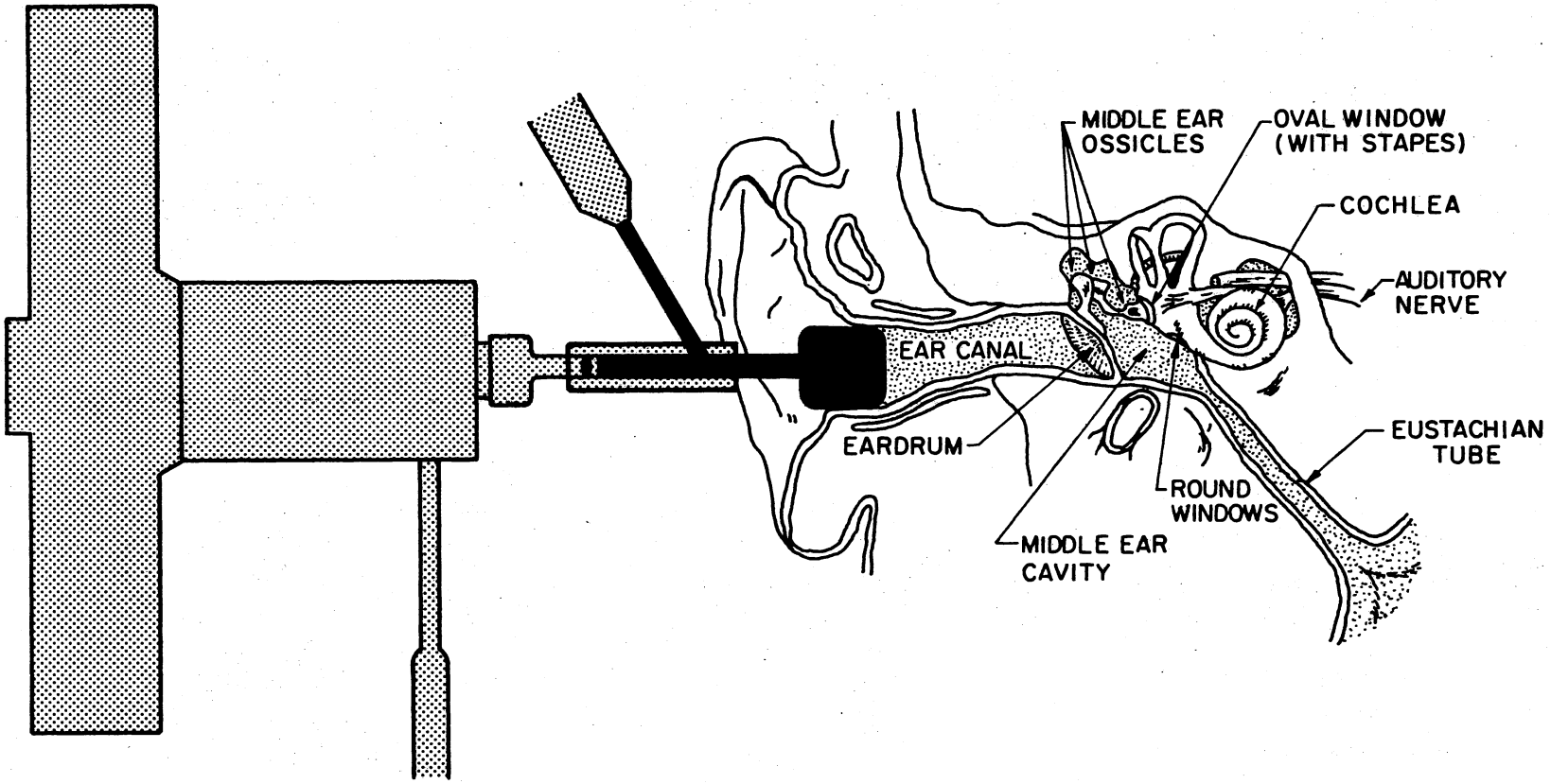

Figure 15. Schematic of Acoustic Impedance Meter Attached to a Human Ear

That eartip was then inserted into the ear canal, as in tympanometry. A dummy headset was used to hold the eartip in place, and the subject was seated in a dentist's chair as demonstrated in Figure 16.

Data was recorded using the form in Table IV of Appendix B. The third column of Table IV contains the probe microphone signal in DBV. By adding the numbers of column two to those of column three, one obtains the SPL inside the ear canal in DB. By continuous reference to Figure 14 one can assure that the acoustic reflex threshold is avoided.

Static acoustic impedance must be measured in the absence of the acoustic reflex. Therefore, the intensity level was monitored to assure that the stimulus intensity was below the minimum 95 percent confidence interval for the acoustic reflex threshold measured by Jepsen (25). Figure 14 is the plot of this threshold in decibels, along with a typical intensity level of the acoustic impedance meter. To minimize adaptation and fatigue every tonal presentation was limited in duration to 10 seconds followed by a 15-second rest (26).

The procedure for measurement of acoustic impedance is as follows. After the ear canal is cleared of serumen, the eartip probe tube is inserted into the ear canal and the rest of the acoustic impedance meter is attached to the eartip probe tube. Stimulus intensity level is checked at 200 hz and at 1000 hz to assure that it is below the minimum acoustic reflex threshold of Figure 14, and above the

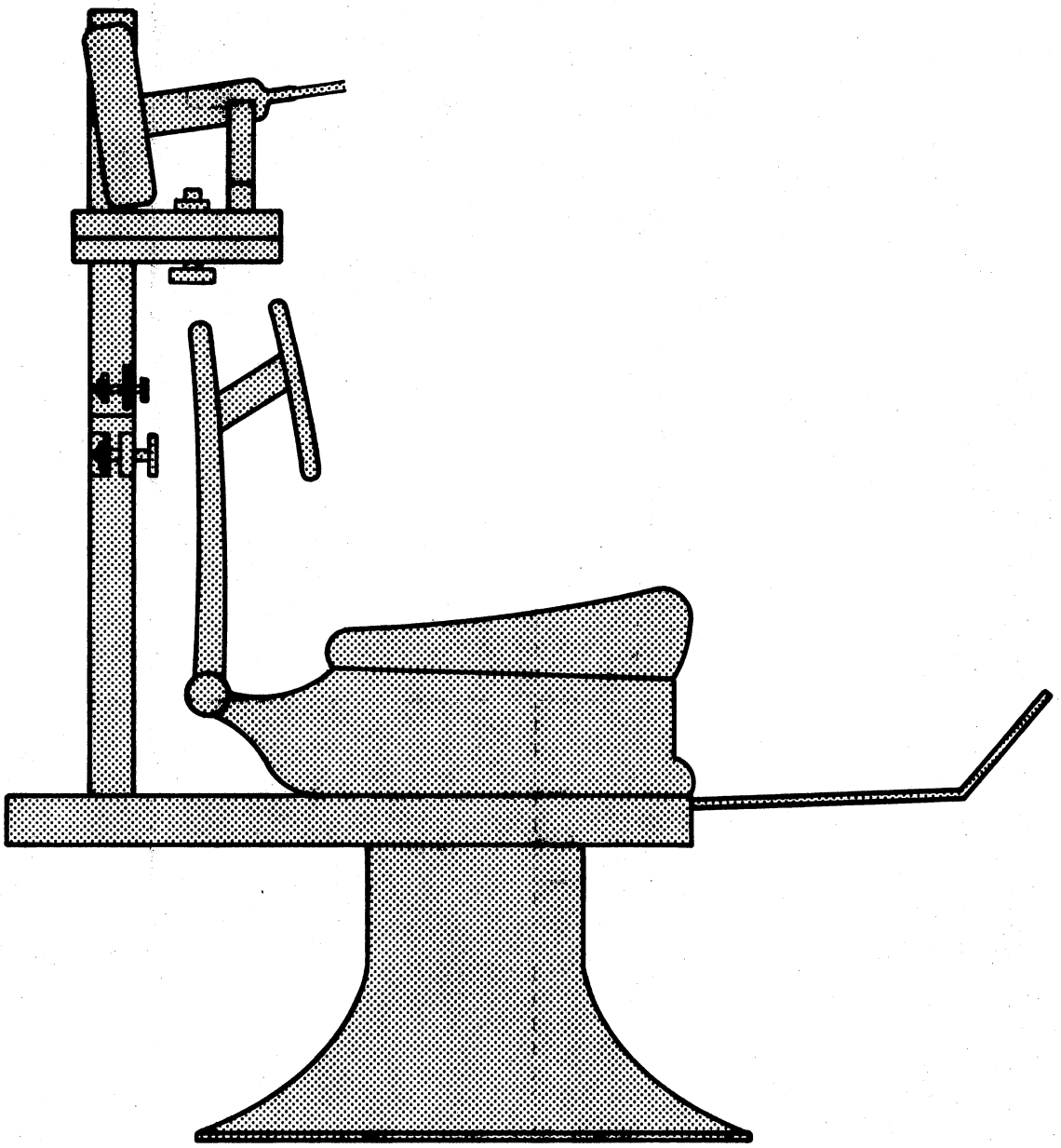

Figure 16. Dentist's Chair Used in the Clinical Study

internal noises (breathing, heart rate, etc.) of the human body. It is necessary to check intensity level at both 200 hz and 1000 hz because the stimulus intensity level and the acoustic reflex threshold depend on frequency. The stimulus tone is presented, and pressure and phase measurements are taken; then the stimulus tone is eliminated. Data is taken at nine different frequencies beginning at 200 hz and ending at 1000 hz, with increments of 100 hz. Data from Table IV is punched onto computer cards, and impedance is calculated using the computer program of Appendix B.

Results

The effect of distance from the eartip to the eardrum was investigated. For one of the normal hearing subjects an impedance profile was measured with placement of the eartip in both the nominal position and about three to five millimeters closer to the eardrum. This subject was chosen because the ear canal was approximately straight with constant cross-sectional area over the distance in question. Other subjects meeting this requirement were not found during the course of this study. Although results based on this experiment cannot be generalized, a preliminary indication may be obtained. As shown in Figure 17, the effect of distance to the eardrum on impedance profile appears to be limited to the variations at 200 hz. Therefore, it appears that the ear canal's effect is negligible at frequencies other than 200 hz.

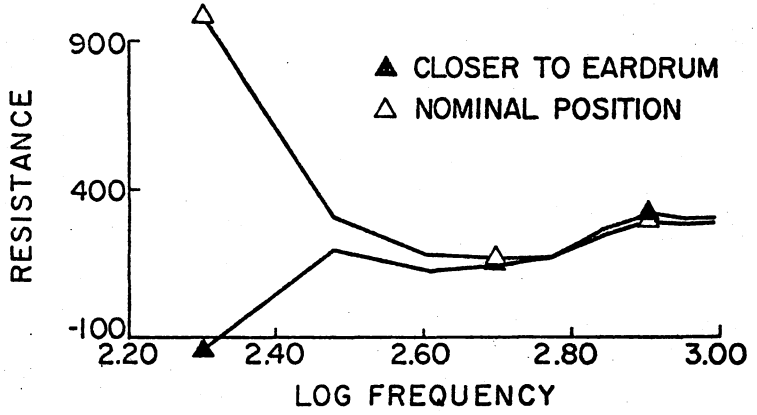

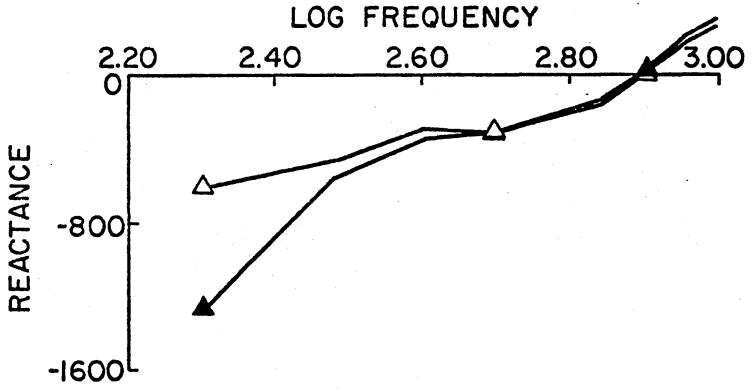

Figure 17. Effect of Distance to the Eardrum

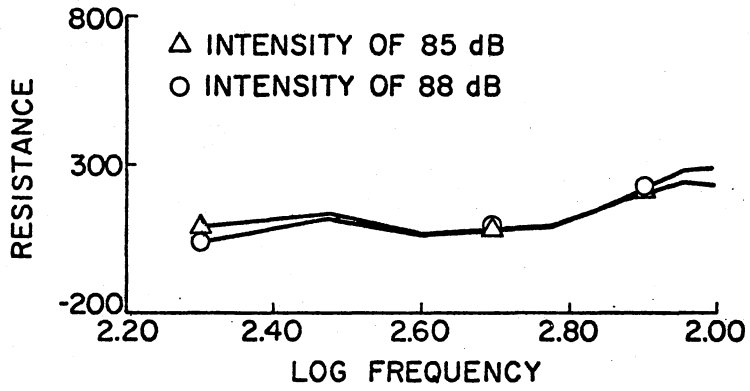

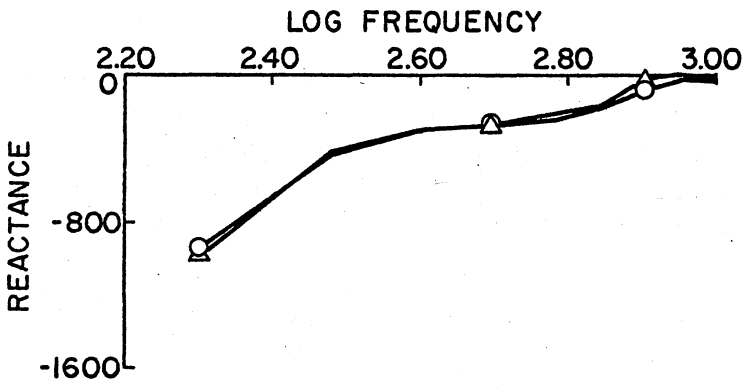

Figure 18. Effect of Intensity Level

Previous investigators have interpreted the ear canal's effect as pure compliance. Figure 17 shows a decreased capacitance because the eartip is closer to the eardrum, decreasing the ear canal's volume. There is also an increased resistance, especially at low frequencies. The amount of increased resistance shown in Figure 17 is not accurate, however, as errors in resistance associated with large stiffness (see Figure 9 in Chapter II) are present.

Although most researchers have used linear models of the ear and have assumed the ear to be approximately linear at moderate intensities, the nonlinear mathematical model used in this study shows impedance profile shape may depend on testing stimulus. In addition, while studying the different intensity levels used in testing, it appeared that impedance profile shape might depend on intensity level. That effect was investigated, and the result is shown in Figure 18. As shown in this figure, there is no appreciable dependence on stimulus intensity as long as the acoustic reflex is avoided. The mathematical model is in error in this respect.

A test was run to check the repeatibility of these impedance profiles. One of the normal hearing subjects was called back for a retest approximately two weeks after the first test. The high repeatibility between the two testing times is shown in Figure 21. This result is based on one subject and is intended as a preliminary indication, not as a general conclusion.

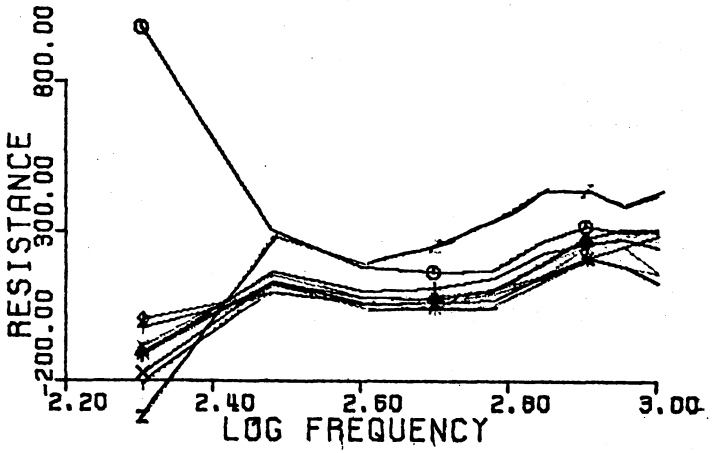

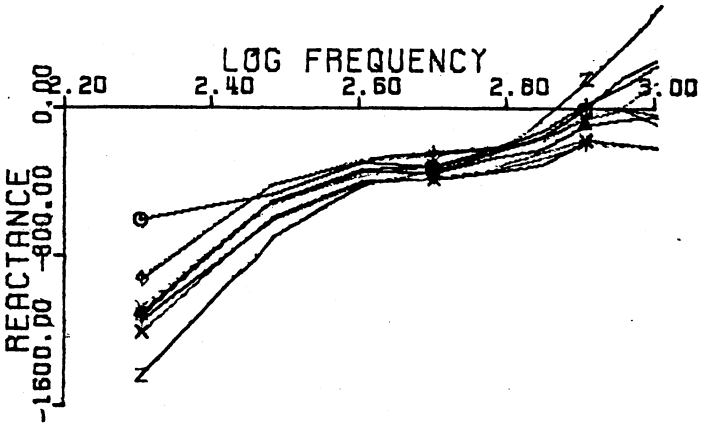

Figure 19. Impedance Profiles of Normal Human Ears

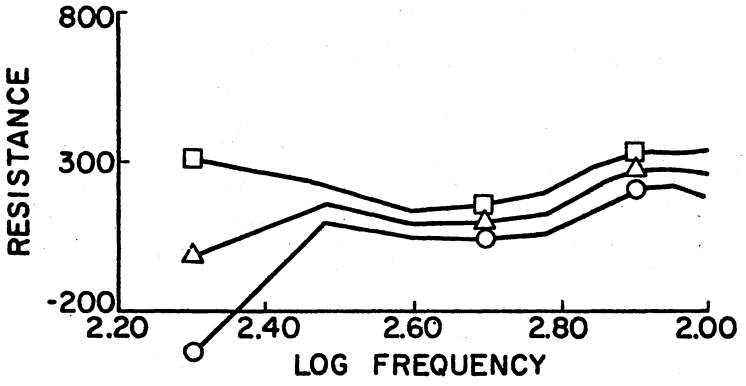

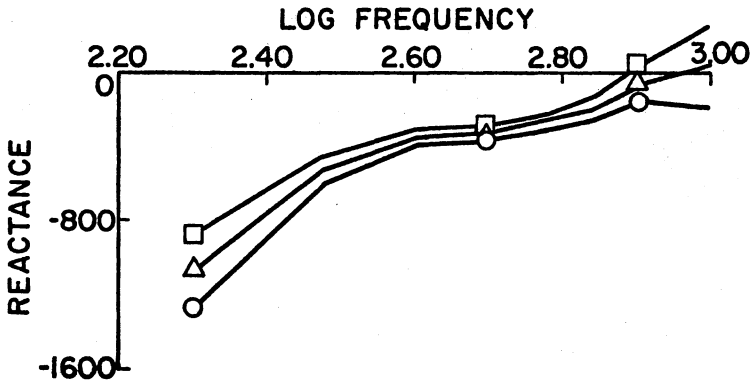

Figure 20. 99% Confidence Interval of Normal Impedance Profiles

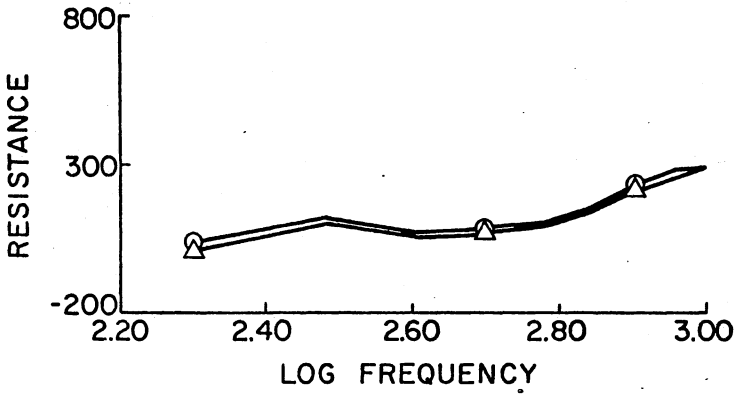

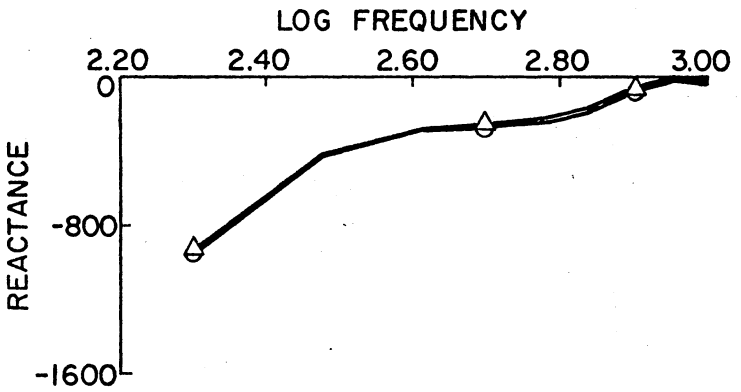

Figure 21. Repeatibility

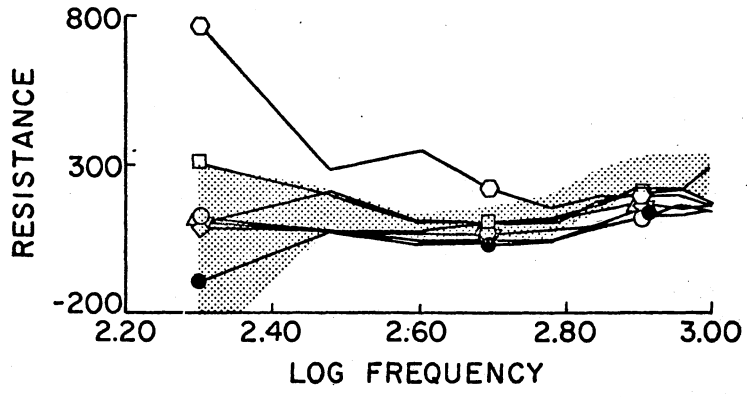

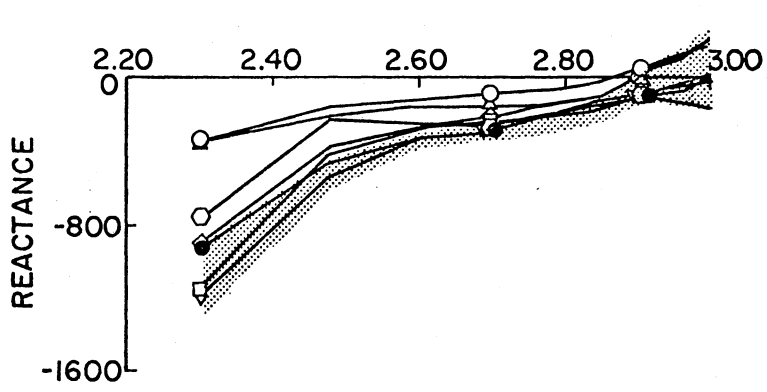

Figure 22. Ears With Sensory Neural Hearing Loss

The results of the tests run on normal ears are shown in Figures 19 and 20. Figure 19 is the plot of the ten normal impedance profiles. The variations at 200 hz are probably caused by variations of the distance from the ear-tip to the eardrum as shown in Figure 17. These data follow approximately the same shape. Figure 20 is a plot of the 90 percent confidence interval of the ten normal ears for hypotheses concerning two means. Statistical analysis of pathological cases for this small amount of data should be undertaken with caution, as there was usually only one of each pathology available (27). If the impedance profile for a pathological ear falls outside the 90 percent confidence interval at any frequency, then that impedance profile differs from normal with 90 percent confidence. For each pathology this confidence interval is shown on the impedance profile as a shaded area.

Impedance profiles of sensory neural ears are shown in Figure 22. The subjects with sensory neural hearing losses were between the ages of 34 and 57. With the exception of two, all had high frequency hearing losses, and most had a history of noise exposure. There was one case of Ménière's disease and one case of mild recurrent external otitis. The sensory neural population should have normal middle ears, and the profiles agree with normals of Figure 19.

With otosclerosis a bony growth appears around the stapes footplate. As otosclerosis progresses this bony growth enlarges in some cases until it reaches the incus,

causing increased resistance to the cochlea. The frequency dependence of otosclerosis is not known.

Four cases of otosclerosis were tested, and the impedance profiles are shown in Figure 23. Due to the wide variations in severity of otosclerosis between these subjects, they will be described individually. Subject EM of Figure 23a is 23 years old, has bilateral otosclerosis, and wears a hearing aid. There is some history of noise exposure, artillery fire during the war. The resistance is increased, indicating added cochlear resistance. Subject CH is 54 years old, and both eardrums show well-healed scars of sclerosis from childhood. This sclerosis was probably due to infection. The incus is immobile, and the diagnosis is bilateral clinical otosclerosis. The extent of otosclerosis of CH is worse than that of EM. Again, there is increased resistance. Subject RE is 44 years old and has a history of hearing loss in the family, the father and a brother both having hearing problems. RE has had significant hearing loss for many years. RE's otosclerosis is the most severe, and the increased resistance is more pronounced. The reactance is a very high inertance, indicating the presence of considerable growth. Subject HA is 69 years old and has clinical otosclerosis. Audiograms and case history information were taken on these subjects and are included in Appendix C.

The otosclerosis subjects of Figure 23 represent wide variations in the extent of disease. There are probably some variations because of the wide range in subjects' ages.

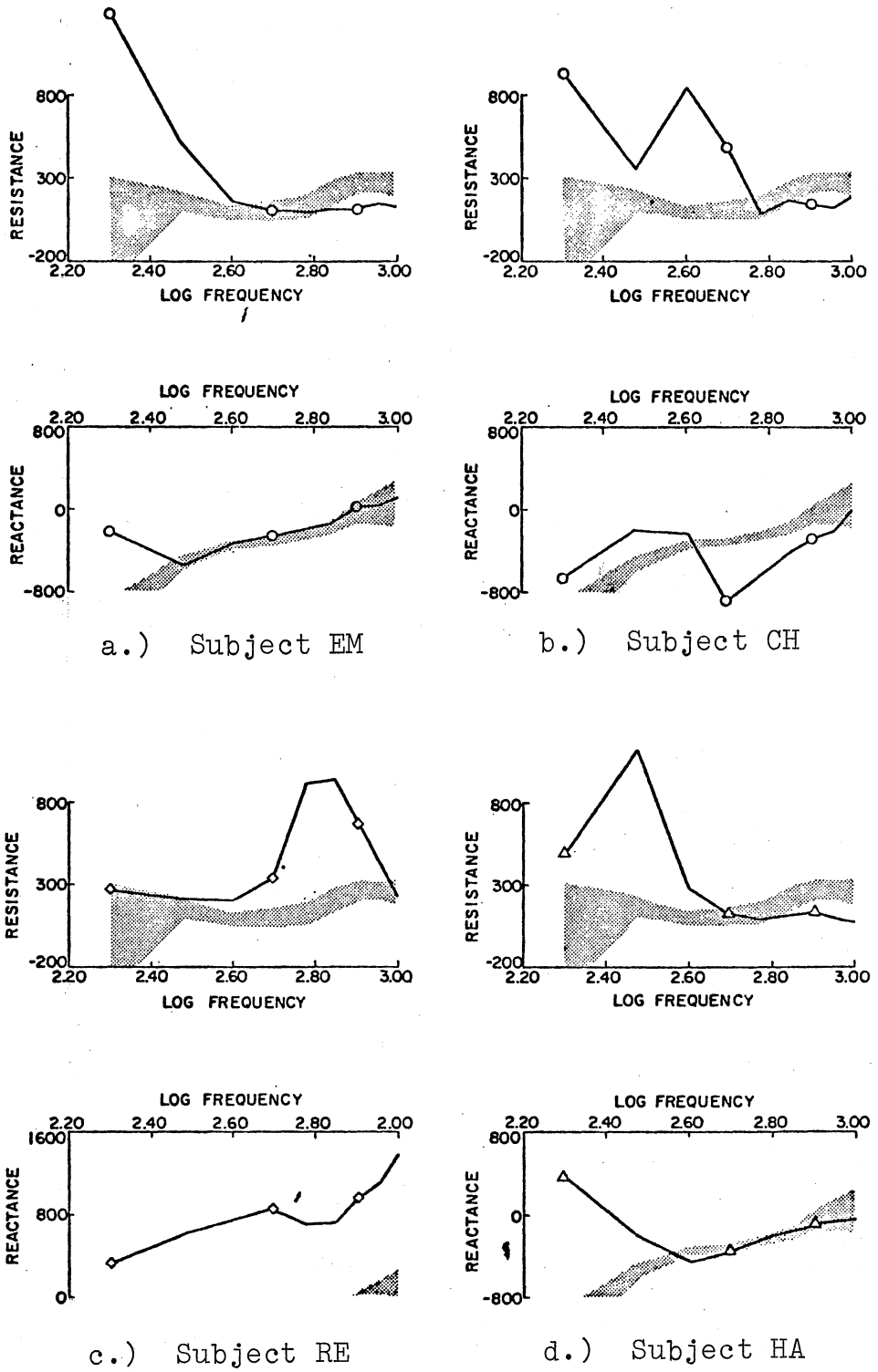

a.) Subject EM

b.) Subject CH

c.) Subject RE

d.) Subject HA

Figure 23. Results for Otosclerosis Compared With 90% Confidence Interval

Subject EM, who is 23 years old, does not have otosclerosis to the extent of the other three subjects. This is consistent with Figure 23a which shows that the impedance profile falls within normal limits at higher frequencies. Subject RE has the most severe case of otosclerosis, having had hearing loss for many years. Figure 23c shows an impedance profile well outside the normal limits. Subject CH's otosclerosis falls somewhere between EM and RE in degree of severity. Notice the differences between Figures 23a and 23c, the impedance profiles of the least and most severe cases, respectively. Due to insufficient information it is not possible to distinctly establish the severity of HA's otosclerosis, but it lies somewhere between EM and RE. Note that the peak in resistance occurs at different frequencies for the four cases, the least and most severe forming the lower and upper frequency bounds, respectively. This indicates that the peak in resistance may occur at a frequency which depends on the severity of otosclerosis. A changing natural frequency of the complex hearing mechanism might be the reason for this, but further investigation is necessary to verify that dependence.

Serous otitis media is a filling of the middle ear cavities with fluid. The two dynamic effects one might expect because of this are increased resistance and a change in stiffness. The stiffness might increase or decrease depending on whether the predominant dynamic effect is the bulk modulus of the fluid or the decreased volume of the

middle ear cavities. In addition, there may be dynamic effects of fluid moving with the eardrum. The mathematical model simulation of Chapter III was conducted under the assumption that a decreased middle ear volume is the predominant effect.

Subjects with serous otitis media are shown in Figure 24. The subject of Figure 24a is 64 years old and has a severe case of serous otitis media as indicated by the fluid level which is visible behind the eardrum. He had complained of tinnitus and has a sensory neural component to his hearing loss. Due to the age, presbycusis effects are probably also present which tend to stiffen the ossicular chain. The impedance profile of Figure 24a is well outside the 90 percent confidence interval at every frequency. The effect is a much higher resistance and either a lower stiffness or a higher inertance. Higher inertance is probably most likely because of the relatively large amount of fluid present. The second peak in resistance is probably due to the acoustic reflex. The reason for increased reactance is not readily apparent and is possibly a combination of reduced stiffness and increased inertance, probably caused by matter adhering to the eardrum and eardrum weakening.

The subject of Figure 24b is 44 years old and has chronic otitis media with a perforation in the eardrum. There is a history of noise exposure which is unrelated to the perforated eardrum. The anticipated dynamic effect is an increased resistance because of the presence of fluid and a

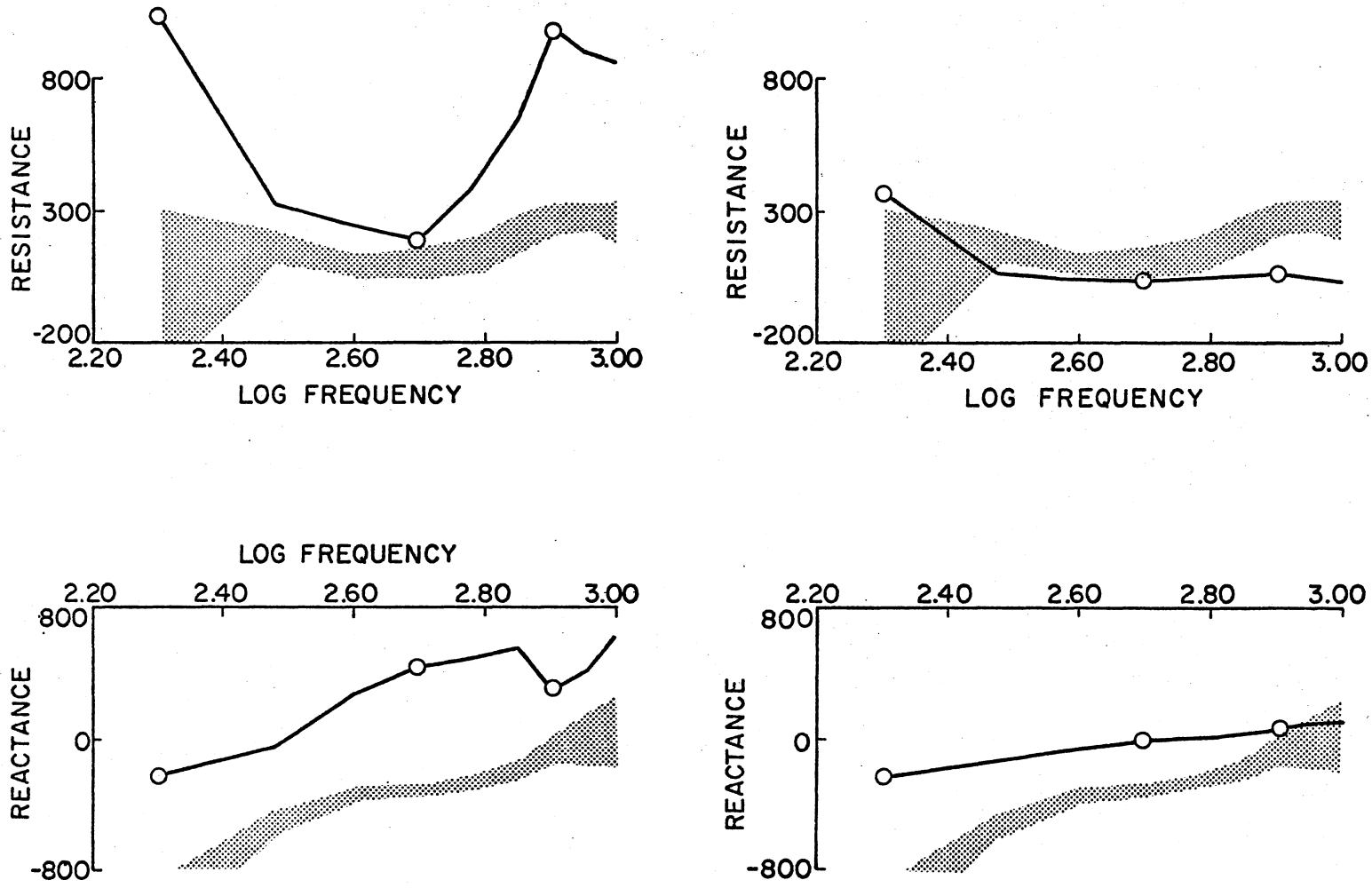

a.) Serous Otitis Media

b.) Mild Serous Otitis Media

Figure 24. Serous Otitis Media Compared With 90 Percent Confidence Interval

reduced stiffness because of the eardrum perforation. Since the subject's perforation is associated with chronic otitis media, the corrosive effect of the fluid provides additional weakening of the eardrum structure. The impedance profile of Figure 24b has a reduced stiffness; but surprisingly, the resistance also appears lower. Since the resistance still falls very close to the 90 percent confidence interval, it is not possible to identify it as a characteristic of this particular pathology.

The mathematical model of Chapter III was designed to show the impedance profile dependence on pathological conditions just discussed, but those model simulations reported earlier appear to have no relationship to the actual pathology. This is possibly because capacitance is not the primary effect of the middle ear cavity. This points out a limitation of the mathematical model, as other middle ear cavity effects cannot be simulated.

A mastoidectomy consists of surgical removal of portions of the middle ear cavity walls and mastoid. For radical mastoidectomy the ossicles are removed, while for modified radical mastoidectomy all or part of the ossicles are left intact. The eardrum is usually repaired during surgery. Ears on which a mastoidectomy was performed are of little interest in terms of predicting hearing loss since the medical history is available. However, in terms of establishing the sensitivity of the acoustic impedance meter to middle ear conditions and in terms of the effect of middle

ear components, mastoidectomy ears are quite valuable. One subject was tested who had a modified radical mastoidectomy, and one was tested who had a radical mastoidectomy. Both of these are shown in Figure 25. The effect of the reduced stiffness and inertance is obvious and differs from the effect of the increased inertance observed with serous otitis media. A decrease of stiffness is the effect of the enlarged middle ear cavities and loss of contact with the cochlea, but there appears to be little effect on the resistance. This suggests that the eardrum and ear canal have resistance. Both cases of mastoidectomy represent drastic changes in middle ear structure, and the impedance profiles fall well outside the 90 percent confidence interval.

The three subjects of Figure 26 are reported together because their impedance profiles look very similar and because they all have chronic otitis media with perforations. Subject HK is 44 years old and had a mastoidectomy at age 13. During recent surgery it was discovered that the incus was missing with a mucuous strand in its place. In addition the stapes was fixed. Subject EE is 24 years old and had a mastoidectomy at age 14. Hearing is deteriorating, and both ears have been draining for about one month. Subject WW has had drainage for several weeks. WW's age and complete case history are not available, but the approximate age is 35.

The profiles of these subjects are very similar to those for subjects who had mastoidectomies, possibly because two

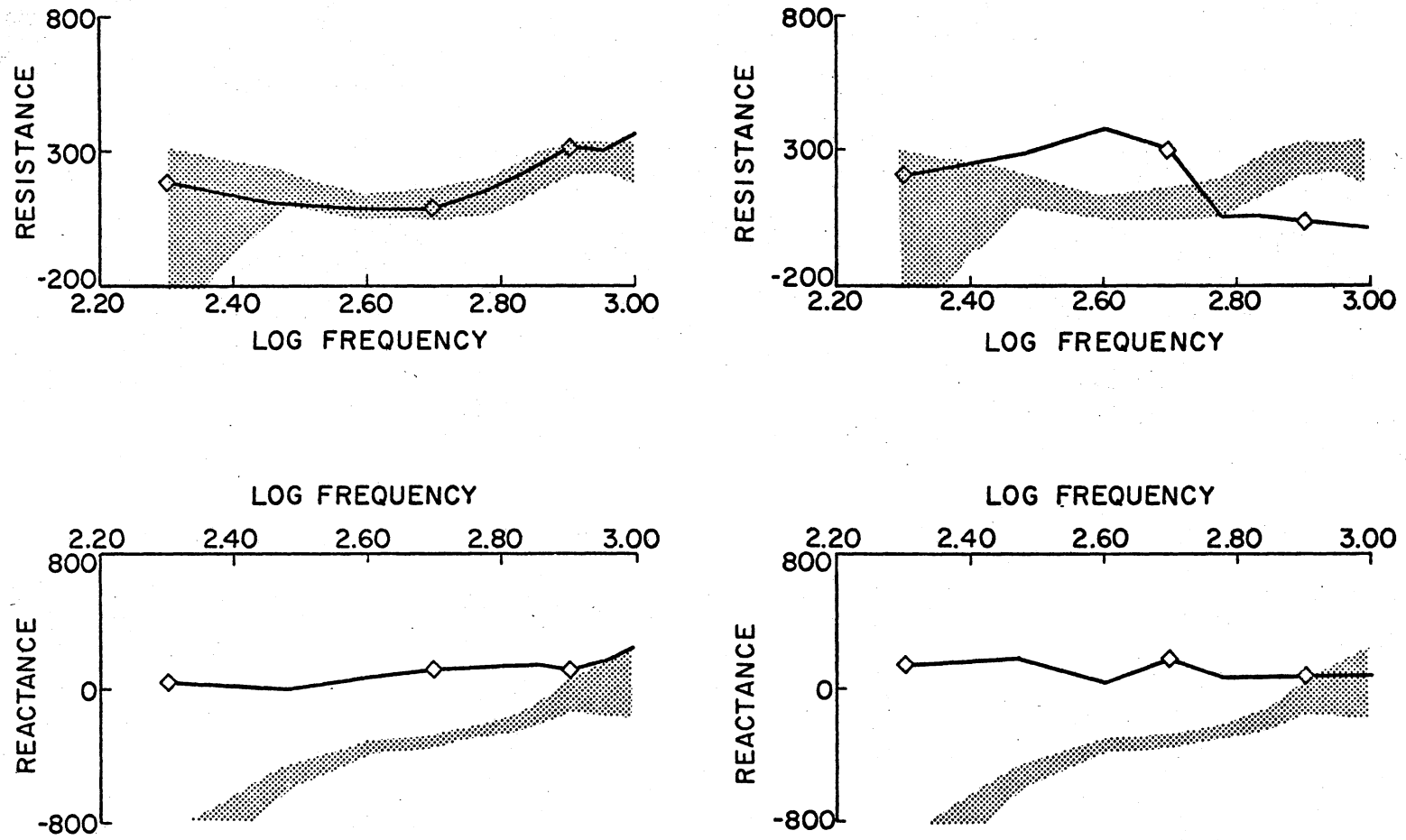

a.) Modified Radical

b.) Radical

Figure 25. Mastoidectomy Patients Compared With 90 Percent Confidence Interval

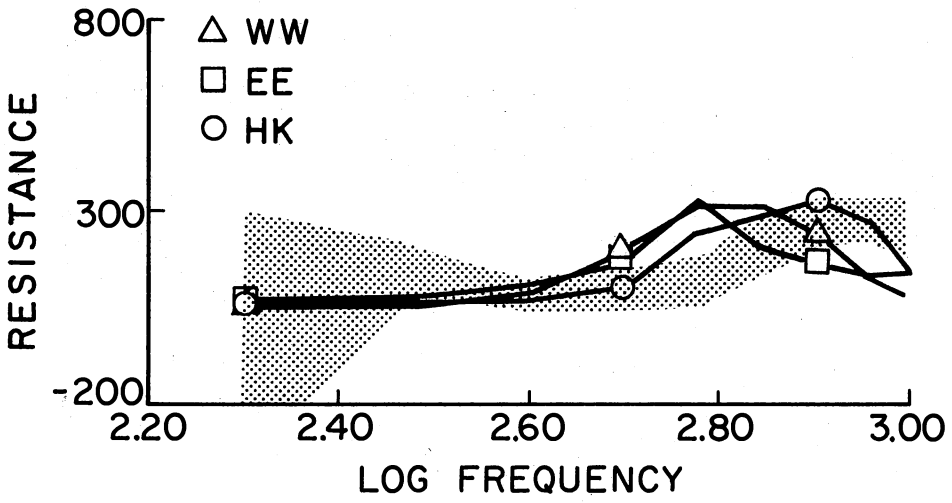

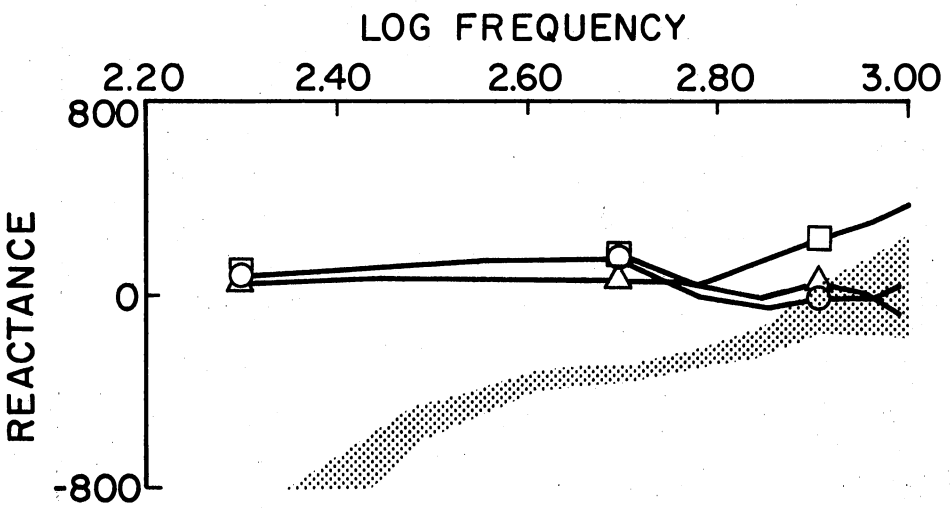

Figure 26. Eardrum Perforations Compared With 90% Confidence Interval

subjects have had mastoidectomies. This suggests that the eardrum undergoes the primary change since the eardrum perforation is the only thing all these ears have in common. The reduced stiffness occurs because of eardrum weakening. The resistance appears to be normal, but the peak at higher frequencies may be a distinguishing feature of eardrum perforation. All profiles fell outside the 90 percent confidence interval. It should be noted that the impedance profiles calculated on the mathematical model for eardrum perforations are similar to the actual pathology in that there is a peak in resistance. The model's reactance shows little change from normal.

Discussion

Sealing in static impedance profile tests is more difficult to identify than with tympanometry. Tympanometry is designed so that when the ear canal is pressurized a leak is immediately detectable by a leaking of the ear canal pressure. The one exception to this is in the case of a perforated eardrum, where a tympanometric seal is difficult. Such a pressurization is not part of the design of this acoustic impedance meter. It is possible to obtain a good seal with reasonable confidence by exercising care in the proper selection of eartip size and in the use of a petroleum jelly lubricant. A lubricant helps provide an airtight seal between the eartip and the ear canal. A faulty seal may be

identified by a very high mass reactance at low frequency or by a large negative resistance.

The clinical study shows two things: (1) Every tested pathological ear had an impedance profile which fell outside the 90 percent confidence interval for a normal ear. This is strong support for the concept of impedance profile shape as a diagnostic tool. (2) The acoustic impedance meter was shown to be capable of measuring acoustic impedance of human ears. Therefore, the dual purpose of this study was satisfied. The acoustic impedance meter was designed, calibrated, and tested. Then it was used in a clinical study which shows that impedance profiles possibly contain diagnostic information. However, the following two problems were encountered. First, it was not always possible to establish a distinct diagnosis before surgery was performed, thus making it difficult to draw conclusions. Second, the acoustic impedance meter's frequency range of operation is quite narrow. Other frequencies should be considered as significant hearing occurs at higher frequencies. In addition, the peaks in the resistance of the otosclerosis impedance profiles appear at different frequencies. It is possible that such peaks also occur at higher frequencies. Therefore, it would be desirable to be able to measure acoustical impedance at higher frequencies.

Considerable information is contained in the relatively narrow frequency range covered in this study. With conventional tympanometry static impedance is measured at a single

frequency, either 220 hz or 660 hz. As demonstrated in Figures 23a, 23d, and 24b the static impedance may appear normal at higher frequencies while at lower frequency there is significant deviation from normal. Thus static impedance profiles measured at several frequencies contain more information than static impedance measured at a single frequency.

Summary

Impedance profiles on ten normal hearing subjects were taken, and 90 percent confidence intervals were calculated. The acoustic impedance meter was shown to be capable of measuring impedance profiles of human ears. Impedance profiles of pathological ears were measured, and they all fell outside the 90 percent confidence interval.

Also, the following variables were checked: (1) repeatibility of impedance profiles from one day to another; (2) dependence on the intensity level of the stimulus tone; and (3) effect of the distance from the eartip to the eardrum. The indication is that none of these have a serious effect on the impedance profiles.

This clinical study shows that the acoustic impedance meter is sensitive to conditions of the middle ear and that those conditions might be reflected in the shape of an impedance profile. Therefore, the acoustic impedance meter appears to be valid for use in clinical audiology, but some improvements are necessary for application in further efforts. Suggestions for these improvements are listed in Chapter V.

CHAPTER V

CONCLUSIONS AND RECOMMENDATIONS

The two-fold purpose of this dissertation was to design an acoustic impedance meter and to investigate its clinical application by examining impedance profile shape as a diagnostic tool since this is an area of potential application of the acoustic impedance meter. That purpose was accomplished, and conclusions of this study are given below:

(1) The acoustic impedance meter was successfully designed and tested, showing improvements in measuring resistance, as well as the ability to measure inertance. Although the frequency range of this acoustic impedance meter is narrow, frequency range is subject to design, rather than being an inherent limitation as with bridges.

(2) Even though the mathematical model did not accurately reproduce acoustical impedance of the ear, it did show impedance profile dependence on middle ear parameters. For eardrum perforation the mathematical model showed increased resistance at a single frequency. Data collected on actual ears with eardrum perforations also showed resistance peaks.

(3) From the clinical testing it was concluded that every middle ear pathology tested had an impedance profile

which fell outside the 90 percent confidence interval. This shows that impedance profiles contain diagnostic information and that the acoustic impedance meter can measure impedance profile changes associated with middle ear pathology which makes them distinctly different from normal impedance profiles.

(4) The static impedance profiles measured and reported in Chapter IV contain inertance information heretofore unavailable because of limitations in previous methods of measuring acoustic impedance. For some normal ears, for two mastoidectomy cases, for three otosclerosis cases, for two serous otitis media cases, and for three chronic otitis media cases with perforations, the ear's reactance became positive. This condition could not have been handled with a bridge. The ability to measure inertance is probably more valuable in static impedance profiles than in tympanometry since tympanograms are measured at low frequencies where inertance information is less important.

(5) The ear canal's effect, approximated as a compliance in earlier studies of static impedance, was handled by measuring impedance profiles at two different distances of eartip insertion on a normal hearing subject. This eliminates the necessity for any assumptions as to the ear canal's dynamic effect because there appears to be no difference in impedance profile shape due to different distance to the eardrum above 200 hz.

(6) Impedance profiles measured over a given frequency range show improvements over static impedance measured at a single frequency because of additional frequency information, ability to measure inertance, and improved ability to measure resistance.

These six conclusions make impedance profiles appear viable as additional diagnostic tools. However, further study is needed in the following basic areas:

(1) A more extensive clinical study should be undertaken with particular consideration given to: (a) quality control of subject population and (b) sufficient patient population. First, maintaining adequate quality control on humans is very difficult, as the ability to determine the ear's exact condition is necessary. This is not always possible, since there may be varying degrees of a characterized disease or injury. It would be helpful to conduct studies on animals in conjunction with a clinical study of humans, since it is possible to vary components of animal ears much more easily than humans. The most promising study is the systematic investigation of a single pathology's impedance profile and its deviation from normal. Second, the qualitative analysis of many different pathologies and varying degrees of each pathology necessitates large amounts of data. It is suggested that any future study be conducted in cooperation with an ear surgeon, as the common treatment for many middle ear problems is surgery. In future clinical studies tympanometry should be a part of the research

procedure to provide equipment comparison capability and to provide all available information concerning each subject's hearing.

(2) Improvements in the mathematical model should be undertaken in the areas of: (a) the function of the eardrum; (b) the effect of the middle ear muscles; and (c) the development of a three-dimensional model. Perfecting this model is thought to be valuable because of the magnitude and complexity of the changes encountered while investigating the pathological effects on the ear's dynamic properties.

(3) The acoustic impedance meter should be modified in the areas of:

(a) Miniaturization.--Miniaturization will improve the method of interface with a human subject. In this respect the heavy horn driver and associated frame should be replaced with smaller equipment so that the acoustic impedance meter can be rigidly attached to the head. Miniaturization would also improve the upper frequency range which is governed by wavelength considerations. By making the acoustic impedance meter smaller, higher frequencies may be handled because the smaller dimensions allow a smaller wavelength and a higher frequency.

(b) Automation.--By using a mechanical drive to sweep the frequency and by designing appropriate control systems to monitor stimulus intensity levels, impedance profiles on humans may be collected more quickly.

Provision for instantaneous availability of the impedance profile would be a significant improvement. This might be accomplished through use of analog circuits which contain the appropriate calibration transfer functions. In this manner the associated computer programs would no longer be necessary.

(c) Calibration.--This could be undertaken either by improving the assumed transfer function or by using an alternate calibration method on which it is possible to estimate volume velocity flowing into the probe tube.

The two-fold purpose of this dissertation has been satisfied. Impedance profiles measured with the acoustic impedance meter described in this dissertation appear to be potentially valuable as diagnostic tools as they were shown to be sensitive to middle ear conditions.

SELECTED BIBLIOGRAPHY

(1) Beranek, L. L. Acoustical Measurements. New York: Wiley, 1949.

(2) Pinto, L. H., and P. J. Dallos. "An Acoustic Bridge for Measuring the Static and Dynamic Impedance of the Eardrum." IEEE Transactions on Bio-Medical Engineering, Vol. BME-15, No. 1 (1968), 10-16.

(3) Salava, T. "Sources of the Constant Volume Velocity and Their Use for Acoustic Measurements." Journal of the Audio Engineering Society, Vol. 22, No. 3 (1974), 146-153.

(4) Zwislocki, J. "An Acoustic Method for Clinical Examination of the Ear." Journal of Speech and Hearing Research, Vol. 16 (1963), 303-314.

(5) Nixon, J. C., and A. Glorig. "Reliability of Acoustic Impedance Measures of the Eardrum." Journal of Auditory Research, Vol. 4 (1964), 261-276.

(6) Lilly, D. J. "Measurement of Acoustic Impedance at the Tympanic Membrane." Modern Developments in Audiology. J. Jerger, ed., 2nd ed. New York: Academic Press, 1973, 115-137.

(7) Metz, O. "The Acoustic Impedance Measured on Normal and Pathological Ears." Acta Oto-Larnygologica Supplementum, Vol. 63 (1946), 1-246.

(8) Feldman, A. S. "Acoustic Impedance Measurement as a Clinical Procedure." Journal of International Audiology, Vol. 3 (1964), 156-166.

(9) Feldman, A. S. "Acoustic Impedance Studies of the Normal Ear." Journal of Speech and Hearing Research, Vol. 10 (1967), 165-176.

(10) Feldman, A. S. "A Report of Further Impedance Studies of the Acoustic Reflex." Journal of Speech and Hearing Research, Vol. 10 (1967), 616-622.

(11) Jerger, J. "Clinical Experience With Impedance Audiometry." Archives of Otolaryngology, Vol. 92 (1970), 311-324.

(12) Coles, R. R. A., and A. R. D. Thornton. "Auditory Research in the I.S.V.R.'s First Decade." Journal of Sound and Vibration, Vol. 20, Pt. 3 (1973), 37.

(13) Zwislocki, J. "Analysis of the Middle Ear Function. Part I: Input Impedance." Journal of the Acoustical Society of America, Vol. 34, No. 8, Pt. 2 (1962), 1514-1523.

(14) Onchi, Y. "Mechanisms of the Middle Ear." Journal of the Acoustical Society of America, Vol. 33 (1961), 794-805.

(15) Moller, A. R. "Transfer Function of the Middle Ear." Journal of the Acoustical Society of America, Vol. 35, No. 10 (1963), 1526-1534.

(16) Stamatinos, S. G. "A Mathematical Model of the Human Ear." (Unpublished M. S. Thesis, University of Florida, 1974.)

(17) Shearer, J. L., A. T. Murphy, and H. H. Richardson. Introduction to System Dynamics. Reading, Massachusetts: MIT Press, 1964, 350.

(18) Bruel and Kjaer. Instructions and Applications One-Half Inch Condenser Microphones, Types 4133, 4134, 4147. New York: Bruel and Kjaer, 1971, 55.

(19) Morton, J. Y., and R. A. Jones. "The Acoustical Impedance Presented by Some Human Ears to Hearing Aid Earphones of the Insert Type." Acustica, Vol. 16 (1956), 339-345.

(20) Bekesy, G. V. Experiments in Hearing. New York: McGraw-Hill, 1960.

(21) Goldstein, J. L. "Auditory Nonlinearity." Journal of the Acoustical Society of America, Vol. 41, No. 3 (1967), 676-689.

(22) Dallos, P. J. The Auditory Periphery Biophysics and Physiology. New York: McGraw-Hill, 1973.

(23) Denes, P. B., and E. N. Pinson. The Speech Chain. New York: Bell Telephone Laboratories, 1963, 68.

(24) Bahler, A. S. "Series Elastic Component of Mammalian Skeletal Muscle." American Journal of Physiology, Vol. 213, No. 6 (1967), 1560-1564.

(25) Jepsen, O. "Middle Ear Muscle Reflexes in Man." Modern Developments in Audiology. J. Jerger, ed., 1st ed. New York: McGraw-Hill, 1963, 125-143.

(26) Ventry, I. M., J. B. Chaiklin, and R. R. Dixon, eds. Hearing Measurement A Book of Readings. New York: McGraw-Hill, 1971.

(27) Miller, I., and J. E. Freund. Probability and Statistics for Engineers. New Jersey: Prentice-Hall, 1965, 166.

(28) Kinsler, L. E., and A. R. Frey. Fundamentals of Acoustics. New York: Wiley, 1962, 201.

(29) Morse, P. M. Vibration and Sound. New York: McGraw-Hill, 1948, 203.

(30) Timoshenko, S. Theory of Plates and Shells. New York: McGraw-Hill, 1940, 58.

(31) McLachlan, N. W. Bessel Functions for Engineers. Oxford: Clarendon Press, 1955.

(32) Hung, I. J. "A Study of the Dynamics of the Acoustic Reflex in Human Beings." (Unpublished Ph.D. Thesis, Northwestern University, 1972.)

(33) Dallos, P. J. "Dynamics of the Acoustic Reflex: Phenomenological Aspects." Journal of the Acoustical Society of America, Vol. 36, No. 11 (1964), 2175-2183.

(34) Price, G. R. "Upper Limit to Stapes Displacement: Implications for Hearing Loss." Journal of the Acoustical Society of America, Vol. 56, No. 1 (1974), 195-197.

(35) Bahler, A. S., J. T. Fales, and K. L. Zierler. "The Dynamic Properties of Mammalian Skeletal Muscle." Journal of General Physiology, Vol. 51 (1968), 369-384.

(36) Bahler, A. S. "Modeling of Mammalian Skeletal Muscle." IEEE Transactions on Bio-Medical Engineering, Vol. BME-15, No. 4 (1968), 249-257.

(37) Hill, A. V. "The Heat of Shortening and the Dynamic Constants of Muscle." Proceedings of the Royal Society, B-126 (1938), 136-195.

APPENDIXES

APPENDIX A

MATHEMATICAL MODEL EQUATIONS

The equation that represents input impedance to a rigid-walled tube of length x with a known impedance Z_e at the other end is (28)

$$Z_o = \frac{\rho_a C_a}{S} \cdot \frac{Z_e + j\rho_a C_a \tan K_a x}{\frac{\rho_a C_a}{S} + jZ_e \tan K_a x} \quad . \tag{1}$$

In Equation (1) the following definitions are necessary:

ρ_a = density of air

C_a = speed of sound in air

ω = frequency, radians/second

K_a = ω/C_a

S = cross-sectional area of the tube.

Z_e is described below.

Acoustical impedance of the eardrum may be obtained by solving for the average transverse velocity of the annular plate and connecting ossicles and forming the ratio of pressure to volume velocity. The starting point is to solve for plate transverse displacement. Velocity is just the time derivative of displacement.

The equation of motion for a flat plate is (29)

$$\frac{\partial^2 y}{\partial t^2} = - C^2 \nabla_r^4 y + \frac{P}{\sigma} e^{j\omega t} + j\frac{\omega R}{\sigma} \bar{y} \quad . \tag{2}$$

The following definitions are necessary:

$$\nabla_r^4 = \left(\frac{\partial^2}{\partial r^2} + \frac{1}{r}\frac{\partial}{\partial r} + \frac{1}{r^2}\frac{\partial^2}{\partial \theta^2}\right)\left(\frac{\partial^2}{\partial r^2} + \frac{1}{r}\frac{\partial}{\partial r} + \frac{1}{r^2}\frac{\partial^2}{\partial \theta^2}\right)$$

$$C^2 = \frac{t^3 E}{12\sigma(1-\nu^2)} \quad , \quad \bar{y} = \int_d^b 2\pi r\, \psi_c(r)\, dr\, e^{j\omega t}$$

$\psi_c(r)$ = homogeneous solution of Equation 2

σ = mass per unit area of the plate

E = modulus of elasticity

ν = Poisson's ratio

P = pressure forcing function

d = inner radius of annular plate

b = outer radius of annular plate.

(See Figure 27.) To solve this equation the method of separation of variables is used. Assume a solution of the form $y(r,t) = \psi(r)e^{j\omega t}$. Substituting this into Equation (2) yields

$$(\nabla_r^4 - K^4)\,\psi(r) = \frac{P}{\sigma C^2} + j\omega\,\psi_{ave}\,\frac{R}{\sigma C^2}$$

where

$$K^4 = \frac{\omega^2}{C^2}$$

$$\psi_{ave} = \bar{y}e^{-j\omega t} \quad .$$

This fourth order, linear, ordinary differential equation has the homogeneous solution of the form

$$\psi_c(r) = A_1 J_0(Kr) + A_2 Y_0(Kr) + A_3 I_0(Kr) + A_4 N_0(Kr) \quad ,$$

where

$J_n(Kr)$ = Bessel function of the first kind, nth order

$Y_n(Kr)$ = Bessel function of the second kind, nth order

$I_n(Kr)$ = modified Bessel function of the first kind, nth order

$N_n(Kr)$ = modified Bessel function of the second kind, nth order.

The particular solution to the differential equation is

$$\psi_p(r) = \frac{-P}{K^4C^2\sigma} - j\,\frac{\omega R}{K^4C^2\sigma}\,\psi_{ave} \quad .$$

The complete solution is the sum of the homogeneous solution and the particular solution

$$\begin{aligned}\psi(r) = {} & A_1J_0(Kr) + A_2Y_0(Kr) + A_3I_0(Kr) + A_4N_0(Kr) \\ & - \frac{P}{K^4C^2\sigma} - j\,\frac{\omega R}{K^4C^2\sigma}\left[A_1J_0(Kd) + A_2Y_0(Kd)\right. \\ & + A_3I_0(Kd) + A_4N_0(Kd) + \frac{2}{K^2(b^2-d^2)}\{A_1K(bJ_1(Kb) \\ & - dJ_1(Kd)) + A_2K(bY_1(Kb) - dY_1(Kd)) \\ & + A_3K(bI_1(Kb) - dI_1(Kd)) + A_4K(bN_1(Kb) \\ & \left. - dN_1(Kd))\}\right] \quad . \end{aligned} \tag{3}$$

The arbitrary constants A_1, A_2, A_3, and A_4 may be solved for provided there are four boundary conditions. These are discussed below. From Figure 27, the four boundary conditions are applied at the two radii of the annual plate.

(1) At r = d, $d\psi/dr = 0$. This is because the flat plate is fixed to the malleus handle at that point; thus the slope is zero.

(2) At r=d, Newton's second law of motion must hold for the malleus disk whose free body diagram is shown in Figure 28.

In Figure 28 the following definitions are necessary:

$$Q = \frac{Et^3}{12(1-\nu^2)} \frac{\partial}{\partial r} \nabla_r^4 y \qquad (30)$$

K_{me} = effective stiffness of middle-ear cavities

$$= \frac{\rho_a C_a}{V_{me}}$$

ρ_a = density of air in middle-ear cavities

C_a = speed of sound of air in middle-ear cavities

V_{me} = volume of middle-ear cavities

Z_m = mechanical input impedance to ossicular chain

$$y_{ave} = y(r,t)\Big|_{r=d} + \frac{1}{\pi b^2 - \pi d^2} \int_d^b 2\pi r\, \psi(r)\, dr\, e^{j\omega t}$$

y_{ave} represents the volume change of the ear cavity. The application of Newton's law yields

$$P\pi d^2 e^{j\omega t} - 2\pi d Q - Z_m \frac{\partial y}{\partial t} - K_{me}\, y_{ave}\, (\pi b^2)^2 = M_e \frac{\partial^2 y}{\partial t^2} \quad ,$$

where M_e is the effective mass of the malleus disk connected to the eardrum.

(3) At r=b, there is shear which is produced by the membrane effect of the eardrum, modeled as a spring. Referring to Figure 29, this force balance may be obtained from that free body diagram. This boundary condition is

$$2\pi b Q = K_d\, y(r,t)\Big|_{r=b} \quad ,$$

where K_d is the effective spring constant of the outer portion of the eardrum.

(4) At r=b, the eardrum behaves mechanically like a membrane - membranes have no stiffness and cannot support a

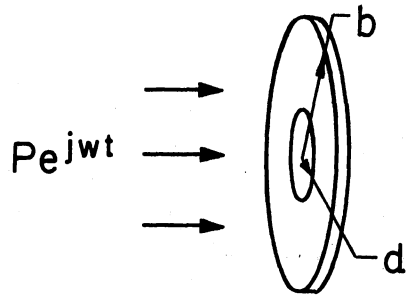

Figure 27. Annular Flat Plate Model of the Eardrum

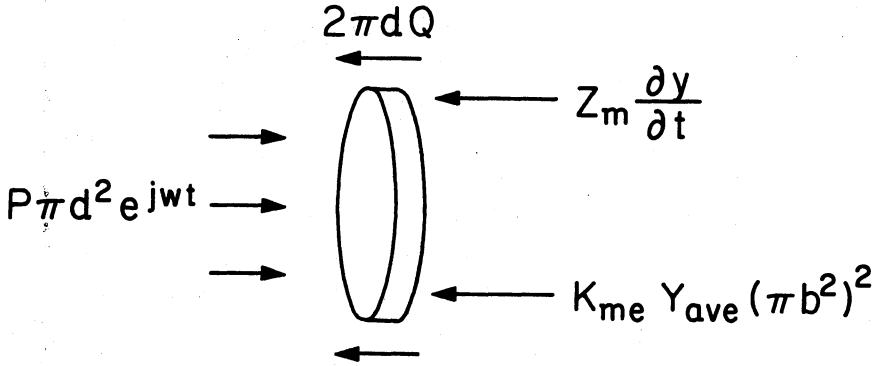

Figure 28. Free Body Diagram for the Malleus Disk

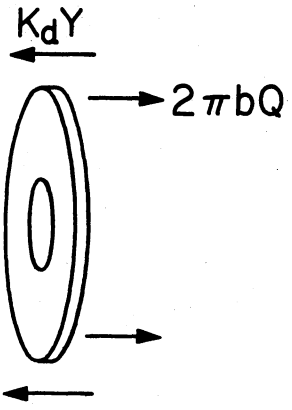

Figure 29. Free Body Diagram of Annular Plate Portion of the Eardrum

moment. Therefore, the moment is zero. This boundary condition then becomes

$$- \frac{Et^3}{12(1-\nu^2)} \left[\frac{d^2\psi}{dr^2} + \frac{\nu}{r} \frac{d\psi}{dr} \right] \Big|_{r=b} = 0 \quad . \quad (22)$$

The above reduces to

$$\frac{d^2\psi}{dr^2} + \frac{\nu}{r} \frac{d\psi}{dr} \Big|_{r=b} = 0 \quad .$$

Substituting into the first boundary condition,

$$\frac{d\psi}{dr} = -A_1 K J_1(Kr) - A_2 K Y_1(Kr) + A_3 K I_1(Kr) - A_4 K N_1(Kr) \quad .$$

Simplifying, this is

$$A_1 J_1(Kd) + A_2 Y_1(Kd) - A_3 I_1(Kd) + A_4 N_1(Kd) = 0 \quad . \quad (4)$$

For the second boundary condition, things are more complicated, so a few preliminary calculations are necessary.

$$\nabla_r^2 \psi = \frac{d^2\psi}{dr^2} + \frac{1}{r} \frac{d\psi}{dr}$$

($\frac{d^2\psi}{d\theta^2} = 0$ because of symmetry assumptions).

From Mclachlan (31),

$$\frac{d}{dZ} J_n(Z) = n \frac{J_n(Z)}{Z} - J_{n+1}(Z)$$

$$\frac{d}{dZ} Y_n(Z) = n \frac{Y_n(Z)}{Z} - Y_{n+1}(Z)$$

$$\frac{d}{dZ} I_n(Z) = n \frac{I_n(Z)}{Z} + I_{n+1}(Z)$$

$$\frac{d}{dZ} N_n(Z) = n \frac{N_n(Z)}{Z} - N_{n+1}(Z) \quad .$$

Substituting these above, the result is

$$\frac{d\psi}{dr} = -KA_1 J_1(Kr) - KA_2 Y_1(Kr) + KA_3 I_1(Kr) - KA_4 N_1(Kr) \quad .$$

$$\frac{d^2\psi}{dr^2} = -K^2\{ A_1\left[\frac{J_1(Kr)}{Kr} - J_2(Kr)\right] + A_2\left[\frac{Y_1(Kr)}{Kr} - Y_2(Kr)\right]$$

$$- A_3\left[\frac{I_1(Kr)}{Kr} + I_2(Kr)\right] + A_4\left[\frac{N_1(Kr)}{Kr} - N_2(Kr)\right] \}$$

$$\nabla_r^2\psi = -K^2\{ A_1\left[\frac{J_1(Kr)}{Kr} - J_2(Kr)\right] + A_2\left[\frac{Y_1(Kr)}{Kr} - Y_2(Kr)\right]$$

$$- A_3\left[\frac{I_1(Kr)}{Kr} + I_2(Kr)\right] + A_4\left[\frac{N_1(Kr)}{Kr} - N_2(Kr)\right] \}$$

$$- \frac{K}{r}\left[A_1J_1(Kr) + A_2Y_1(Kr) - A_3I_1(Kr) + A_4N_1(Kr)\right] .$$

Simplifying the above,

$$\nabla_r^2\psi = A_1\{K^2J_2(Kr) - \frac{2K}{r}J_1(Kr)\} + A_2\{K^2Y_2(Kr) - \frac{2K}{r}Y_1(Kr)\}$$

$$+ A_3\{K^2I_2(Kr) + \frac{2K}{r}I_1(Kr)\} + A_4\{K^2N_2(Kr) - \frac{2K}{r}N_1(Kr)\}$$

$$\frac{\partial}{\partial r}\nabla_r^2\psi = A_1\{K^2\left[K(2\frac{J_2(Kr)}{Kr} - J_3(Kr))\right] - \frac{2K}{r}\left[K(\frac{J_1(Kr)}{Kr}\right.$$

$$\left. - J_2(Kr))\right] + \frac{2K}{r^2}J_1(Kr)\} + A_2\{K^2\left[K(2\frac{Y_2(Kr)}{Kr}\right.$$

$$\left. - Y_3(Kr))\right] - \frac{2K}{r}\left[K(\frac{Y_1(Kr)}{Kr} - Y_2(Kr))\right]$$

$$+ \frac{2K}{r^2}Y_1(Kr)\} + A_3\{K^2\left[K(2\frac{I_2(Kr)}{Kr} + I_3(Kr))\right]$$

$$+ \frac{2K}{r}\left[K(\frac{I_1(Kr)}{Kr} + I_2(Kr))\right] - \frac{2K}{r^2}I_1(Kr)\}$$

$$+A_4\{K^2\left[K(2\frac{N_2(Kr)}{Kr} - N_3(Kr))\right] + \frac{2K}{r}\left[K(\frac{N_1(Kr)}{Kr}\right.$$

$$\left. - N_2(Kr))\right] + \frac{2K}{r^2}N_1(Kr)\} \quad .$$

Simplifying, the above may be written as

$$\frac{\partial}{\partial r}\nabla_r^2\psi = A_1\{-K^3J_3(Kr) + 2(\frac{K+K^2}{r})J_2(Kr)\} + A_2\{-K^3Y_3(Kr)$$

$$+ 2(\frac{K+K^2}{r})Y_2(Kr)\} + A_3\{K^3I_3(Kr) + 2(\frac{K+K^2}{r})I_2(Kr)\}$$

$$+ A_4\{-K^3N_3(Kr) + 2(\frac{K+K^2}{r})N_2(Kr)\} \quad .$$

If the following definitions are made,

$$C_1 = \frac{-j\omega R}{K^4C^2\sigma}\left[J_0(Kd) + \frac{2}{K(b^2-d^2)}\left(bJ_1(Kb) - dJ_1(Kd)\right)\right]$$

$$C_2 = \frac{-j\omega R}{K^4C^2\sigma}\left[Y_0(Kd) + \frac{2}{K(b^2-d^2)}\left(bY_1(Kb) - dY_1(Kd)\right)\right]$$

$$C_3 = \frac{-j\omega R}{K^4C^2\sigma}\left[I_0(Kd) + \frac{2}{K(b^2-d^2)}\left(bI_1(Kb) - dY_1(Kd)\right)\right]$$

$$C_4 = \frac{-j\omega R}{K^4C^2\sigma}\left[N_0(Kd) + \frac{2}{K(b^2-d^2)}\left(bN_1(Kb) - dN_1(Kd)\right)\right] \quad ,$$

then $\psi(r)$ becomes

$$\psi(r) = A_1(J_0(Kr) + C_1) + A_2(Y_0(Kr) + C_2) + A_3(I_0(Kr) + C_3) + A_4(N_0(Kr) + C_4) - \frac{P}{K^4C^2\sigma} \quad .$$

Solving for y_{ave},

$$y_{ave} = A_1(J_0(Kd) + C_1) + A_2(Y_0(Kd) + C_2) + A_3(I_0(Kd) + C_3) + A_4(N_0(Kd) + C_4) - \frac{P}{K^4C^2\sigma} + \frac{2}{K^2(b^2-d^2)}\left[A_1K(bJ_1(Kb) - dJ_1(Kd)) + A_2K(bY_1(Kb) - dY_1(Kd)) + A_3K(bI_1(Kb) - dI_1(Kd)) + A_4K(bN_1(Kb) - dN_1(Kd))\right] \quad .$$

Substituting back into the second boundary condition,

$$P\pi d^2 - \frac{2\pi dEt^3}{12(1-\nu^2)}\left\{A_1\left[\frac{2(K+K^2)}{d}J_2(Kd) - K^3J_3(Kd)\right] + A_2\left[\frac{2(K+K^2)}{d}Y_2(Kd) - K^3Y_3(Kd)\right] + A_3\left[\frac{2(K+K^2)}{d}I_2(Kd) + K^3I_3(Kd)\right] + A_4\left[\frac{2(K+K^2)}{d}N_2(Kd) - K^3N_3(Kd)\right]\right\} - j\omega Z_m\left[A_1(J_0(Kd) + C_1) + A_2(Y_0(Kd) + C_2) + A_3(I_0(Kd) + C_3) + A_4(N_0(Kd) + C_4) - \frac{P}{K^4C^2\sigma}\right] -$$

$$- K_{me}(\pi b^2)^2\Big[A_1(J_0(Kd) + C_1) + A_2(Y_0(Kd) + C_2)$$

$$+ A_3(I_0(Kd) + C_3) + A_4(N_0(Kd) + C_4) - \frac{P}{K^4C^2\sigma}$$

$$+ \frac{2}{K^2(b^2-d^2)}\Big[A_1K(bJ_1(Kb) - dJ_1(Kd)) + A_2K(bY_1(Kb)$$

$$- dY_1(Kd)) + A_3K(bI_1(Kb) - dI_1(Kd)) + A_4K(bN_1(Kb)$$

$$- dN_1(Kd))\Big]$$

$$= (j\omega)^2M_e\Big[A_1(J_0(Kd) + C_1) + A_2(Y_0(Kd) + C_2)$$

$$+ A_3(I_0(Kd) + C_3) + A_4(N_0(Kd) + C_4) - \frac{P}{K^4C^2\sigma}\Big] \quad .$$

Collecting terms, this may be written as

$$P\pi d^2 + j\omega Z_m \frac{P}{K^4C^2\sigma} + K_{me}(\pi b^2)^2\frac{P}{K^4C^2\sigma} + (j\omega)^2M_e \frac{P}{K^4C^2\sigma}$$

$$+ A_1\{-\frac{2\pi dEt^3}{12(1-\nu^2)}\Big[\frac{2(K+K^2)}{d}J_2(Kd) - K^3J_3(Kd)\Big]$$

$$- j\omega Z_m(J_0(Kd) + C_1) - K_{me}(\pi b^2)^2\Big[(J_0(Kd) + C_1)$$

$$+ \frac{2}{K(b^2-d^2)}(bJ_1(Kb) - dJ_1(Kd))\Big] - (j\omega)^2M_e(J_0(kd)$$

$$+ C_1)\} + A_2\{-\frac{2\pi dEt^3}{12(1-\nu^2)}\Big[\frac{2(K+K^2)}{d}Y_2(Kd) - K^3Y_3(Kd)\Big]$$

$$- j\omega Z_m(Y_0(Kd) + C_2) - K_{me}(\pi b^2)^2\Big[(Y_0(Kd) + C_2)$$

$$+ \frac{2}{K(b^2-d^2)}(bY_1(Kb) - dY_1(Kd))\Big] - (j\omega)^2M_e(Y_0(Kd)$$

$$+C_2)\} + A_3\{\frac{-2\pi dEt^3}{12(1-\nu^2)}\Big[\frac{2(K+K^2)}{d}I_2(Kd) + K^3I_3(Kd)\Big]$$

$$- j\omega Z_m(I_0(Kd) + C_3) - K_{me}(\pi b^2)^2\Big[(I_0(Kd) + C_3)$$

$$+ \frac{2}{K(b^2-d^2)}(bI_1(Kb) - dI_1(Kd))\Big] - (j\omega)^2M_e(I_0(Kd)$$

$$+ C_3)\} + A_4\{-\frac{2\pi dEt^3}{12(1-\nu^2)}\left[\frac{2(K+K^2)}{d} N_2(Kd) - K^3N_3(Kd)\right]$$

$$- j\omega Z_m(N_0(Kd) + C_4) - K_{me}(\pi b^2)^2\left[(N_0(Kd) + C_4)\right.$$

$$\left. + \frac{2}{K(b^2-d^2)}(bN_1(Kb) - dN_1(Kd))\right] - (j\omega)^2M_e(N_0(Kd)$$

$$+ C_4)\} = 0 \quad .$$

An expression this complicated obviously prohibits solution by hand, so the following definitions are made to facilitate a computerized solution.

$$P_1 = \frac{-2\pi dEt^3}{12(1-\nu^2)}\left[\frac{2(K+K^2)}{d} J_2(Kd) - K^3J_3(Kd)\right] - \left[j\omega Z_m\right.$$

$$\left. + (j\omega)^2M_e + K_{me}(\pi b^2)^2\right](J_0(Kd) + C_1)$$

$$- K_{me}(\pi b^2)^2\left[\frac{2(bJ_1(Kb) - dJ_1(Kd))}{K(b^2-d^2)}\right]$$

$$P_2 = \frac{-2\pi dEt^3}{12(1-\nu^2)}\left[\frac{2(K+K^2)}{d} Y_2(Kd) - K^3Y_3(Kd)\right] - \left[j\omega Z_m\right.$$

$$\left. +(j\omega)^2M_e + K_{me}(\pi b^2)^2\right](Y_0(Kd) + C_2)$$

$$- K_{me}(\pi b^2)^2\left[\frac{2(bY_1(Kb) - dY_1(Kd))}{K(b^2-d^2)}\right]$$

$$P_3 = \frac{-2\pi dEt^3}{12(1-\nu^2)}\left[\frac{2(K+K^2)}{d} I_2(Kd) + K^3I_3(Kd)\right] - \left[j\omega Z_m\right.$$

$$\left. + (j\omega)^2M_e + K_{me}(\pi b^2)^2\right](I_0(Kd) + C_3)$$

$$- K_{me}(\pi b^2)^2\left[\frac{2(bI_1(Kb) - dI_1(Kd))}{K(b^2-d^2)}\right]$$

$$P_4 = \frac{-2\pi dEt^3}{12(1-\nu^2)}\left[\frac{2(K+K^2)}{d} N_2(Kd) - K^3N_3(Kd)\right] - \left[j\omega Z_m\right.$$

$$\left. + (j\omega)^2M_e + K_{me}(\pi b^2)^2\right](N_0(Kd) + C_4)$$

$$- K_{me}(\pi b^2)^2\left[\frac{2(bN_1(Kb) - dN_1(Kd))}{K(b^2-d^2)}\right]$$

$$P_9 = -\left[P\pi d^2 + (j\omega Z_m + (j\omega)^2 M_e + K_{me}(\pi b^2)^2)\frac{P}{K^4C^2\sigma}\right] \quad .$$

Using these definitions the second boundary condition becomes

$$P_1A_1 + P_2A_2 + P_3A_3 + P_4A_4 = P_9 \quad . \tag{5}$$

By using those relationships already developed, the third boundary condition may be written directly as

$$\frac{2\pi bEt^3}{12(1-\nu^2)}\{A_1\left[-K^3J_3(Kb) - \frac{2(K+K^2)}{d}J_2(Kb)\right] + A_2\left[-K^3Y_3(Kb) + \frac{2(K+K^2)}{b}Y_2(Kb)\right] + A_3\left[K^3I_3(Kb) + \frac{2(K+K^2)}{b}I_2(Kb)\right] + A_4\left[-K^3N_3(Kb) + \frac{2(K+K^2)}{b}N_2(Kb)\right] = K_d\left[A_1(J_0(Kb) + C_1) + A_2(Y_0(Kb) + C_2) + A_3(I_0(Kb) + C_3) + A_4(N_0(Kb) + C_4) - \frac{P}{K^4C^2\sigma}\right] \quad .$$

Making the following definitions,

$$P_{10} = \frac{2\pi bEt^3}{12(1-\nu^2)}\left[-K^3J_3(Kb) + \frac{2(K+K^2)}{b}J_2(Kb)\right] - K_d\,(J_0(Kb) + C_1)$$

$$P_{11} = \frac{2\pi bEt^3}{12(1-\nu^2)}\left[-K^3Y_3(Kb) + \frac{2(K+K^2)}{b}Y_2(Kb)\right] - K_d(Y_0(Kb) + C_2)$$

$$P_{12} = \frac{2\pi bEt^3}{12(1-\nu^2)}\left[K^3I_3(Kb) + \frac{2(K+K^2)}{b}\,I_2(Kb)\right] - K_d(I_0(Kb) + C_3)$$

$$P_{13} = \frac{2\pi bEt^3}{12(1-\nu^2)}\left[-K^3N_3(Kb) + \frac{2(K+K^2)}{b}\,N_2(Kb)\right] - K_d(N_0(Kb) + C_4) \quad ,$$

the third boundary condition becomes

$$P_{10}A_1 + P_{11}A_2 + P_{12}A_3 + P_{13}A_4 = \frac{-K_d P}{K^4 C^2 \sigma} \quad . \qquad (6)$$

The fourth boundary condition is obtained from previously developed relationships.

$$-K^2\{A_1\left[\frac{J_1(Kb)}{Kb} - J_2(Kb)\right] + A_2\left[\frac{Y_1(Kb)}{Kb} - Y_2(Kb)\right]$$
$$- A_3\left[\frac{I_1(Kb)}{Kb} + I_2(Kb)\right] + A_4\left[\frac{N_1(Kb)}{Kb} - N_2(Kb)\right]\}$$
$$+ \frac{\nu}{b}\left[-K(A_1J_1(Kb) + A_2Y_1(Kb) - A_3I_1(Kb) + A_4N_1(Kb))\right]$$
$$= 0 \quad .$$

Collecting terms, the above is

$$A_1\{-K^2\left[\frac{J_1(Kb)}{Kb} - J_2(Kb)\right] - \frac{K\nu}{b}J_1(Kb)\} + A_2\{-K^2\left[\frac{Y_1(Kb)}{Kb}\right.$$
$$\left. - Y_2(Kb)\right] - \frac{K\nu}{b}Y_1(Kb)\} + A_3\{K^2\left[\frac{I_1(Kb)}{Kb} + I_2(Kb)\right]$$
$$+ \frac{K\nu}{b} I_1(Kb)\} + A_4\{-K^2\left[\frac{N_1(Kb)}{Kb} - N_2(Kb)\right] - \frac{K\nu}{b} N_1(Kb)$$
$$= 0 \quad .$$

Making the following definitions,

$$P_5 = K^2J_2(Kb) - \frac{K(1+\nu)}{b} J_1(Kb)$$

$$P_6 = K^2Y_2(Kb) - \frac{K(1+\nu)}{b} Y_1(Kb)$$

$$P_7 = K^2I_2(Kb) + \frac{K(1+\nu)}{b} I_1(Kb)$$

$$P_8 = K^2N_2(Kb) - \frac{K(1+\nu)}{b} N_1(Kb) \quad ,$$

the fourth boundary condition is

$$P_5A_1 + P_6A_2 + P_7A_3 + P_8A_4 = 0 \quad . \qquad (7)$$

Arranging in matrix form and regrouping, the result is given below.

$$\begin{bmatrix} P_1 & P_2 & P_3 & P_4 \\ P_{10} & P_{11} & P_{12} & P_{13} \\ J_1(Kd) & Y_1(Kd) & -I_1(Kd) & N_1(Kd) \\ P_5 & P_6 & P_7 & P_8 \end{bmatrix} \begin{bmatrix} A_1 \\ A_2 \\ A_3 \\ A_4 \end{bmatrix} = \begin{bmatrix} P_9 \\ \frac{-PK_d}{K^4C^2\sigma} \\ 0 \\ 0 \end{bmatrix}$$

The above matrix equation may be solved for the constants A_1, A_2, A_3, and A_4 by a number of methods. The particular method is not important, but Cramer's rule was used here. When the constants A_1, A_2, A_3, and A_4 are known, then the eardrum displacement may be calculated. The average displacement of the eardrum is

$$\psi_{ave} = \psi(d) + \frac{1}{\pi(b^2-d^2)} \int_d^b 2\pi r\, \psi(r)\, dr \quad .$$

Carrying out the above integration and substituting for $\psi(r)$,

$$\begin{aligned} \psi_{ave} = {} & A_1 J_0(Kd) + A_2 Y_0(Kd) + A_3 I_0(Kd) + A_4 N_0(Kd) \\ & - \frac{P}{K^4C^2\sigma} + \frac{2}{K(b^2-d^2)} \Big[A_1(bJ_1(Kb) - dJ_1(Kd)) \\ & + A_2(bY_1(Kb) - dY_1(Kd)) + A_3(bI_1(Kb) - dI_1(Kd)) \\ & + A_4(bN_1(Kb) - dN_1(Kd)) \Big] \quad . \end{aligned} \tag{8}$$

The average acoustical impedance at the eardrum is

$$Z_e = \frac{P}{U} = \frac{Pe^{j\omega t}}{j\omega\psi_{ave}\, e^{j\omega t}(\pi b^2)} \quad ,$$

which may be simplified as given below.

$$Z_e = \frac{P}{j\omega\psi_{ave}(\pi b^2)} \tag{9}$$

The mechanism of the acoustic reflex on the static impedance of the ear is not known precisely, but it has been

described by Hung (32) to be primarily due to the stapedius muscle which provides a tension on the incus in the lateral direction. Although it has not been definitely established in the literature, it has been suggested that the effect of the acoustic reflex is to provide a different mode of vibration for the ear, which causes the static acoustic impedance to increase (33) (34). From the standpoint of modeling the ossicular chain for static impedance, it is necessary only to describe the static properties of the middle-ear muscles as the acoustic reflex is not operating for static impedance. For the static impedance profiles, the acoustic reflex mechanism is not included.

Several researchers have described the action of mammalian skeletal muscle (21) (35) (36) (37), and the result is the model shown in Figure 30. This model consists of a contractile component plus a series elastic component. Since this model is intended only for use in predicting static impedance, the series elastic component is all that is used. Force-displacement data is given by Bahler (21), shown in Figure 31.

Both linear and nonlinear ossicle models are developed. Since Bahler's force-displacement data is nonlinear, it is desirable to have a nonlinear muscle model. However, precise nonlinear analysis in the frequency domain is not possible at this time, so a linear ossicle muscle model is also used. By including both linear and nonlinear models, it is possible to examine the effect of nonlinear muscle properties on

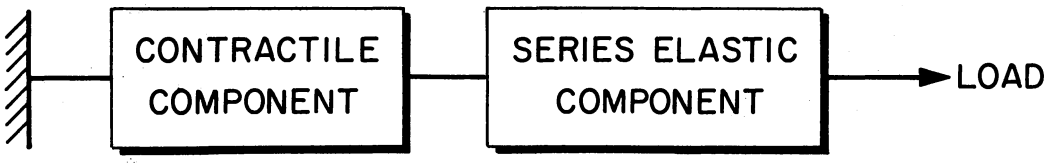

Figure 30. Model of Mammalian Skeletal Muscle

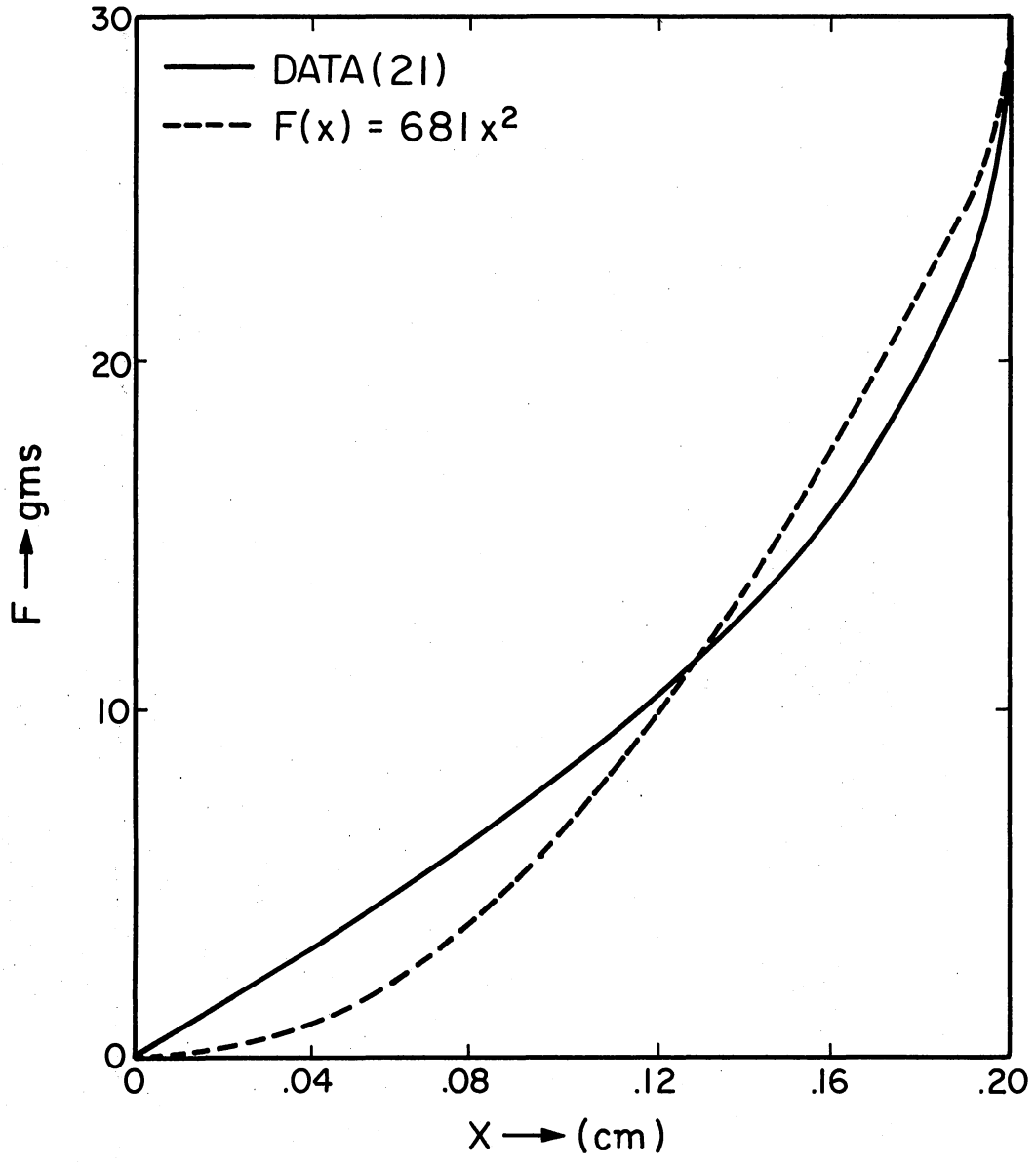

Figure 31. Force Displacement Data of Series Elastic Component

impedance profiles and in this manner investigate the value of including nonlinear effects. This comparison will also provide some additional information as to the accuracy of linear ossicle models. Although the middle ear may be essentially linear at moderate intensities as is commonly accepted, its nonlinearity might have a significant effect on the shape of the impedance profiles at all intensities.

The free body diagram shown in Figure 32 represents the mathematical model of the ossicles. The spring constants and Z_c are assumed to be linear. From Figure 32 applying Newton's law, the equation of motion results.

$$\frac{1}{3}\left[M_m\ell_m^2 + M_I\ell_I^2\right]\ddot{\theta} + Z_c\ell_I^2\dot{\theta} + \left[k_S\ell_I^2 + k_t\ell_m^2\right]\theta = F\ell_m e^{j\omega t} \tag{10}$$

where Z_c is the input impedance to the cochlea. The ossicles are assumed to be circular rods for purposes of taking moments of inertia. This equation is linear and may easily be solved for θ by assuming $\theta=Ae^{j\omega t}$ and substituting back into the original equation to solve for A. When this is done, Z_m may be calculated by taking the ratio of force to velocity.

$$Z_m = \frac{R_C\ell_I^2}{\ell_m} + j\left\{\left[\frac{1}{3}M_m\ell_m^2 + \frac{1}{3}\frac{M_I\ell_I^2}{\ell_m}\right]\omega - \left[\frac{\frac{k_S\ell_I^2}{\ell_m} + \frac{k_C\ell_I^2}{\ell_m^2} + k_t\ell_m}{\omega}\right]\right\} \tag{11}$$

From Figure 32 if the spring characteristic is now a square law, the following equation holds.

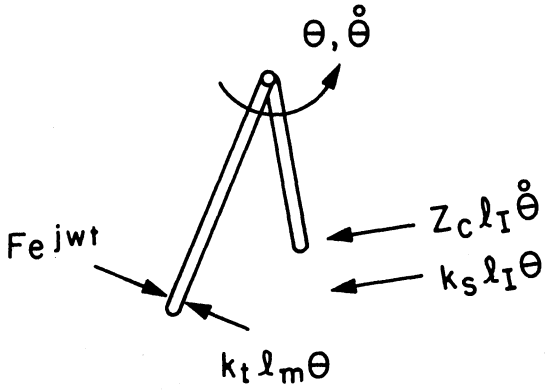

Figure 32. Free Body Diagram of Ossicles

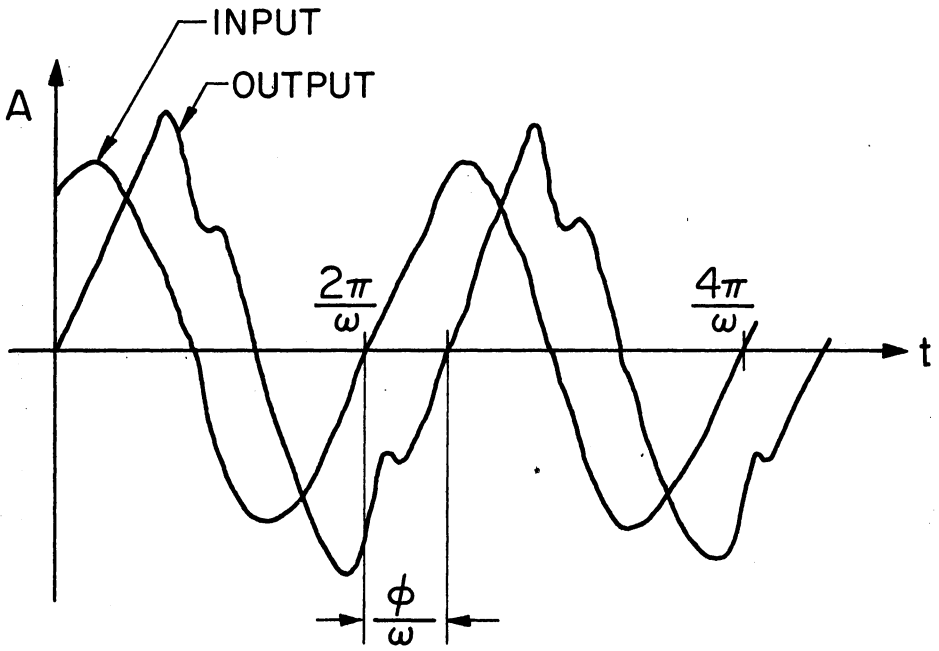

Figure 33. Nonlinear Impedance Algorithm

$$\frac{1}{3}\left[M_m \ell_m + \frac{M_I \ell_I^2}{\ell_m}\right]\ddot{\theta} + \frac{Z_C \ell_I^2}{\ell_m}\dot{\theta} + \left[\frac{k_S \ell_I^2}{\ell_m} + k_t \ell_m\right]\theta|\theta| = F\ell_m \sin \omega t$$

By making the following definitions,

$$Q_1 = \frac{R_C \ell_I^2/\ell_m}{\frac{1}{3}\left[M_m \ell_m + M_I \ell_I^2/\ell_m\right]}$$

$$Q_2 = \frac{\left[k_S \ell_I^2/\ell_m + k_C \ell_I^2/\ell_m + k_t \ell_m\right]}{\frac{1}{3}\left[M_m \ell_m + M_I \ell_I^2/\ell_m\right]}$$

$$P_0 = \frac{F\ell_m}{\frac{1}{3}\left[M_m \ell_m + M_I \ell_I^2/\ell_m\right]} \quad ,$$

the following equation results:

$$\ddot{\theta} + Q_1\dot{\theta} + Q_2\theta|\theta| = P_0 \sin \omega t \quad . \tag{12}$$

The above nonlinear equation cannot presently be solved in closed form. Approximate solutions may be obtained using a variety of methods, or the numerical solution can be generated using the digital computer. An approximate solution for displacement using Galerkin's method was generated initially because a closed form solution is much easier with which to work. This approximate solution when differentiated to get velocity introduced large errors, so a different method was used.

Since impedance is force divided by velocity, the quantity to be solved for is velocity. The basic idea for approximating this nonlinear velocity was to numerically integrate in time for one full cycle to allow all transients to die out. At the end of one cycle, the computer was

programmed to keep track of maximum and minimum values of velocity and also zero crossing. In this way, approximate amplitude and phase information was obtained as demonstrated in Figure 33. For complete programming details see the next section.

Parameter Selection

The above mathematical models are coded as separate subroutines named MEATUS, EARDUM, and OSSCLE for ease in making changes in the models. An appropriate choice of parameters is necessary in order for the mathematical model to be effective. Many of the parameters have been measured by Bekesy, others are available from other sources, and still others may be estimated. The mathematical model only approximates the behavior of the real ear, however, so adjustments in the parameters may be necessary. The parameters readily available from literature are listed below.

$P = .2$ dynes/cm^2 (80dB)

$S = .5$ cm^2

$M_m = .025$ gms

$M_I = .025$ gms

$\ell_m = .3$ cm

$\ell_I = .3$ cm

$\rho_a = 1.23 \times 10^{-3}$ gm/cm^3

$C_a = 3.62 \times 10^4$ cm/sec

$V_{me} = 2.0$ cm^3

These parameters are satisfactory as they are. Others that are available from Bekesy are:

R_c = 100 dyne-sec/cm

b = .55cm

d = .45 cm

E = 2.0×10^8 dynes/cm^2

t = .005 cm

σ = 44.5×10^{-3} gms/cm^2

The parameters b and d come from Bekesy's estimates as to the total area of the eardrum that moves with the malleus handle and the total area of the eardrum. Still other parameters have not been measured or reported elsewhere. Those are given below, along with their estimates.

X = 2.5 cm

k_S = 1.0×10^5 dyne/cm

k_t = 1.0×10^5 dyne/cm

M_e = 2.0×10^{-2} gm

K_d = 6×10^4 dynes/cm

In the above, K_d comes from Bekesy's measurement of the stiffness of the outer segment of the eardrum. Subsequent trial runs on the computer indicated that the dynamics of the eardrum predominates. The four most important parameters in eardrum dynamics were determined to be E, t, σ, and K_d. These were used as unknowns in a parameter fitting computer program and the results are given below.

K_d = 6×10^4 dynes/cm

σ = .95 gms/cm^2

$E = 2.0 \times 10^8$ dynes/cm^2

$t = 0.17$ cm

Most computer runs were made, and the following estimates for the remaining parameters are:

$R_c = 1600$ dyne-sec/cm

$X = 2.5$ cm

$d - .49$ cm

$b = .50$ cm

$\sigma = 1.9$ gms/cm^2

$M_e = 2.0$ gms

The computer program used to calculate impedance along with associated plotting routines is given in the next section.

Computer Programs

This mathematical model was programmed on the computer. Tables I and II are descriptions of input data and computer parameters, respectively. A complete source listing follows.

TABLE I

INPUT DATA

CARD NO.	COLUMN	FORMAT	PARAMETER
1	4	I4	NPLOT = 1,2,3 1 new axes drawn for each data set 2 data plotted on same axes 3 no plot
1	8	I4	NRUNS = number of runs
1	12	I4	NLIN = 1,2 1 linear ossicle model 2 nonlinear ossicle model
1	16	I4	M = number of frequency data points
1	20	I4	NUM = 40
1	24	I4	IPHAS = 0,1,2 0 resistance-reactance impedance plots 1 magnitude and phase impedance plots 2 both of the above
2	1-10	E10.2	RPLATE
2	11-20	E10.2	AR
2	21-30	E10.2	X
2	31-40	E10.2	B
2	41-50	E10.2	D
2	51-60	E10.2	E
2	61-70	E10.2	TK
2	71-80	E10.2	PMU
3	1-10	E10.2	SIGM
3	11-20	E10.2	RME
3	21-30	E10.2	RKD
3	31-40	E10.2	P

TABLE I (Continued)

CARD NO.	COLUMN	FORMAT	PARAMETER
4	1-10	E10.2	RKTS
4	11-20	E10.2	EL
4	21-30	E10.2	EA
4	31-40	E10.2	RC
4	41-50	E10.2	VC
4	51-60	E10.2	RM
4	61-70	E10.2	RI
4	71-80	E10.2	RLM
5	1-10	E10.2	RLI
5	11-20	E10.2	C
5	21-30	E10.2	V
5	31-40	E10.2	DENS
5	41-50	E10.2	RKS
5	51-60	E10.2	RKT
5	61-70	E10.2	CA

TABLE II

GLOSSARY OF COMPUTER PARAMETERS

COMPUTER PARAMETER	DEFINITION
RPLATE	Flat plate damping coefficient
AR	Ear canal cross-sectional area
X	Distance to the eardrum
B	Outer radius of annular flate plate
D	Inner radius of annular flate plate
E	Flat plate modulus of elasticity
TK	Flat plate thickness
PMU	Flat plate Poisson's ratio
SIGM	Flat plate mass/unit area
RME	Malleus disk mass
RKD	Outer eardrum linear spring constant
P	Driving pressure intensity
RKTS	Rotary spring constant between malleus and incus
EL	Length of eustachian tube
EA	Radius of eustachian tube
RC	Cochlear resistance
VC	Unused dummy parameter
RM	Malleus effective mass
RI	Incus effective mass
RLM	Malleus effective length
RLI	Incus effective length
C	Nonlinear ossicle quadratic spring coefficient
V	Volume of middle ear cavities

TABLE II (Continued)

COMPUTER PARAMETER	DEFINITION
DENS	Density of fluid in middle ear cavities
RKS	Linear spring constant of stapedius
RKT	Linear spring constant of tensor tympani
CA	Speed of sound of fluid in middle ear cavities

```
000000000111111111122222222223333333333444444444455555555556666666667777
123456789012345678901234567890123456789012345678901234567890123456789012345673901

      IMPLICIT REAL*8 (A-H,O-Z)
      REAL*4 XARRAY,X1,Y1,Y2,XSTART,XDELTA,YSTART,YDELTA,RSTART,RDELTA
      REAL*4 VALUE,TITLE,VARBLE
      COMPLEX*16 DCMPLX,ZC,ZM,ZE,ZO,S,ZSTOR
      COMPLEX CMPLX
      DIMENSION ZO(56),XARRAY(58),Y1(58),Y2(58),X1(58),ZSTOR(10,56)
      DIMENSION VALUE(10),TITLE(10)
      COMMON/PARAM/  ZC,ZM,ZE,P,PMU,CA,SIGM,E,D,B,V,DENS,RM,RI,RLM,
     *RLI,RKS,RKT,RHO,C,VC,TK,RC,RME,RKO,RPLATE,EL,EA,RKTS
      READ(5,199)(TITLE(I),I=1,10),VARBLE
C
C*************************
C
C     READ IN PARAMETERS WHICH CONTROL PLOTTING INFORMATION
      READ(5,200) NPLOT,NRUNS,NLIN,M,NUM,IPHAS
C
C***********************
C
C     READ IN PARAMETERS WHICH PERTAIN TO EARDUM AND MEATUS
      READ(5,210) RPLATE,AR,X,B,D,E,TK,PMU,SIGM,RME,RKO,P
C
C*******************************
C
C     READ IN PARAMETERS WHICH PERTAIN TO OSSCLE
      READ(5,220) RKTS,EL,EA,RC,VC,RM,RI,RLM,RLI,C,V,DENS,RKS,RKT,CA
C
      WRITE(6,300) NPLOT,NRUNS,NLIN,M,IPHAS
      WRITE(6,310) RPLATE,AR,X,B,D,E,TK,PMU,SIGM,RME,RKO,P
      WRITE(6,320) RKTS,EL,EA,RC,VC,RM,RI,RLM,RLI,C,V,DENS,RKS,RKT,CA
      DO 10 IL=1,NRUNS
      WRITE(6,110)
      FRQ = 1.0D2
      DELFRQ = 20.
      CALL MEATUS(AR,X,DELFRQ,FRQ,M,ZO,NLIN)
      FRQ = 100.
      DELFRQ = 20.
      DO 11 IQ=1,M
      WRITE(6,100) FRQ,ZO(IQ)
      X1(IQ) = FRQ
      ZSTOR(IL,IQ) = ZO(IQ)
      XARRAY(IQ) = DLOG10(FRQ)
      IF(FRQ.GE.1000.) DELFRQ = 100.
   11 FRQ = FRQ+DELFRQ
      VALUE(IL) = RKO
      RKO = RKO/2.
   10 CONTINUE
      IF(NPLOT.EQ.3) GO TO 5
      CALL PLOTS
      CALL PLOTC(0.0,-11.,-3)
      LINTIC=3
      RLABEL = 1.5
      IF(IPHAS.EQ.1) GO TO 400
      DO 7 KL=1,NRUNS
      DO 2 K=1,M
```



```
000000000111111111122222222223333333333444444444455555555556666666667777
123456789012345678901234567890123456789012345678901234567890123456789012345673901

      Y1(K)=DIMAG(ZSTOR(KL,K))
    2 Y2(K)=DREAL(ZSTOR(KL,K))
      IF(NPLOT.EQ.2.AND.KL.GT.1) GO TO 4
      CALL SCALE(XARRAY,3.0,M,1)
      CALL SCALE(Y1,2.0,M,1)
      CALL SCALE(Y2,2.0,M,1)
      XSTART=XARRAY(M+1)
      XDELTA=XARRAY(M+2)
      YSTART=Y1(M+1)
      YDELTA=Y1(M+2)
      RSTART=Y2(M+1)
      RDELTA=Y2(M+2)
      CALL PLOTC(0.0,2.5,-3)
      CALL AXIS(0.0,2.0,'LOG FREQUENCY',+13,3.0,0.0,XSTART,XDELTA)
      CALL AXIS(0.0,0.0,'REACTANCE',9,2.0,90.0,YSTART,YDELTA)
      CALL PLOTC(0.0,4.0,-3)
      CALL AXIS(0.0,0.0,'LOG FREQUENGY',-13,3.0,0.0,XSTART,XDELTA)
      CALL AXIS(0.0,0.0,'RESISTANCE',10,2.0,90.0,RSTART,RDELTA)
      CALL SYMBOL(1.0,2.0,.14,TITLE,0.0,NUM)
    4 CONTINUE
      CALL LINE(XARRAY,Y2,M,1,LINTIC,KL)
      CALL SYMBOL(2.0,RLABEL,.14,KL,0.0,-1)
      CALL SYMBOL(999.0,999.0,.14,VARBLE,0.0,4)
      CALL NUMBER(999.0,999.0,.14,VALUE(KL),0.0,0)
      RLABEL = RLABEL - .20
      CALL PLOTC(0.0,-4.0,-3)
      CALL LINE(XARRAY,Y1,M,1,LINTIC,KL)
      LINTIC=LINTIC+2
      IF(NPLOT.EQ.1) GO TO 6
      CALL PLOTC(0.0,4.0,-3)
      GO TO 7
    6 CALL PLOTC(8.0,-2.5,-3)
    7 CONTINUE
      IF(IPHAS.EQ.0) GO TO 5
      IF(NPLOT.NE.1) CALL PLOTC(0.0,-4.0,-3)
      CALL PLOTC(8.0,-2.5,-3)
      RLABEL = 1.5
  400 DO 71 KL=1,NRUNS
      DO 72 K=1,M
      Y1(K)=CDABS(ZSTOR(KL,K))
   72 Y2(K)=DATAN(DIMAG(ZSTOR(KL,K))/DREAL(ZSTOR(KL,K)))*180./3.141592
      IF(NPLOT.EQ.2.AND.KL.GT.1) GO TO 74
      CALL SCALE(XARRAY,3.0,M,1)
      CALL SCALE(Y1,2.0,M,1)
      CALL SCALE(Y2,2.0,M,1)
      XSTART=XARRAY(M+1)
      XDELTA=XARRAY(M+2)
      YSTART=Y1(M+1)
      YDELTA=Y1(M+2)
      RSTART=Y2(M+1)
      RDELTA=Y2(M+2)
      CALL PLOTC(0.0,2.5,-3)
      CALL AXIS(0.0,0.0,'LOG FREQUENCY',-13,3.0,0.0,XSTART,XDELTA)
      CALL AXIS(0.0,0.0,'IMPEDANCE MAGNITUDE',19,2.0,90.0,YSTART,YDELTA)
```

```
                                                80/80 LIST

00000000011111111112222222222333333333344444444455555555556666666667777
12345678901234567890123456789012345678901234567890123456789012345678901123

      SUBROUTINE MEATUS(AR,X,DELFRQ,FRQ,M,ZO,NLIN)
      IMPLICIT REAL*8 (A-H,O-Z)
C
C
      COMPLEX*16 DCMPLX,ZO,ZC,ZM,ZE,Z,S
      COMPLEX CMPLX,DU,DUM
      DIMENSION ZO(1)
      COMMON/PARAM/  ZC,ZM,ZE,P,PMU,CA,SIGM,E,D,B,V,DENS,RM,RI,RLM,
     *RLI,RKS,RKT,RHO,C,VC,TK,RC,RME,RKO,RPLATE,EL,EA,RKTS
C
      DUM= CMPLX(1.,0.)
      DU  = CMPLX(0.,1.)
      DO 20 K=1,M
      IF(FRQ.GE.1000.) DELFRQ = 100.
      FRR = FRQ*2.*3.141592
      S = DCMPLX(0.0D0,FRR)
      Z = S/DU/CA
      CK =DREAL(Z)
      CALL EARDUM(S,NLIN)
      DUF = DENS*CA/AR
      ZO(K) =DUF*DUM*(ZE+DU*DUF*DTAN(CK*X))/(DUM*DUF+DU*ZE*DTAN(CK*X))
20    FRQ = FRQ+DELFRQ
      RETURN
      END
```

```
                                                80/80 LIST

00000000011111111112222222222333333333344444444455555555556666666667777
12345678901234567890123456789012345678901234567890123456789012345678901123

      CALL PLOTC(0.0,4.0,-3)
      CALL AXIS(0.0,0.0,'LOG FREQUENCY',-13,3.0,0.0,XSTART,XDELTA)
      CALL AXIS(0.0,0.0,'IMPEDANCE PHASE',15,2.0,90.0,RSTART,RDELTA)
      CALL SYMBOL(1.0,2.0,.14,TITLE,0.0,NUM)
   74 CONTINUE
      CALL LINE(XARRAY,Y2,M,1,LINTIC,KL)
      CALL SYMBOL(2.0,PLABEL,.14,KL,0.0,-1)
      CALL SYMBOL(999.0,999.0,.14,VARBLE,0.0,4)
      CALL NUMBER(999.0,999.0,.14,VALUE(KL),0.0,0)
      RLABEL = RLABEL - .20
      CALL PLOTC(0.0,-4.0,-3)
      CALL LINE(XARRAY,Y1,M,1,LINTIC,KL)
      LINTIC=LINTIC+2
      IF(NPLOT.EQ.1) GO TO 76
      CALL PLOTC(0.0,4.0,-3)
      GO TO 71
   76 CALL PLOTC(8.0,-2.5,-3)
   71 CONTINUE
    5 CONTINUE
  100 FORMAT(10X,F10.4,5X,E11.4,5X,E11.4)
  110 FORMAT(/,11X,'FREQUENCY',7X,'RESISTANCE',5X,'REACTANCE',//)
  199 FORMAT(11A4)
  200 FORMAT(6I4)
  210 FORMAT(8E10.2/4E10.2)
  220 FORMAT(8E10.2/7E10.2)
  300 FORMAT(5X,'NPLOT=',I4,'NRUNS=',I4,'NLIN=',I4,'M=',I4,'IPHAS=',I4)
  310 FORMAT(5X,'RPLATE=',E10.2,'AR=',E10.2,'X=',E10.2,'B=',E10.2,'D=',
     *E10.2,'E=',E10.2,'TK=',E10.2,'PMU=',E10.2,'SIGM=',E10.2,/,5X,
     *'RME=',E10.2,'RKO=',E10.2,'P=',E10.2)
  320 FORMAT(5X,'RKTS=',E10.2,'EL=',E10.2,'EA=',E10.2,'RC=',E10.2,/,5X,
     *'VC=',E10.2,'RM=',E10.2,'RI=',E10.2,'RLM=',E10.2,'RLI=',E10.2,/,5X
     *,'C=',E10.2,'V=',E10.2,'DENS=',E10.2,'RKS=',E10.2,'RKT=',E10.2,
     *'CA=',E10.2)
      STOP
      END
```

```
                                                    80/80 LIST

00000000011111111112222222222333333333344444444445555555556666666666577
12345678901234567890123456789012345678901234567890123456789012345678901234567890

      SUBROUTINE EAROUM(S,NLIN)
      IMPLICIT REAL*8 (A-H,O-Z)
      COMPLEX*16 DCMPLX,ZM,ZC,ZE,S,Z,Y,P1,P2,P3,P4,P5,P6,P7,P8,P9,P10,
     *P11,P12,P13,A1,A2,A3,A4,DET,XR1,XR2,XR3,XR4,ER2,ER1,CR2,CR1,
     *DUMMY,BR3,BR2,BR1,C1,C2,C3,C4
      COMPLEX CMPLX,DU,DUM
C
C
      COMMON/PARAM/  ZC,ZM,ZE,P,PMU,CA,SIGM,E,D,B,V,DENS,RM,RI,RLM,
     *RLI,RKS,RKT,RHO,C,VC,TK,RC,RME,RKD,RPLATE,EL,EA,RKTS
      DU = CMPLX(0.,1.)
      DUM = CMPLX(1.,0.)
      CE = DSQRT(E*TK*TK*TK/(12.*(1.0D0-PMU*PMU)*SIGM))
C
C     COMPUTE ALL REQUIRED CONSTANTS.
C
      Z = S/(DU*CE)
      CK =DREAL(Z)
      CK = DSQRT(CK)
C
      CALL OSSCLE(S,NLIN)
C
C
      X1 = CK*D
      X2 = CK*B
C
C     COMPUTE ALL REQUIRED BESSEL FUNCTIONS OF THE FIRST KIND
C
      CALL BESJ(X1,0,RJ0D,1.0D-4,IER)
      CALL BESJ(X1,1,PJ1D,1.0D-4,IER)
      CALL BESJ(X1,2,PJ2D,1.0D-4,IER)
      CALL BESJ(X1,3,RJ3D,1.0D-4,IER)
      CALL BESJ(X2,1,RJ1B,1.0D-4,IER)
      CALL BESJ(X2,2,PJ2B,1.0D-4,IER)
      CALL BESJ(X2,0,RJ0B,1.0D-4,IER)
      CALL BESJ(X2,3,RJ3B,1.0D-4,IER)
C
C     COMPUTE ALL BESSEL FUNCTIONS OF THE SECOND KIND.
C
      CALL BESY(X1,0,Y0D,IER)
      CALL BESY(X1,1,Y1D,IER)
      CALL BESY(X1,2,Y2D,IER)
      CALL BESY(X1,3,Y3D,IER)
      CALL BESY(X2,1,Y1B,IER)
      CALL BESY(X2,2,Y2B,IER)
      CALL BESY(X2,0,Y0B,IER)
      CALL BESY(X2,3,Y3B,IER)
C
C     COMPUTE ALL MODIFIED BESSEL FUNCTIONS OF THE FIRST KIND.
C
      CALL BESI(X1,0,RI0D)
      CALL BESI(X1,1,RI1D)
      CALL BESI(X1,2,RI2D)
      CALL BESI(X1,3,RI3D)
```



```
00000000011111111112222222223333333333444444444455555555556666666666777
12345678901234567890123456789012345678901234567890123456789012345678901234567890123

      CALL BESI(X2,1,RI1B)
      CALL BESI(X2,2,RI2B)
      CALL BESI(X2,0,RI0B)
      CALL BESI(X2,3,RI3B)
C
C     COMPUTE ALL MODIFIED BESSEL FUNCTIONS OF THE SECOND KIND.
C
      CALL BESK(X1,0,RK0D,IER)
      CALL BESK(X1,1,RK1D,IER)
      CALL BESK(X1,2,RK2D,IER)
      CALL BESK(X1,3,RK3D,IER)
      CALL BESK(X2,1,RK1B,IER)
      CALL BESK(X2,2,RK2B,IER)
      CALL BESK(X2,0,RK0B,IER)
      CALL BESK(X2,3,RK3B,IER)
C
C     COMPUTE THOSE COEFFICIENTS NECESSARY TO EVALUATE THE BOUNDARY
C     CONDITIONS.
C
      COF = 2.0*3.141592*E*TK*TK*TK  /(12.0*(1.0-PMU*PMU))
      CME = CA*CA*DENS/V*(3.141592*B*B)*(3.141592*B*B)+DENS*(EL+16.*EA/
     *(3.*3.141592))*3.141592*B*B*S*S
      COFE = 2./(CK*(B*B-D*D))
C
      C1= -S*RPLATE/(CK*CK*CK*CK*CE*CE*SIGM)*(RJ0D+COFE*(B*RJ1B-D*RJ1D))
      C2 = -S*RPLATE/(CK*CK*CK*CK*CE*CE*SIGM)*(Y0D+COFE*(B*Y1B-D*Y1D))
      C3=-S*RPLATE/(CK*CK*CK*CK*CE*CE*SIGM)*(RI0D+COFE*(B*RI1B-D*RI1D))
      C4=-S*RPLATE/(CK*CK*CK*CK*CE*CE*SIGM)*(RK0D+COFE*(B*RK1B-D*RK1D))
C
C
      P1= -D*COF*(2.*(CK+CK*CK)/D*RJ2D-CK*CK*CK*RJ3D)-(S*ZM+S*S*PME+CME)
     **(RJ0D+C1)-CME*COFE*(B*RJ1B-D*RJ1D)
C
C
      P2=-D*COF*(2.*(CK+CK*CK)/D*Y2D-CK*CK*CK*Y3D)-(S*ZM+S*S*RME+CME)
     **(Y0D+C2)-CME*COFE*(B*Y1B-D*Y1D)
C
C
      P3= -D*COF*(2.*(CK+CK*CK)/D*RI2D+CK*CK*CK*RI3D)-(S*ZM+S*S*RME+CME)
     **(RI0D+C3)-CME*COFE*(B*RI1B-D*RI1D)
C
C
      P4= -D*COF*(2.*(CK+CK*CK)/D*RK2D-CK*CK*CK*RK3D)-(S*ZM+S*S*RME+CME)
     **(RK0D+C4)-CME*COFE*(B*RK1B-D*RK1D)
C
C
      COK = CK*(1.+PMU)/B
C
      P5 = CK*CK*RJ2B-COK*PJ1B
      P6 = CK*CK*Y2B-COK*Y1B
      P7 = CK*CK*RI2B+COK*RI1B
      P8 = CK*CK*RK2B-COK*RK1B
C
      CDET = P/(SIGM*CE*CE*CK*CK*CK*CK)
```

```
                                80/80 LIST

00000000011111111112222222222333333333444444444455555555556666666666777
12345678901234567890123456789012345678901234567890123456789012345678901234

      COCT =CDET*RKD
C
      P10= B*COF*(2./B*(CK+CK*CK)*RJ2B-CK*CK*CK*RJ3B)-RKD*(RJOB+C1)
      P11= B*COF*(2./B*(CK+CK*CK)*Y2B-CK*CK*CK*Y3B)-RKD*(YOD+C2)
      P12= B*COF*(2./B*(CK+CK*CK)*RI2B+CK*CK*CK*RI3B)-RKD*(RIOD+C3)
      P13= B*COF*(2./B*(CK+CK*CK)*RK2B-CK*CK*CK*RK3B)-RKD*(RKOD+C4)
C
      P9 = -(P*3.141592*D*D+(S*ZM+S*S*RME+CME)*CDET)
C
C     COMPUTE THE COEFFICIENTS IN THE DIFFERENTIAL EQUATION
C
      DET = P1*(P13 *(Y1D*P7+RI1D*P6)-P12 *(Y1D*P8-RK1D*P6)-P11*(RI1D*P8
     *+RK1D*P7))-P2*(P13 *(RJ1D*P7+RI1D*P5)-P12 *(RJ1D*P8-RK1D*P5)-P10 *
     *(RI1D*P8+RK1D*P7)J+P3*(P10 *(Y1D*P8-RK1D*P6)-P11*(RJ1D*P8-RK1D*P5)
     *+ P13*(RJ1D*P6-Y1D*P5))-P4*( P10*(Y1D*P7+RI1D*P6)-P11*(RJ1D*P7+
     *RI1D*P5)+ P12*(RJ1D*P6-Y1D*P5))
C
C
       A1 = (P9*( P13*(Y1D*P7+RI1D*P6)- P12*(Y1D*P8-RK1D*P6)-P11*(RI1D*
     *P8+RK1D*P7))-P2*CDCT*(RI1D*P8+RK1D*P7)-P3*CDCT*(Y1D*P8-RK1D*P6)+
     *P4*CDCT*(Y1D*P7+RI1D*P6))/DET
C
C
       A2 = (P9*( P10*(RI1D*P8+RK1D*P7)+ P12*(RJ1D*P8-RK1D*P5)- P13*
     *(RJ1D*P7+RI1D*P5))+P1*CDCT*(RI1D*P8+RK1D*P7)-P3*CDCT*(RJ1D*P8-
     *RK1D*P5)+P4*CDCT*(RJ1D*P7+RI1D*P5))/DET
C
C
       A3 = (P9*( P10*(Y1D*P8-RK1D*P6)-P11*(RJ1D*P8-RK1D*P5)+ P13*
     *(RJ1D*P6-Y1D*P5))-P1*CDCT*(Y1D*P8-RK1D*P6)+P2*CDCT*(RJ1D*P8-RK1D*
     *P5)+P4*CDCT*(RJ1D*P6-Y1D*P5))/DET
C
C
       A4 = (P9*(P11*(RJ1D*P7+RI1D*P5)- P12*(RJ1D*P6-Y1D*P5)- P10*(Y1D*
     *P7+RI1D*P6))-P1*CDCT*(Y1D*P7+RI1D*P6)+P2*CDCT*(RJ1D*P7+RI1D*P5)-
     *P3*CDCT*(RJ1D*P6-Y1D*P5))/DET
C
C
      Y =  A1*(RJOD+COFE*(B*RJ1B-D*RJ1D))+ A2*(YOD+COFE*(B*Y1B-D*Y1D))+
     * A3*(RIOD+COFE*(B*RI1B-D*RI1D))+ A4*(RKOD+COFE*(B*RK1B-D*RK1D))-
     *CDET
C
C
      PE = P/3.141592
      ZE = PE/(S*Y*B*B)
      RETURN
      END
```

```
                                   80/80 LIST

00000000011111111112222222222333333333344444444455555555556666666666777
12345678901234567890123456789012345678901234567890123455789012345678901 2

      SUBROUTINE OSSCLE(S,NLIN)
      IMPLICIT REAL*8 (A-H,O-Z)
      COMPLEX*16 ZM,ZC,XM,ZE,S,DSP,R1
      COMPLEX*16 DCMPLX
      DIMENSION DX(4),X(4),XA(4),DXA(4)
      DIMENSION VEL(1000)
C
C
      COMMON/PARAM/  ZC,ZM,ZE,P,PMU,CA,SIGM,E,D,B,V,DENS,RM,RI,RLM,
     *RLI,RKS,RKT,RHO,C,VC,TK,RC,RME,RKD,RPLATE,EL,EA,RKTS
      Q3(X) = 681.8*X*DABS(X)*980.
C
      ZC = RC*VC/S
      GO TO(100,200,200),NLIN
  100 ZM = ((S*S*RI*RLI*RLI/3.+S*ZC*RLI+RKS*RLI+RKTS)*(S*S*RM*RLM*RLM/3.
     *+RKT*RLM+RKTS)-RKTS*RKTS)/(S*(S*S*RLI*RLI/3.+S*ZC*RLI+RKS*RLI+
     *RKTS))
      RETURN
  200 PO = P*3.141592*B*B*RLM
      IF(RKTS.GT.1.0D6) RKTS=1.0D6
      FRR = DIMAG(S)
      DT = 2.*3.141592/(500.*FRR)
      RCY=1.0D0
      TF = 2.*3.141592*RCY/FRR
      IN = TF/DT
      X(1) = 0.0
      X(2) = 0.0
      X(3) = 0.0
      X(4) = 0.0
      T = 0.0
      TS = 2.*3.141592*(RCY-1.0D0)/FRR
      NN = 2
      THETA = 0.0
      DO 220 IT=1,IN
      DO 210 KUTTA=1,4
      DX(1) = X(3)
      DX(2) = X(4)
      DX(3) = RKTS/(RM*RLM*RLM)*3.*(X(2)-X(1))-RKT*RLM*3./(RM*RLM*RLM)
     **Q3(X(1))+PO*DSIN(FRR*T)
      DX(4) = RKTS*3./(RI*RLI*RLI)*(X(1)-X(2))-ZC*RLI*3./(RI*RLI*RLI)
     **X(4)-RKS*RLI*3./(RI*RLI*RLI)*Q3(X(2))
    1 HDT = 0.5*DT
      GO TO(10,20,30,40),KUTTA
   10 DO 11 I=1,4
      XA(I) = X(I)
      DXA(I) = DX(I)
   11 X(I) = X(I)+HDT*DX(I)
      GO TO 210
   20 DO 21 I=1,4
      DXA(I) = DXA(I)+DX(I)+DX(I)
   21 X(I) = XA(I)+HDT*DX(I)
      GO TO 210
   30 DO 31 I=1,4
      DXA(I) = DXA(I)+DX(I)+DX(I)
```

```
                                   80/80 LIST

00000000011111111112222222222333333333344444444455555555556666666555
12345678901234567890123456789012345678901234567890123455789012345678901 2

   31 X(I) = XA(I)+DT*DX(I)
      GO TO 210
   40 VDT = DT*.166666666667
      DO 41 I=1,4
   41 X(I) = XA(I)+VDT*(DXA(I)+DX(I))
  210 CONTINUE
      IF(T.LE.(TS-DT)) VEL(1) = X(3)
      IF(T.LT.TS) GO TO 220
      VEL(NN) = X(3)
      NNM = NN-1
      PHAS = VEL(NN)*VEL(NNM)
      IF(PHAS.LT.0.0D0) TIM = THETA
      THETA = THETA+DT
      IF(VEL(NN).GT.VEL(NNM)) VMAX = VEL(NN)
      IF(VEL(NN).LT.VEL(NNM)) VMIN = VEL(NN)
      NN = NN+1
  220 T = T+DT
      PHI = 3.141592*FRR*TIM
      VCR = (VMAX-VMIN)*DCOS(PHI)
      VCX =-(VMAX-VMIN)*DSIN(PHI)
      DSP = DCMPLX(VCR,VCX)
      ZM = PO/DSP
      RETURN
      END
```

APPENDIX B

IMPEDANCE MEASUREMENT DETAILS

Appendix B contains a description of the instrumentation, a description of the input data required to process the experimental data, and a source listing of the computer program. In addition, Table IV is included which is an example of the forms used in taking data on human subjects.

As shown in Figure 34, the two microphones of the device must be connected to different voltmeters for measurement of pressure ratio and phase. The sound source to the horn driver was provided by a Hewlett Packard 200 CD audio oscillator through a McIntosh audio amplifier. The two B&K microphone outputs are taken from the microphone power supply (B&K 2804 dual channel) into two Ballantine RMS voltmeters. This is for two reasons: (1) provision for accurate measurement of the various pressure ratios, and (2) the Ballantine RMS voltmeters each have amplifier outputs for use in phase measurement. The phase measurement is accomplished by a North Atlantic 202R phase angle voltmeter. The accuracy of the phase angle measurement depends on the amplitude of the input signals, so the amplifier output of the Ballantine RMS voltmeter is crucial for accurate phase measurement.

TABLE III

EXPERIMENTAL DATA REDUCTION INPUT DATA

CARD NO.	COLUMN	FORMAT	VARIABLE
1	1-20	5A4	label for several groups statistically reduced and placed on one plot
1	23	I3	NCOMP = number of data groups
1	26	I3	NGROUP = 0,1 0 new grid drawn for each group 1 all groups plotted on same grid
2	1-20	5A4	title for each data group
3	4	I4	NDATA = number of data sets
3	8	I4	NPLOT = 3 statistical reduction desired otherwise same as Appendix A
3	12	I4	NRUNS = NDATA 3 for statistical reduction
3	16	I4	NLIN = 0 calcomp routines scale plot 1 use limits supplied
3	20	I4	M = same as Appendix A
3	24	I4	NUM = same as Appendix A
3	28	I4	IPHAS = same as Appendix A
3	29	F10.3	YSTART = starting reactance coordinate
3	39	F10.3	RSTART = starting resistance coordinate
3	49	F10.3	YDELTA = reactance increment
3	59	F10.3	RDELTA = resistance increment
4	1-55	11F5.3	Experimental microphone magnitude response
4	64	I3	Subject number
5	1-55	I3	Experimental microphone phase response
5	56-60	F5.4	Reference microphone voltage level

TABLE IV

IMPEDANCE DATA FORM[a]

Frequency	Probe Tube Correction	Microphone Voltage in DBV	Ear SPL in DB	Microphone Voltage	Microphone Phase
200	133				
300	132				
400	131				
500	129				
600	129				
700	128				
800	129				
900	131				
1000	133				
1200	135				
1400	137				

[a]Raw Impedance Data for Subject Number _____

V_r = _____

Notes: _____

_____

_____

```
                                                80/80 LIST

00000000011111111112222222222333333333344444444455555555556666666557777
12345678901234567890123456789012345678901234567890123456789012345678901

C      IMPEDANCE METER BASED ON THEVININ'S EQUIVALENT CIRCUIT THEOREM.
C      COMPUTER PROGRAM TO CALCULATE UNKNOWN IMPEDANCE USING ACOUSTIC
C
C
C   DEFINITIONS
C
C      GOC = OPEN CIRCUIT PRESSURE RESPONSE.
C      GMAG = MAGNITUDE OF GOC.
C      GPHAS = PHASE ANGLE OF GOC.
C      GTEST = TEST PRESSURE RESPONSE USING CAPACATIVE LOAD.
C      GTMAG = MAGNITUDE OF GTEST.
C      GTPHAS = PHASE ANGLE OF GTEST.
C      GK = TEST PRESSURE RESPONSE USING GENERAL LOAD.
C      GKMAG = MAGNITUDE OF GK.
C      GKPHAS = PHASE ANGLE OF GK.
C      GM = TEST PRESSURE RESPONSE OF MICROPHONE PROBE TUBE.
C      GMMAG = MAGNITUDE OF GM.
C      GMPHAS = PHASE ANGLE OF GM.
C      ZT = VALUE OF KNOWN TEST IMPEDANCE.
C      ZB = VALUE OF DEVICE INTERNAL IMPEDANCE.
C      Z = VALUE OF KNOWN TEST IMPEDANCE USED IN GENERATING GM.
C      ZCAL = CALCULATED VALUE OF TEST IMPEDANCE.
C      ZK = VALUE OF MEASURED ACOUSTIC IMPEDANCE.
C
C
       DIMENSION GMAG(11),GPHAS(11),GTMAG(11),GTPHAS(11)
      *,GKMAG(11),GKPHAS(11),GMMAG(11),GMPHAS(11),CORR(11)
       DIMENSION SUMX1(11),SUMX2(11),SSQX1(11),SSQX2(11),RBAR(11),
      *RVAR(11),XBAR(11),XVAR(11)
       DIMENSION XARRAY(13),Y1(13),Y2(13),ZSTOR(3,11),RLOOP(11),XLOOP(11)
       DIMENSION TITLE(10)
       COMPLEX CMPLX,GOS,GTEST,ZB,ZT,GK,GM,ZC,ZK,ZCAL,ZM,ZS,DU,CABS,ZSTOR
C
C   INPUT CALIBRATION CHARTS
C
       DATA CORR/31.,16.,1.,-8.,-18.,-25.,-31.,-34.,-37.,-41.,-43./
       DATA GMMAG/.0415,.0449,.0502,.0570,.0631,.0645,.0588,.0495,
      *.0402,.0298,.0238/
       DATA GMPHAS/       325.,334.,338.,337.,325.,302.,274.,259.,250.,
      *242.,239./
       DATA VRM/.005/
       DATA GMAG/        .0441,.0510,.0600,.0646,.0628,.0578,.0537,.0521,
      *.0511,.0447,.0316/
       DATA GPHAS/        319.,316.,301.,276.,252.,236.,227.,221.,214.,179.
      *,87./
       DATA VRO/.005/
       DATA GTMAG/       .143,.112,.09,.0765,.066,.054,.0398,.0281,.0189,
      *.0099,.0055/
       DATA GTPHAS/        284.,249.,224.,211.,198.,177.,142.,103.,80.,60.,
      *50./
       DATA VRT/.05/
C
       READ(5,1999)(TITLE(I),I=1,10)
       DO 9 I=1,11
```



```
00000000011111111112222222222333333333344444444455555555556666666666
12345678901234567890123456789012345678901234567890123456789012345678999

       SUMX1(I) = 0.
       SUMX2(I) = 0.
       SSQX1(I) = 0.
       SSQX2(I) = 0.
       GPHAS(I) = (GPHAS(I)+CORR(I))*3.141592/180.
       GTPHAS(I) =(GTPHAS(I)+CORR(I))*3.141592/180.
       GMPHAS(I) =(GMPHAS(I)+CORR(I))*3.141592/180.
       GMMAG(I) = GMMAG(I)*14.6/(VRM*115.)
       GMAG(I) = GMAG(I)*14.6/(VRO*115.)
       GTMAG(I) = GTMAG(I)*14.6/(VRT*115.)
     9 CONTINUE
C
       DENS = 1.23E-3
       CA = 3.43E4
       C1 = 2./(DENS*CA*CA)
       V = 1.7*1.7*1.7*3.141592/4.0  +.6*.6*.1*3.141592/4.
       C=V/(DENS*CA*CA)
       L1 = 1.725/((3.141592E-2)*(3.141592E-2))
       C2 = 0.465E-11*(3.141592E-2)*(3.141592E-2)
       DU = CMPLX(0.,1.)
C
       READ(5,299) NDATA ,NPLOT,NRUNS,NLIN,M,NUM,IPHAS
       DO 199 K=1,NDATA
       READ(5,100) (GKMAG(I),I=1,11),ITUBE,NSUB
       READ(5,102) (GKPHAS(I),I=1,11),VR
       WRITE(6,399) NSUB,VR
       WRITE(6,99)
       FRQ = 200.
       DELFRQ = 100.
       DO 10 I=1,11
       IF(FRQ.GE.1000.) DELFRQ=200.
       WRITE(6,101) FRQ,GKMAG(I),GKPHAS(I)
C
C      CONVERT TO RADIANS
       GKMAG(I) = GKMAG(I)*14.6/(VR*115.)
       GKPHAS(I) = (GKPHAS(I)+CORR(I))*3.141592/180.
    10 FRQ = FRQ+DELFRQ
       WRITE(6,499)
       DELFRQ=100.
       FRQ = 200.
       DO 11 I=1,11
       FRR = FRQ*2.*3.141592
       GR = GMAG(I)*COS(GPHAS(I))
       GX = GMAG(I)*SIN(GPHAS(I))
       GOS = CMPLX(GR,GX)
       GTR = GTMAG(I)*COS(GTPHAS(I))
       GTX = GTMAG(I)*SIN(GTPHAS(I))
       GTEST = CMPLX(GTR,GTX)
       GMR = GMMAG(I)*COS(GMPHAS(I))
       GMX = GMMAG(I)*SIN(GMPHAS(I))
       GM = CMPLX(GMR,GMX)
       GKR = GKMAG(I)*COS(GKPHAS(I))
       GKX=GKMAG(I)*SIN(GKPHAS(I))
       GK = CMPLX(GKR,GKX)
```

```
                                                80/80 LIST

0000000001111111111222222222233333333344444444445555555556666666655577
1234567890123456789012345678901234567890123456789012345678901234567890

      FRR=2.*3.141592*FRQ
      IF(FRQ.GE.1000.) DELFRQ=200.
C   COMPUTE TEST IMPEDANCES.
      U = .354*FRR-1./(13.64E-8*FRR)
      UC = -1./FRR/C
      ZT = CMPLX(GO.,UC)
      ZM = CMPLX(1.12E4,U)
      ZB = (GCS/GTEST-1.)*ZT/(1.+(1.-GOS/GTEST)*ZT/ZM)
      GCC = GOS*(1.+ZB/ZM)
      ZK = GK/((GCC-GK)/ZB-GK/ZM)                              /ZM)
      ZSTOR(K,I)=ZK

   29 SUMX1(I) = SUMX1(I)+REAL(ZK)
      SUMX2(I) = SUMX2(I)+AIMAG(ZK)
      SSQX1(I) = SSQX1(I)+REAL(ZK)*REAL(ZK)
      SSQX2(I) = SSQX2(I)+AIMAG(ZK)*AIMAG(ZK)
      X = DENS*(1.8*16.*.15/3./3.141592)/3.141592/.15/.15/2.*FRR-1./FRR
     */C1
      ZEAL = CMPLX(383.,X)
      WRITE(6,200) FRQ,ZK
   11 FRQ = FRQ+DELFRQ
  199 CONTINUE
      IF(NDATA.EQ.1) GO TO 1111
      DELFRQ = 100.
      FRQ = 200.
      WRITE(6,799) NDATA
      WRITE(6,899)
      WRITE(6,699)
      XDATA = NDATA
      DO 1000 ISTAT=1,11
      XARRAY(ISTAT) = ALOG10(FRQ)
      RBAR(ISTAT) = SUMX1(ISTAT)/XDATA
      XBAR(ISTAT) = SUMX2(ISTAT)/XDATA
      RVAR(ISTAT)= SSQX1(ISTAT)/(XDATA-1.)-RBAR(ISTAT)*RBAR(ISTAT)*
     *XDATA/(XDATA-1.)
      XVAR(ISTAT)= SSQX2(ISTAT)/(XDATA-1.)-XBAR(ISTAT)*XBAR(ISTAT)*
     *XDATA/(XDATA-1.)
      WRITE(6,599) FRQ,RBAR(ISTAT),RVAR(ISTAT),XBAR(ISTAT),XVAR(ISTAT)
      IF(FRQ.GE.1000.) DELFRQ = 200.
      RLOOP(ISTAT) = SQRT(RVAR(ISTAT))
      XLOOP(ISTAT) = SQRT(XVAR(ISTAT))
 1000 FRQ = FRQ+DELFRQ
      DO 3000 K=1,3
      DO 2000 I=1,M
      ZSTOR(K,I) = RBAR(I)+DU*XBAR(I)-RLOOP(I)-DU*XLOOP(I)
      RLOOP(I) = RLOOP(I)-SQRT(RVAR(I))
      XLOOP(I) = XLOOP(I)-SQRT(XVAR(I))
 2000 CONTINUE
 3000 CONTINUE
      IF(NPLOT.EQ.3) GO TO 5
      CALL PLOTS
      CALL PLOTC(0.0,-11.,-3)
      LINTIC=3
      RLABEL = 1.5
```

```
                                                80/80 LIST

0000000001111111111222222222233333333344444444445555555556666666667777
1234567890123456789012345678901234567890123456789012345678901234567890

      IF(IPHAS.EQ.1) GO TO 400
      DO 7 KL=1,NRUNS
      DO 2 K=1,M
      Y1(K)=AIMAG(ZSTOR(KL,K))
    2 Y2(K)= REAL(ZSTOR(KL,K))
      IF(NPLOT.EQ.2.AND.KL.GT.1) GO TO 4
      CALL SCALE(XARRAY,4.0,M,1)
      CALL SCALE(Y1,2.0,M,1)
      CALL SCALE(Y2,2.0,M,1)
      XSTART=XARRAY(M+1)
      XDELTA=XARRAY(M+2)
      YSTART=Y1(M+1)
      YDELTA=Y1(M+2)
      RSTART=Y2(M+1)
      RDELTA=Y2(M+2)
      CALL PLOTC(0.0,2.5,-3)
      CALL AXIS(0.0,2.0,'LOG FREQUENCY',+13,4.0,0.0,XSTART,XDELTA)
      CALL AXIS(0.0,0.0,'REACTANCE',9,2.0,90.0,YSTART,YDELTA)
      CALL PLOTC(0.0,4.0,-3)
      CALL AXIS(0.0,0.0,'LOG FREQUENCY',-13,4.0,0.0,XSTART,XDELTA)
      CALL AXIS(0.0,0.0,'RESISTANCE',10,2.0,90.0,RSTART,RDELTA)
      CALL SYMBOL(1.0,2.0,.14,TITLE,0.0,NUM)
      CALL NUMBER(1.0,1.7,.14,XDATA,0.0,0)
      CALL SYMBOL(999.,999.,.14,' DATA SETS',0.0,10)
    4 CONTINUE
      CALL LINE(XARRAY,Y2,M,1,LINTIC,KL)
      CALL PLOTC(0.0,-4.0,-3)
      CALL LINE(XARRAY,Y1,M,1,LINTIC,KL)
      LINTIC=LINTIC+2
      IF(NPLOT.EQ.1) GO TO 6
      CALL PLOTC(0.0,4.0,-3)
      GO TO 7
    6 CALL PLOTC(8.0,-2.5,-3)
    7 CONTINUE
      IF(IPHAS.EQ.0) GO TO 5
      IF(NPLOT.NE.1) CALL PLOTC(0.0,-4.0,-3)
      CALL PLOTC(8.0,-2.5,-3)
  400 DO 71 KL=1,NRUNS
      DO 72 K=1,M
      Y1(K)= CABS(ZSTOR(KL,K))
   72 Y2(K)= ATAN(AIMAG(ZSTOR(KL,K))/ REAL(ZSTOR(KL,K)))*180./3.141592
      IF(NPLOT.EQ.2.AND.KL.GT.1) GO TO 74
      CALL SCALE(XARRAY,4.0,M,1)
      CALL SCALE(Y1,2.0,M,1)
      CALL SCALE(Y2,2.0,M,1)
      XSTART=XARRAY(M+1)
      XDELTA=XARRAY(M+2)
      YSTART=Y1(M+1)
      YDELTA=Y1(M+2)
      RSTART=Y2(M+1)
      RDELTA=Y2(M+2)
      CALL PLOTC(0.0,2.5,-3)
      CALL AXIS(0.0,0.0,'LOG FREQUENCY',-13,4.0,0.0,XSTART,XDELTA)
      CALL AXIS(0.0,0.0,'IMPEDANCE MAGNITUDE',19,2.0,90.0,YSTART,YDELTA)
```

```
                                    80/80 LIST

0000000001111111111222222222233333333344444444455555555556666666666777
1234567890123456789012345678901234567890123456789012345678901234567890123

      CALL PLOTC(0.0,4.0,-3)
      CALL AXIS(0.0,0.0,'LOG FREQUENCY',-13,4.0,0.0,XSTART,XDELTA)
      CALL AXIS(0.0,0.0,'IMPEDANCE PHASE',15,2.0,90.0,RSTART,RDELTA)
      CALL SYMBOL(1.0,2.0,.14,TITLE,0.0,NUM)
      CALL NUMBER(1.0,1.7,.14,XDATA,0.0,0)
      CALL SYMBOL(999.,999.,.14,' DATA SETS',0.0,10)
   74 CONTINUE
      CALL LINE(XARRAY,Y2,M,1,LINTIC,KL)
      CALL PLOTC(0.0,-4.0,-3)
      CALL LINE(XARRAY,Y1,M,1,LINTIC,KL)
      LINTIC=LINTIC+2
      IF(NPLOT.EQ.1) GO TO 76
      CALL PLOTC(0.0,4.0,-3)
      GO TO 71
   76 CALL PLOTC(8.0,-2.5,-3)
   71 CONTINUE
    5 CONTINUE
  299 FORMAT(7I4)
  100 FORMAT(11F5.3,I2,I3)
  102 FORMAT(11F5.0,F5.4)
  399 FORMAT(/,15X,'RAW IMPEDANCE DATA FOR SUBJECT NUMBER',I5,3X,'VR=',
     *F10.4,/)
   99 FORMAT(11X,'FREQUENCY',11X,'MAGNITUDE',10X,'PHASE')
  101 FORMAT(8X,F10.0,10X,F10.4,7X,F10.3)
  499 FORMAT(/,20X,'RESULTING ACCUSTICAL IMPEDANCE',/)
  200 FORMAT(9X,'FRQ=',F10.4,2X,'RK=',E11.4,2X,'XK=',E11.4)
  599 FORMAT(26X,F10.0,5X,E11.4,5X,E11.4,5X,E11.4,5X,E11.4)
  699 FORMAT(///,30X,'FREQUENCY',5X,'MEAN',10X,'VARIANCE',11X,'MEAN',10X
     *,'VARIANCE')
  799 FORMAT(//,40X,I4,3X,'DATA SETS')
  699 FORMAT(//,50X,'RESISTANCE',23X,'REACTANCE')
 1999 FORMAT(10A4)
 1111 STOP
      END
```

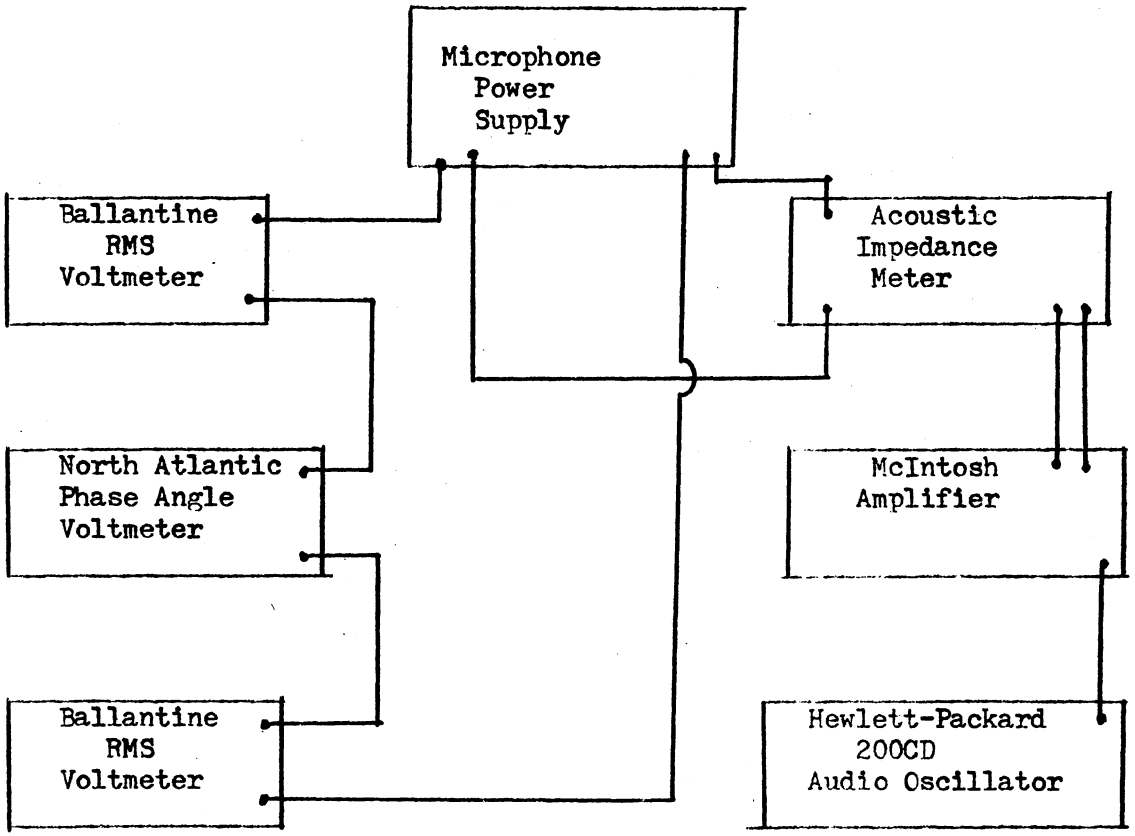

Figure 34. Instrumentation Details

APPENDIX C

AUDIOGRAMS AND CASE HISTORY INFORMATION

Appendix C contains the audiometric information and case history that was available on those volunteers tested in the clinical study. Some of the case history reports are incomplete, but the data that was available is given. Groups which are reported are the sensory neural hearing losses, cases of otosclerosis, cases of otitis media, cases of eardrum perforations, and two mastoidectomy patients.

Subject JB Age 50 Sex Male Occupation _____

Type of Hearing Loss Sensory Neural Bilateral

History: Considerable Exposure to noise, no surgery.

Audiogram

Air Conduction

Right							Left						
125	250	500	1000	2000	4000	8000	125	250	500	1000	2000	4000	8000
25	35	55	70	65	65	nr /85	20	35	60	70	65	60	nr /80

Bone Conduction

Right					Left				
250	500	1000	2000	4000	250	500	1000	2000	4000
30	nr /60	nr /70	nr /65		35	nr /60	nr /70	nr /65	

Speech Audiometry

Speech Reception Threshold					Discrimination Score					Pure Tone Averages		
Ear	1	2	3	4		1 26SL	2	3	4	Ear	Two Freq.	Three Freq.
R	60					64	58			R	60	63
L	58				Mask					L	63	65
Mask						78	72					

Inter Test Consistency: Right: good Left: good

Remarks: Aided SRT 46 (SDT = 38)
Aided DISC @ 50 32%

Subject TT Age 34 Sex Male Occupation _____

Type of Hearing Loss no diagnosis

History: Reported dizziness and blackouts due to head trauma. Normal hearing.

Audiograms

Air Conduction

Right							Left						
125	250	500	1000	2000	4000	8000	125	250	500	1000	2000	4000	8000
20	20	15	20	15	15	25	15	20	15	20	5	20	25

Bone Conduction

Right					Left				
250	500	1000	2000	4000	250	500	1000	2000	4000
15	15	10	5	20	15	10	10	5	20

Speech Audiometry

Speech Reception Threshold					Discrimination Score					Pure Tone Averages		
Ear	1	2	3	4		1 26SL	2	3	4	Ear	Two Freq.	Three Freq.
R		14				98				R	15	17
L		12				98				L	10	13
Mask					Mask							

Inter-Test Consistency: Right: good Left: good

Remarks:

Subject CM Age 41 Sex Male Occupation

Type of Hearing Loss Mild Sensory Neural with recurrent external Otitis

History: Has had mild recurrent external otitis since 12/30/74 in the left ear.

Audiogram

Air Conduction

Right							Left						
125	250	500	1000	2000	4000	8000	125	250	500	1000	2000	4000	8000
20	20	15	20	10	20	10	25	30	20	15	15	55	30

Bone Conduction

Right					Left				
250	500	1000	2000	4000	250	500	1000	2000	4000
20	20	20	15	25	20	20	15	15	30
									60
									70

Speech Audiometry

Speech Reception Threshold					Discrimination Score					Pure Tone Averages		
Ear	1	2	3	4		1 26SL	2	3	4	Ear	Two Freq.	Three Freq.
R	14					100				R	12	15
L	14					100				L	15	18
Mask					Mask							

Inter-Test Consistency: Right: Left:

Remarks:

Subject LW Age 53 Sex Male Occupation _____

Type of Hearing Loss Sensory Neural

History: Has Menieries disease, suffers from vertigo, profound sensory neural hearing loss right ear, mild sensory neural hearing loss left ear.

Audiogram

Air Conduction

Right							Left						
125	250	500	1000	2000	4000	8000	125	250	500	1000	2000	4000	8000
55	65	80	80	70	80	nr /85	20	20	30	35	35	55	nr /85
nr /70	80	80	70										
				75	80								
50	50	65	65	65	80								

Bone Conduction

Right					Left				
250	500	1000	2000	4000	250	500	1000	2000	4000
nr /35	35	40	40	nr /65	nr /35	35	40	40	60
	nr /65	nr /70	nr /65						
	80	80	70						

Speech Audiometry

Speech Reception Threshold					Discrimination Score					Pure Tone Averages		
Ear	1	2	3	4		1 40SL	2 0SL	3	4	Ear	Two Freq.	Three Freq.
R	78	nr /96				94				R	73	75
L	26						14			L	33	33
Mask			50 P/N		Mask			50SPN				

Inter-Test Consistency: Right: Left:

Remarks: Unable to establish SRT at 96 db-patient complained of discomfort

Subject JJ Age 44 Sex Male Occupation _____

Type of Hearing Loss Sensory Neural

History: Subject to artillary fire for 22 years

Audiogram

Air Conduction

Right							Left						
125	250	500	1000	2000	4000	8000	125	250	500	1000	2000	4000	8000
20	35	50	55	60	nr /105	nr /85	20	35	45	55	60	95	nr /80
	20	35	45	50	nr /600			20	30	45	50	90	

Bone Conduction

Right					Left				
250	500	1000	2000	4000	250	500	1000	2000	4000
35	55	50	60	nr /60	35	55	50	55	nr /60

Speech Audiometry

Speech Reception Threshold					Discrimination Score					Pure Tone Averages		
Ear	1	2	3	4		1 40SL	2	3	4	Ear	Two Freq.	Three Freq.
R				32		74				R	52	55
L				36		68				L	50	53
Mask					Mask							

Inter-Test Consistency: Right: good Left: good

Remarks:

Subject WM Age 57 Sex Male Occupation _____

Type of Hearing Loss Sensory Neural

History: History of exposure to bombs and blasts during the war. High frequency sensory neural hearing loss bilaterally.

Audiogram

Air Conduction

Right							Left						
125	250	500	1000	2000	4000	8000	125	250	500	1000	2000	4000	8000
25	20	10	15	15	40	45	20	20	15	20	10	40	60
	5	0	5	5	35			5	0	10	0	35	

Bone Conduction

Right					Left				
250	500	1000	2000	4000	250	500	1000	2000	4000
20	20	20	25	35	20	25	15	20	35

Speech Audiometry

Speech Reception Threshold					Discrimination Score					Pure Tone Averages		
Ear	1	2	3	4		1 40SL	2	3	4	Ear	Two Freq.	Three Freq.
R	12			2		100				R	12	13
L	14			4		100				L	12	15
Mask					Mask							

Inter-Test Consistency: Right: good Left: good

Remarks:

Subject EM Age 23 Sex Male Occupation Mechanic

Type of Hearing Loss Conduction

History: History of noise exposure-was around artillary, worked in grain elevator. 11/4/74 was diagnosed to have bilateral clinical otosclerosis. Uses hearing aid in left ear.

Audiogram

Air Conduction

Right							Left						
125	250	500	1000	2000	4000	8000	125	250	500	1000	2000	4000	8000
55	65	50	55	55	55	80	65	65	70	65	70	90	nr /80
					65				70	65	70	90	
									75	70	70	90	

Bone Conduction

Right					Left				
250	500	1000	2000	4000	250	500	1000	2000	4000
5	20	20	30	30	20	25	30	45	40
		CNM			20	25	30	50	40
					70	80	75	85	90

Speech Audiometry

Speech Reception Threshold					Discrimination Score					Pure Tone Averages		
Ear	1	2	3	4		1 26SL	2	3	4	Ear	Two Freq.	Three Freq.
R	46					94				R	52	52
L	64					82				L	68	68
Mask					Mask		65W/N					

Inter-Test Consistency: Right: good Left: good

Subject CH Age 54 Sex Male Occupation Carpenter

Type of Hearing Loss Conductive

History: Both eardrums show sclerosis from childhood, due to infection probably. No head injuries, vertigo, or discharge. External canals and TM intact, mobile. Diagnosis bilateral otosclerosis, incus is immobile.

Audiogram

Air Conduction

Right							Left						
125	250	500	1000	2000	4000	8000	125	250	500	1000	2000	4000	8000
50	55	55	60	45	65	65	40	50	60	50	45	65	70

Bone Conduction

Right					Left				
250	500	1000	2000	4000	250	500	1000	2000	4000
10	10	20	20	30	0	10	20	30	35
10	10	20	30	30	0	15	30	30	50
70	80	80	90	90	70	80	90	80	90

Speech Audiometry

Speech Reception Threshold					Discrimination Score					Pure Tone Averages		
Ear	1	2	3	4		1 26SL	2	3	4	Ear	Two Freq.	Three Freq.
R	56					96				R	50	53
L	50					100				L	47	52
Mask					Mask							

Inter-Test Consistency: Right: good Left: good

Remarks:

Subject RE Age 44 Sex Male Occupation _____

Type of Hearing Loss Conductive

History: History of hearing loss in family-both father and brother suffered from deafness. Has had bilateral hearing loss for many years, especially bad in left ear. 5/13/75 Both ear canals and TM's intact and mobile. Diagnosis bilateral clinical otosclerosis.

Audiogram

Air Conduction

Right							Left						
125	250	500	1000	2000	4000	8000	125	250	500	1000	2000	4000	8000
20	30	45	45	50	55	70	40	50	55	55	95	55	85

Bone Conductance

Right					Left				
250	500	1000	2000	4000	250	500	1000	2000	4000
0	15	20	30	45	0	10	15	35	30
	CNM				0	10	20	35	30
					65	70	80	90	80

Speech Audiometry

Speech Reception Threshold					Discrimination Score					Pure Tone Averages		
Ear	1	2	3	4		1 26SL	2	3	4	Ear	Two Freq.	Three Freq.
R	50					82				R	45	48
L	56					84				L	55	65
Mask					Mask	20						

Inter-Test Consistency: Right: good Left: good

Remarks:

Subject HA Age 69 Sex Male Occupation retired policeman

Type of Hearing Loss Conductive

History: Limited history available. Subject has clinical otosclerosis, no audiograms are available.

Audiogram

Air Conduction

Right							Left						
125	250	500	1000	2000	4000	8000	125	250	500	1000	2000	4000	8000

Bone Conduction

Right					Left				
250	500	1000	2000	4000	250	500	1000	2000	4000

Speech Audiometry

Speech Reception Threshold					Discrimination Score					Pure Tone Averages		
Ear	1	2	3	4		1	2	3	4	Ear	Two Freq.	Three Freq.
R										R		
L										L		
Mask					Mask							

Inter-Test Consistency: Right: Left:

Remarks:

Subject LC Age 64 Sex Male Occupation Laborer

Type of Hearing Loss Conductive

History: Has complained of tinnitus. Hearing loss in both ears, on 5/7/75 right TM's intact and mobile, but fluid was visible behind eardrums. Left TM retracted, dull, immobile. Diagnosis is serous otitis media, both ears, and high frequency sensory neural hearing loss, bilaterally.

Audiogram

Air Conduction

Right							Left						
125	250	500	1000	2000	4000	8000	125	250	500	1000	2000	4000	8000
20	20	20	30	35	80	nr /85	30	35	40	45	45	90	nr /80
								40	45	50			
							45	45	45				

Bone Conduction

Right					Left				
250	500	1000	2000	4000	250	500	1000	2000	4000
0	5	5	25	nr /60	0	0	0	45	nr /60
	CNM				10	15	0		
					50	60	60		

Speech Audiometry

Speech Reception Threshold					Discrimination Score					Pure Tone Averages		
Ear	1	2	3	4		1 26SL	2	3	4	Ear	Two Freq.	Three Freq.
R	22					84				R	25	28
L	44	48				82				L	45	47
Mask		45WBW			Mask							

Inter-Test Consistency: Right: good Left: good

Remarks

Subject BB Age 50 Sex Male Occupation _____

Type of Hearing Loss Conductive

History: History of noise exposure-infantry noise in VietNam. Chronic otitis Media left ear, Perforation in eardrum.

Audiogram

Air Conduction

Right							Left						
125	250	500	1000	2000	4000	8000	125	250	500	1000	2000	4000	8000
15	15	10	15	30	50	75	40	55	45	35	50	70	80
								60	50		55		
	0	0	5	20	45			45	35	25	45	65	
								50	50		55		

Bone Conduction

Right					Left				
250	500	1000	2000	4000	250	500	1000	2000	4000
10	0	15	15	35	15	15	10	15	25
			15	35	15	15	10	20	25
			70	90	60	55	40	65	80

Speech Audiometry

Speech Reception Threshold					Discrimination Score					Pure Tone Averages		
Ear	1	2	3	4		1 40SL	2	3	4	Ear	Two Freq.	Three Freq.
R	16			6		96				R	13	18
L	36			26		94				L	43	47
Mask					Mask							

Inter-Test Consistency: Right: good Left: good

Remarks: Negative Speech slenger
Negative pure tone slenger @ 1k, 2k, 3k, 4k, 5k.

Subject LA Age 54 Sex Male Occupation Machinist

Type of Hearing Loss _____

History: Has history of noise exposure-bombing during the war, machinery noise because of job. Had radical mastoidectomy in right ear.

Audiogram

Air Conduction

Right							Left						
125	250	500	1000	2000	4000	8000	125	250	500	1000	2000	4000	8000
40	40	40	45	40	55	60	30	35	20	20	15	25	45
			45		55	65							
			50		60	85							

Bone Conduction

Right					Left				
250	500	1000	2000	4000	250	500	1000	2000	4000
0	10	15	10	10	5	10	10	10	0
10	20	15	15	10	5				
55	60	60	50	60	55				CNM

Speech Audiometry

Speech Reception Threshold					Discrimination Score					Pure Tone Averages		
Ear	1	2	3	4		1 26SL	2	3	4	Ear	Two Freq.	Three Freq.
R	38					98				R	40	42
L	14					96				L	17	18
Mask					Mask							

Inter-Test Consistency: Right: good Left: good

Remarks: Negative speech stenger
Negative pure tone stenger @ 1k, 2k, 5k.

Subject WA Age 54 Sex Male Occupation _____

Type of Hearing Loss Conductive

History: on 1/6/75 examination showed severe retraction and tympanosclerosis in left ear. Subject has chronic otitis media bilaterally. Right modified radical mastoidectomy.

Audiogram

Air Conduction

Right							Left						
125	250	500	1000	2000	4000	8000	125	250	500	1000	2000	4000	8000
nr /65	60	55	55	35	55	80	35	20	25	20	10	15	35
	65	60	55		55	nr /90							
	55	55	45		60	60							

Bone Conduction

Right					Left				
250	500	1000	2000	4000	250	500	1000	2000	4000
0	10	5	15	15	10	15	10	10	5
0	10	5	20	25					
40	45	40	40	55					

Speech Audiometry

Speech Reception Threshold					Discrimination Score					Pure Tone Averages		
Ear	1	2	3	4		1 26SL	2	3	4	Ear	Two Freq.	Three Freq.
R	48	50				94				R	45	52
L	10					92				L	15	18
Mask		40 SPN			Mask							

Inter-Test Consistency: Right: Left:

Remarks:

Subject HK Age 44 Sex Male Occupation _____

Type of Hearing Loss Conductive

History: Had left mastoidectomy at age 13. Seems to be well healed. Left ear drains at intervals, subject complains of sensation of something in trachea. There is granulation of left TM and evidence of a hole. Diagnosis-chronic otitis media and trachea irritation due to post nasal drip. (30% perforation) Post-op: Subject had incus missing, mucuous in its place. The stapes footplate was fixed.

Audiogram

Air Conduction

Right							Left						
125	250	500	1000	2000	4000	8000	125	250	500	1000	2000	4000	8000
5	10	10	20	15	40	15	40	50	55	60	55	25	40
								50	55	60	55		

Bone Conduction

Right					Left				
250	500	1000	2000	4000	250	500	1000	2000	4000
15	10	25	10	5	0	0	15	20	5
				40	0	0	15	20	CNM
				80	60	60	60	60	

Speech Audiometry

Speech Reception Threshold					Discrimination Score					Pure Tone Averages		
Ear	1	2	3	4		1 26SL	2	3	4	Ear	Two Freq.	Three Freq.
R	14					90				R	12	15
L	48					96				L	55	57
Mask					Mask							

Inter-Test Consistency: Right: good Left: good

Remarks:

Subject EE Age 24 Sex Female Occupation _____

Type of Hearing Loss Conductive

History: Complains of bilateral hearing loss since childhood. Had mastoidectomy at age 14, left ear. Hearing is deteriorating, there is discharge from both ears. Right ear has TM perforation at center with mucuous discharge. Left ear has TM perforation, discharge. 5/5/75.

Audiogram

Air Conduction

Right							Left						
125	250	500	1000	2000	4000	8000	125	250	500	1000	2000	4000	8000
45	40	50	45	30	45	45	60	45	55	40	20	30	35
		50	50		45		60	45	55				
CNM		70	75		40	CNM	65	60	70				

Bone Conduction

Right					Left				
250	500	1000	2000	4000	250	500	1000	2000	4000
0	0	0	0	5	0	0	5	0	10
			5	5				10	
			40	40				40	

Speech Audiometry

Speech Reception Threshold					Discrimination Score					Pure Tone Averages		
Ear	1	2	3	4		1 26SL	2	3	4	Ear	Two Freq.	Three Freq.
R	48					98				R	38	42
L	40					100				L	30	38
Mask					Mask							

Inter-Test Consistency: Right: good Left: good

Remarks:

Subject WW Age ___ Sex Male Occupation _____

Type of Hearing Loss Conductive

History: Limited information available. Right ear is normal. Left ear has chronic otitis media with TM perforation, drainage. No audiograms available.

Audiogram

Air Conduction

Right							Left						
125	250	500	1000	2000	4000	8000	125	250	500	1000	2000	4000	8000

Bone Conduction

Right					Left				
250	500	1000	2000	4000	250	500	1000	2000	4000

Speech Audiometry

Speech Reception Threshold					Discrimination Score					Pure Tone Averages		
Ear	1	2	3	4		1	2	3	4	Ear	Two Freq.	Three Freq.
R										R		
L										L		
Mask					Mask							

Inter-Test Consistency: Right: Left:

Remarks:

VITA

Paul Wayne Whaley

Candidate for the Degree of

Doctor of Philosophy

Thesis: AN ACOUSTIC IMPEDANCE METER AND ITS VALUE AS A DIAGNOSTIC TOOL

Major Field: Mechanical Engineering

Biographical:

Personal Data: Born in Duncan, Oklahoma, December 9, 1948, the son of Mr. and Mrs. John W. Whaley. Married May 27, 1969 to Karen Collins.

Education: Graduated from Adrian High School, Adrian, Texas, in May, 1967; received Bachelor of Science degree in Mechanical Engineering from Oklahoma State University in May, 1971; received Master of of Science degree in Mechanical Engineering from Oklahoma State University in May, 1973.

Professional Experience: Graduate Teaching Assistant, Oklahoma State University, College of Engineering, 1971-1972; Graduate Research Assistant, Oklahoma State University, College of Engineering, 1972-1975.